Regulation of the DNA Damage Response by the Ubiquitin System

Regulierung der DNA-Schadensreaktion durch das Ubiquitin System

Doctoral thesis

for a doctoral degree

at the Graduate School of Life Sciences,

Julius-Maximilians-Universität Würzburg,

Section: Biomedicine

submitted by

Wenshan Xu

from Anhui, China

Würzburg 2017

Submitted on:

Members of the Thesis Committee:

Chairperson:

Primary Supervisor: **Dr. Nikita Popov**

Supervisor (Second): **Prof. Dr. Alexander Buchberger**

Supervisor (Third): **Dr. Sonja Lorenz**

Date of Public Defence:

Date of Receipt of Certificates:

Table of Contents

Summary

DNA damage occurs frequently during normal cellular progresses or by environmental factors. To preserve the genome integrity, DNA damage response (DDR) has evolved to repair DNA and the non-properly repaired DNA induces human diseases like immune deficiency and cancer. Since a large number of proteins involved in DDR are enzymes of ubiquitin system, it is critical to investigate how the ubiquitin system regulates cellular response to DNA damage. Hereby, we reveal a novel mechanism for DDR regulation via activation of SCF ubiquitin ligase upon DNA damage.

As an essential step for DNA damage-induced inhibition of DNA replication, Cdc25A degradation by the E3 ligase β-TrCP upon DNA damage requires the deubiquitinase Usp28. Usp28 deubiquitinates β-TrCP in response to DNA damage, thereby promotes its dimerization, which is required for its activity in substrate ubiquitination and degradation. Particularly, ubiquitination at a specific lysine on β-TrCP suppresses dimerization.

The key mediator protein of DDR, 53BP1, forms oligomers and associates with β-TrCP to inhibit its activity in unstressed cells. Upon DNA damage, 53BP1 is degraded in the nucleoplasm, which requires oligomerization and is promoted by Usp28 in a β-TrCP-dependent manner. Consequently, 53BP1 destruction releases and activates β-TrCP during DNA damage response.

Moreover, 53BP1 deletion and DNA damage promote β-TrCP dimerization and recruitment to chromatin sites that locate in the vicinity of putative replication origins. Subsequently, the chromatin-associated Cdc25A is degraded by β-TrCP at the origins. The stimulation of β-TrCP binding to the origins upon DNA damage is accompanied by unloading of Cdc45, a crucial component of pre-initiation complexes for replication. Loading of Cdc45 to origins is a key Cdk2-dependent step for DNA replication initiation, indicating that localized Cdc25A degradation by β-TrCP at origins inactivates Cdk2, thereby inhibits the initiation of DNA replication.

Collectively, this study suggests a novel mechanism for the regulation of DNA replication upon DNA damage, which involves 53BP1- and Usp28-dependent activation of the SCF(β-TrCP) ligase in Cdc25A degradation.

Zusammenfassung

DNA-Schäden treten häufig in Folge zellulären Fortschrittes oder durch externe Faktoren auf. Um die Integrität des Genoms zu bewahren und DNA Schäden zu reparieren, die Ursache für viele Autoimmunkrankheiten und Krebs sind, hat sich ein durch DNA Schäden getriggertes Geflecht aus Reparaturprozessen (englisch: “DNA damage response (DDR)”) entwickelt. Hierbei ist es von großem Interesse zu verstehen, wie das Ubiquitin-Proteasom-System die zelluläre Antwort auf DNA-Schäden reguliert. Wir konnten zeigen, dass die SCF Ubiquitin Ligase β-TrCP durch geschädigte DNA aktiviert wird, was einen bisher unbekannten Mechanismus für die Regulation der DDR darstellt.

Für den grundlegenden Schritt der durch DNA Schäden ausgelösten Inhibition der DNA Replikation – der Abbau von Cdc25A durch die E3 Ligase β-TrCP – wird die Deubiquitinase Usp28 benötigt. Diese deubiquitiniert β-TrCP als Antwort auf DNA-Schäden und fördert dadurch seine Dimerisierung, die für die Substrat-Ubiquitinierung und dem anschließenden Abbau erforderlich ist. Hierbei unterdrückt die Ubiquitinierung eines spezifischen Lysin-Rests von β-TrCP dessen Dimerisierung.

Das Schlüsselprotein vom DDR, 53BP1, oligomerisiert und assoziiert mit β-TrCP, was seine Aktivität in gesunden Zellen inhibiert. Auf DNA-Schäden hin oligomerisiert 53BP1 und wird mit Hilfe von Usp28 abhängig von β-TrCP im Nukleoplasma abgebaut. Durch den Abbau von 53BP1 wird β-TrCP freigesetzt, aktiviert und kann auf DNA Schäden reagieren.

Die Deletion von 53BP1 fördert die Dimerisierung von β-TrCP. Die Reparaturmaschinerie wird daraufhin an Stellen des Chromatins rekrutiert, die in der Nähe von vermeintlichen Replikationsursprüngen liegen. Chromatin-assoziiertes Cdc25A wird dann durch β-TrCP ubiquitiniert. Die Bindung von β-TrCP an die Replikationsursprünge in Folge von DNA Schädigung wird begleitet von der Freisetzung von Cdc45, das eine entscheidende Komponente des Präinitiationskomplexes darstellt. Das Beladen von Cdc45 an die Replikationsursprünge stellt eine Schlüsselfunktion der Cdc25A-abhängigen DNA Replikationsinititation dar. Gezielter Abbau von Cdc25A durch β-TrCP an den Replikationsursprüngen inaktiviert Cdk2 und inhibiert dadurch DNA Replikation.

Zusammenfassend lässt sich konstatieren, dass unsere Studien einen neuartigen Mechanismus für die Regulation der DNA Replikation auf DNA Schäden hin aufgezeigt haben, der die 53BP1- und Usp28-abhängige Aktivierung der SCF(β-TrCP) Ubiquitin Ligase im Abbau von Cdc25A beinhaltet.

1 Introduction

1.1 Overview of the ubiquitin system

1.1.1 Ubiquitin-conjugation cascade

Ubiquitin is a highly conserved protein with 76 amino acids. The critical feature of ubiquitin is its C-terminal tail and seven lysine residues. Ubiquitination is a covalent enzymatic modification of a substrate protein with ubiquitin. Typically, via an iso-peptide bond, the C-terminal glycine of ubiquitin covalently binds to the epsilon-amino group of a lysine on a substrate (Pickart, 2001). Additionally, ubiquitin can attach to the N-terminal amine group of a substrate protein rather than the lysine residues (McDowell and Philpott, 2013). Non-amine groups in non-lysine residues have also been shown to be ubiquitination targets, such as the sulfhydryl group on cysteine, and the hydroxyl group on threonine and serine.

Ubiquitination requires at least three types of enzymes including ubiquitin-activating enzymes (E1), ubiquitin-conjugating enzymes (E2), and ubiquitin ligases (E3). First, E1 enzymes form a thiol ester with the C-terminal glycine of ubiquitin in an ATP-dependent manner. In this step, ubiquitin is activated for nucleophilic attack and then transiently transferred to E2 enzymes. The subsequent transfer of ubiquitin from the E2s to the substrates is catalyzed by E3 ligases that are responsible mainly for the substrate specificity (Hershko and Ciechanover, 1998). This three-step reaction results in proteolytic or non-proteolytic regulation of substrates (Fig 1.1).

The proteolytic function of ubiquitination is mediated by the 26S proteasome, a large multi-protein complex which contains a single catalytic 20S complex (core particle) and one or two 19S regulatory particles. The 20S complex is essential to provide the central catalytic chamber for degradation, while the 19S regulatory complex is responsible for binding, deubiquitination and unfolding of the substrates (Budenholzer *et al.*, 2017). The broad range of proteins targeted for proteolytic ubiquitination results in regulation of multiple cellular progresses including cell cycle, signal transduction, stress response, transcriptional regulation, DNA repair, *etc*.

Figure 1.1

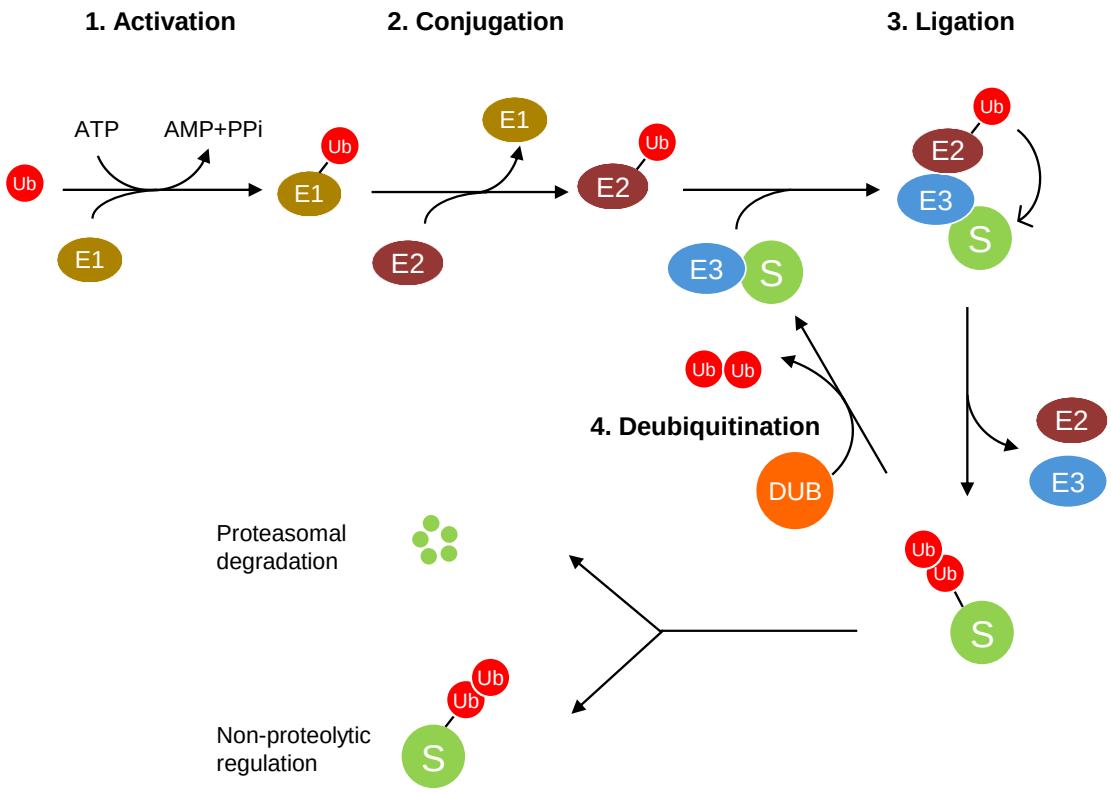

Figure 1.1. Schematic of the ubiquitin-conjugation cascade.

Ubiquitination is achieved by a multiple step reaction mediated by at least three enzymes. The ubiquitin molecules are first activated by the ubiquitin-activating enzyme E1 in an ATP-dependent manner (1) and then transferred to the ubiquitin-conjugating enzyme (E2) (2). The E2 enzymes associate with the E3 ligases which recognize and bind to substrates. Subsequently, E3 enzymes transfer ubiquitin to substrates, either via catalysis by RING E3 ligases or via a ubiquitin-HECT E3 ligases intermediately binding (3). The substrate ubiquitination results in proteasomal degradation or non-proteolytic regulation. Ubiquitin can be removed from proteins by the deubiquitinases (DUB) via deubiquitination (4).

The nonproteolytic ubiquitination of substrates is involved in multiple cellular events as well, such as kinase activation, DNA repair, chromatin dynamics and membrane trafficking. In this case, ubiquitin and polyubiquitin chains can recruit proteins to specific sites, activate kinases or ligases, or serve as a scaffold to associate proteins in diverse signaling, thereby regulate them to perform specific functions (Chen and Sun, 2009; Welchman *et al.*, 2005).

Substrates are monoubiquitinated when a single ubiquitin is attached to one substrate lysine, which is involved in cellular functions like histone regulation, endocytosis and virus budding (Hicke, 2001). Substrates can also be multi-ubiquitinated on several lysines. The seven lysine residues (K6, K11, K27, K29, K33, K48, K63) or the N-terminus M1 on ubiquitin can all serve as the sites of ubiquitination to form polyubiquitin chains (Komander and Rape, 2012; Sadowski and Sarcevic, 2010). The multiple sites on ubiquitin allow the formation of diverse ubiquitin chains which target proteins to different fates. Classically, polyubiquitin chains via K48-linkage with at least 4 ubiquitin molecules, as well as K11-linkage, target proteins for degradation by the 26S proteasome. K63-linked Ub chains can regulate kinase activation, DNA damage repair and protein activity in a non-degradative manner (Sadowski *et al.*, 2012). However, more and more evidence shows that K63-linked chains and multiple other types of Ub chains lead to proteasomal degradation, while K48-linked chains can also drive non-proteolytic regulation, such as transcription factor modulation (Cano *et al.*, 2015; Flick *et al.*, 2006; Kim *et al.*, 2011; Kirkpatrick *et al.*, 2006). This indicates that the functions of ubiquitination in cellular regulation do not only depend on chain topology, but also on some other factors, such as the interactions between E3s and effectors, the subcellular location of enzymes or substrate, or the reversibility of ubiquitination (Komander *et al.*, 2012).

1.1.2 E3 ligases in the ubiquitin system

Typically, ubiquitination involves with one E1 enzyme, but many species of E2s and multiple E3s families or E3-multiple proteins complexes. The large number of E3 ligases and complexes are responsible for the extraordinary diversity of the substrates, which is the most remarkable feature of ubiquitin system and leads to diverse biological functions (Hershko *et al.*, 1998).

Based on the structure domains, E3 ligases can be subdivided into three protein families: Homologous to E6AP Carboxy Terminus (HECT), Really Interesting New Gene (RING), and UFD2 homology (U-box) proteins. The HECT proteins contain an active cysteine in the HECT domains which forms a thiol ester intermediately with ubiquitin prior to transfer it to the substrates. With the RING domain consisting of a short motif rich in cysteine and histidine residues, the RING E3 ligases facilitate direct transfer of ubiquitin from the E2 enzymes to the substrates as scaffolds (Fig

1.1). The U-box proteins lack their own substrates, but promote the polyubiquitination of other E3 ligases' substrates (Aravind and Koonin, 2000; Lorick *et al.*, 1999; Pickart and Eddins, 2004). Other than ubiquitin attaching to HECT E3 ligases, some RING E3 ligases are also known to be self-ubiquitinated, catalyzed by themselves or other ligases (Lorick *et al.*, 1999; Min *et al.*, 2012).

RING E3 ligases are the largest E3 family and function as monomers, dimers, and multi-subunit complex assemblies such as the anaphase-promoting complex / cyclosome (APC/C) and the SCF complex (Skp1-Cullin-F-box protein complex). One of the functions of APC/C ligase is to trigger metaphase-anaphase transition by degrading specific substrates. APC/C ligase consists of at least 12 core subunits, while its activity is regulated by its co-activators Cdc20 and Cdh1 (Visintin *et al.*, 1997). The SCF complex is composed of the adapter protein Skp1, the scaffolding protein Cul1, the RING-domain containing protein Rbx1 and a F-box protein (FBP) as a substrate adaptor. Cul1 acts as the major structural scaffold of the SCF complex and links Skp1 with Rbx1, which recruits E2 enzymes. The F-box protein determines the specificity of E3 ligases and binds to Skp1 which allows the substrates to be brought into close proximity with the E2 enzymes (Fig 1.2) (Vodermaier, 2004).

Figure 1.2

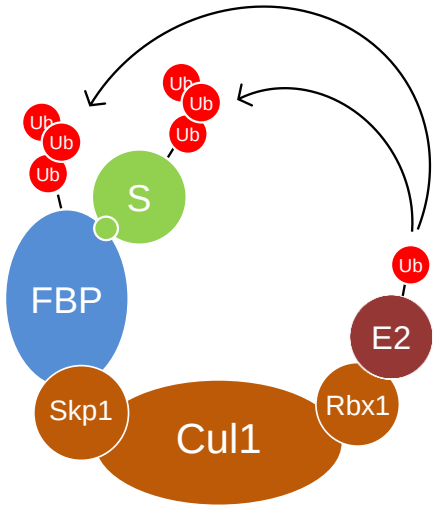

Figure 1.2. Schematic model for ubiquitination by SCF E3 ligases.

SCF complex consists of Skp1, Cul1, Rbx1 with a F-box protein. Rbx1 recruits E2 enzymes, while Skp1 binds to the F-box protein that recognizes substrates. Cul1 serves as a scaffold protein to link Skp1 and Rbx1 and brings E2 enzymes close to the substrates. The F-box proteins also undergoes self-ubiquitination.

F-box proteins contain the F-box domain of approximately 50 amino acids that functions as a Skp1 binding site. For substrate recognition, the F-box proteins interact with substrates via its C-terminal protein binding domains, which can be subdivided into three categories: WD40 repeats, leucine-rich repeats (LRR) and other domains. The WD40 repeat is a structural motif containing about 40 amino acids and typically 4-16 repeats are assembled together to form a circular β-propeller structure (Li and Roberts, 2001). A LRR consists of repeating 20-30 amino acid stretches that form an α/β horseshoe fold. Many of such repeats form a LRR domain in a horseshoe shape (Kobe and Kajava, 2001). The phosphorylation on specific epitopes (phospho-degrons) in substrates are required for the recognition by the F-box proteins (Kipreos and Pagano, 2000). F-box proteins are also known to be self-ubiquitinated and degraded, which was suggested to be necessary for rapid switching among different SCF complexes during cell cycle progression, which allows cells to rapidly adapt to physiological condition alterations (Galan and Peter, 1999). Moreover, it has been observed that F-box proteins form dimers and dimerization is required for their activities (Skaar *et al.*, 2013).

In addition to catalyzing substrate ubiquitination, some of E3 ligases are self-ubiquitinated, resulting in proteolytic or non-proteolytic regulation. Self-ubiquitination can lead to auto-catalyzed proteasomal degradation of ligases such as Mdm2, CBL ligases and the substrate adaptors of some SCF ligases (Fang *et al.*, 2000; Ryan *et al.*, 2006). Besides, the ubiquitination of E3 ligases like TRAF6 (TNF receptor-associated factor 6) and Diap1 (Drosophila melanogaster inhibitor of apoptosis 1) is mediated by other E3 ligases (Herman-Bachinsky *et al.*, 2007; Zaaroor-Regev *et al.*, 2010).

E3 ligases self-ubiquitination has also been reported to modulate their activities and substrate recruitment. The self-ubiquitination of RING1B ligase enhances its activity, but do not target RING1B for degradation (Ben-Saadon *et al.*, 2006). Auto-ubiquitinated BRCA1 (breast cancer 1) also have enhanced activity in substrate ubiquitination (Mallery *et al.*, 2002). In contrast, Diap1 ubiquitinates itself with K63-linked chains that inhibit its activity, potentially via preventing efficient binding to substrates (Herman-Bachinsky *et al.*, 2007). The auto-ubiquitination of Nrdp1 (neuregulin receptor degradation pathway protein 1) and Mdm2 targets themselves for proteolytic degradation, thereby resulting in stabilization of their substrates (Fang *et al.*, 2000; Honda and Yasuda, 1999; Wu *et al.*, 2004). In addition, the ubiquitin

attracted to some E3 ligases like TRAF6 and NEDD4 (neural precursor cell-expressed developmentally downregulated 4), functions to recruit substrates with ubiquitin binding properties (Baud *et al.*, 1999; de Bie and Ciechanover, 2011; Woelk *et al.*, 2006; Yin *et al.*, 2009).

Auto-ubiquitination also correlates with the ability to dimerize. The self-ubiquitinated RING ligases SIAH1 (seven in absentia 1) (Hu and Fearon, 1999), TRAF6, and the F-box protein Fbw7 and its *S.cerevisiae* ortholog Cdc4 are found to form dimers. The dimerization of TRAF6 is required for its auto-ubiquitination (Yin *et al.*, 2009). Conversely, dimer-deficient Fbw7 and Cdc4 variants show high levels of self-ubiquitination and the dimers exhibit stronger activity in substrate ubiquitination (Min *et al.*, 2012; Tang *et al.*, 2007; Welcker *et al.*, 2013). In contrast, the auto-ubiquitination of RNF144 requires its self-association that promotes its activity in substrate ubiquitination (Ho *et al.*, 2015).

1.1.3 Role of F-box protein β-TrCP in regulating cellular processes

β-TrCP (β-transducin repeat containing protein) is one of the well-studied F-box proteins and is highly conserved in multiple species. β-TrCP belongs to the family of Fbw (F-box/WD40 repeat containing) proteins which are featured by containing the N-terminal F-box domain that recruits Skp1-Cul1-Rbx1 complex, and seven WD40 repeats at the C-terminus that binds to substrates (Fuchs *et al.*, 2004). β-TrCP also contains a conserved D domain at the N-terminus that mediates dimerization (Fig 1.3) (Suzuki *et al.*, 2000). Mammalian cells encode two paralogues, β-TrCP1 and β-TrCP2 proteins that are highly homologous. The differences in sequences between β-TrCP1 and β-TrCP2 encoding genes are most remarkable in the N-terminal parts neighbouring the F-box domain. These two paralogues are equivalent in many functions and might be redundant in biological roles (Fuchs *et al.*, 2004). It has been shown that mice lacking β-TrCP1 develop normally with only minor defects in spermatogenesis, since β-TrCP2 might compensate for β-TrCP1 loss (Guardavaccaro *et al.*, 2003; Nakayama *et al.*, 2003). Indeed, β-TrCP1 and β-TrCP2 are redundant in mediating degradation of IκB and β-catenin, while Emi1 is a target of β-TrCP1/β-TrCP2 heterodimers (Guardavaccaro *et al.*, 2003). Thus, in this study we refer to the two paralogues below as β-TrCP unless specifically indicated.

Figure 1.3

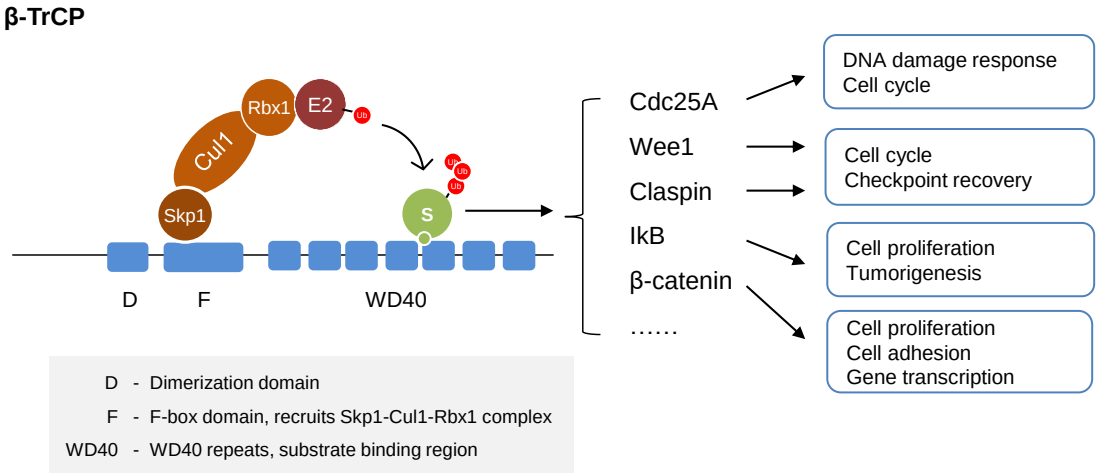

Figure 1.3. Schematic structure of β-TrCP.

β-TrCP contains the D domain for dimerization and the F-box domain for Skp1-Cul1-Rbx1 complex recruitment at the N-terminus. The C-terminus of β-TrCP is the substrate binding region with WD40 repeats. β-TrCP regulates various cellular processes via mediating the ubiquitination and degradation of a wide range of substrates.

β-TrCP recognizes a wide range of substrates for degradation and thereby regulates various cellular processes. The characteristics of β-TrCP substrates contain the $DSG(X)_{2+n}S$ motifs (DSGXXS or its variants, *e.g.*, DSG/DDG/EEG/SSGXXS/E/D) with serine residues phosphorylated by various kinases (Frescas and Pagano, 2008).

NFκB (nuclear factor kappa-light-chain-enhancer of activated B cells) is an inducible transcription factor that is involved in multiple cell progresses such as immune response and tumor development. The NFκB signaling pathway is modulated by β-TrCP via targeting IκB, the inhibitory protein of NFκB (Hattori *et al.*, 1999). β-TrCP is also shown to colocalize in the nucleus with the transcription factor Atf4 (activating transcription factor 4) to mediate its degradation (Lassot *et al.*, 2001).

Additionally, β-TrCP plays roles in cell adhesion and migration through its substrate β-catenin, a critical mediator of Wnt signaling that regulates cell proliferation and cell fate determination (Hart *et al.*, 1999; Winston *et al.*, 1999). The polycomb group protein Bmi1 is crucial for cellular homeostasis via regulating cell proliferation and senescence. Phosphorylated Bmi1 is targeted by β-TrCP for

ubiquitination and degradation (Banerjee Mustafi *et al*., 2017). Bim (Bcl-2 Interacting Mediator of cell death) belongs to the Bcl-2 protein family and activates proapoptotic Bak and Bax upon stress. β-TrCP targets Bim-extra long (BimEL) for destruction after phosphorylation by Rsk1/2 (ribosomal S6 kinase 1/2) and Erk1/2 (extracellular-signal-regulated kinases 1/2) to promote cell survival (Dehan *et al.*, 2009).

Cell cycle progression is regulated by β-TrCP via targeting multiple cell cycle regulators for ubiquitination and degradation. As an early mitotic inhibitor 1, Emi1 degradation mediated by β-TrCP results in the destruction of Cyclin B and mitotic exit (Margottin-Goguet *et al.*, 2003). Wee1 is a nuclear kinase that phosphorylates Cdk1 (cyclin-dependent kinase 1) at tyrosine 15 and thereby inactivates Cdk1-Cyclin B1 complex to inhibit the mitotic entry. β-TrCP-dependent Wee1 degradation is required for the rapid activation of Cdk1 at the onset of mitosis (Watanabe *et al.*, 2004). In addition, Wee1-dependent phosphorylation of Cdk2 is necessary for replication fork progression (Dominguez-Kelly *et al.*, 2011; Hughes *et al.*, 2013). Therefore, β-TrCP is critically involved in determining the timing of the mitotic onset via mediating Emi1 and Wee1 degradation. Moreover, β-TrCP ubiquitinates and thereby stabilizes Myc, a protein that stimulates exit from quiescence and elicits progression through G1 phase. Myc ubiquitination by β-TrCP is required for Myc-dependent acceleration of cell cycle progression in S and G2 phase (Popov *et al.*, 2010).

Another well-established β-TrCP substrate for cell cycle regulation is Cdc25A (cell division cycle 25A), a phosphatase which activates Cdks by mediating their dephosphorylation during S phase and DNA damage response. β-TrCP recognizes Cdc25A after phosphorylation by the checkpoint kinases Chk1 and Chk2 which are activated by DNA damage or stalled DNA replication. Cdc25A destruction by β-TrCP promotes the accumulation of inactive phosphorylated Cdk2, thereby inhibits DNA replication (Busino *et al.*, 2003; Jin *et al.*, 2003).

The p53 inhibitor Mdm2 is phosphorylated by CK1δ (Casein Kinase 1 delta) and ATM kinases that are activated by DNA damage, and is subsequently recognized and degraded by β-TrCP, which results in p53 activation (Wang *et al.*, 2012). β-TrCP substrate Bmi1 is required for ubiquitination of histone H2A induced by DNA damage (Ginjala *et al.*, 2011; Nacerddine *et al.*, 2012). During cell recovery from a checkpoint response in G2 phase, the destruction of Claspin mediated by β-TrCP prevents further activation of Chk1 (Freire *et al.*, 2006). Thus, β-TrCP plays a prominent role in regulating DNA damage response and checkpoint recovery (Fig 1.4).

Figure 1.4

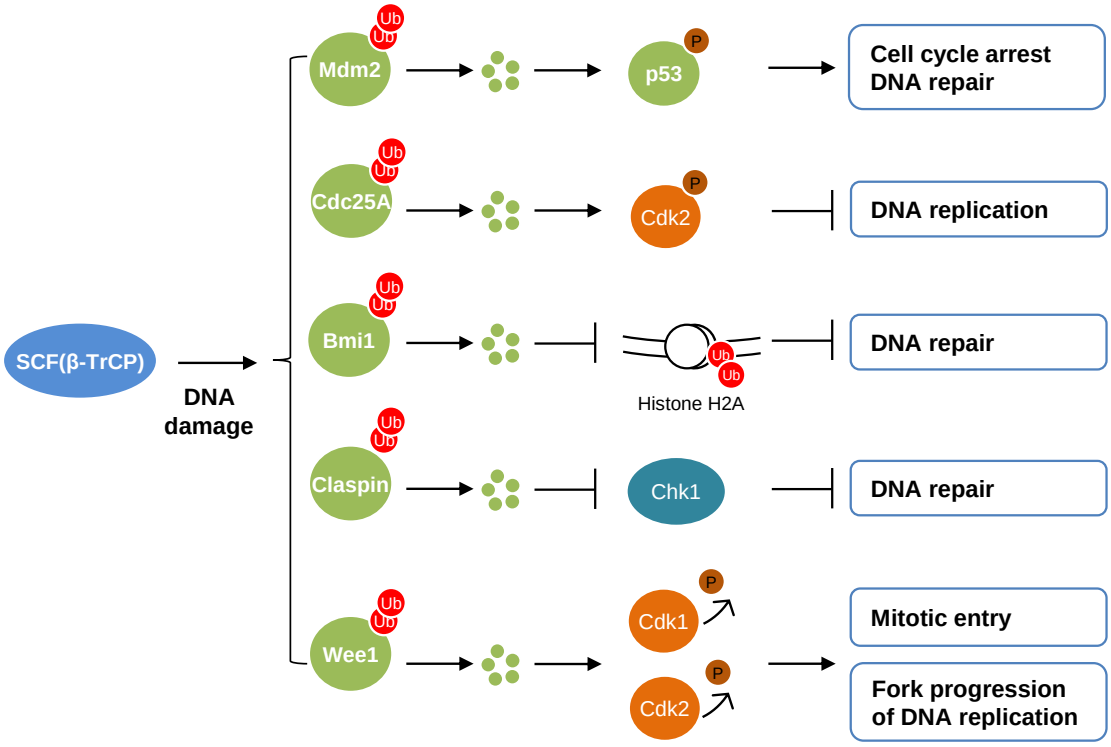

Figure 1.4. β-TrCP-mediated substrate degradation regulates DNA damage response.

Upon DNA damage, Mdm2 is degraded by β-TrCP, which promotes the activation of p53 pathway for DNA repair. β-TrCP-mediated degradation of Cdc25A leads to accumulation of pCdk2 and inhibition of DNA replication. Bmi1 is necessary for DNA damage-induced ubiquitination of histone H2A which recruits DNA repair factors.

During checkpoint recovery, Claspin degradation by β-TrCP inhibits further activation of Chk1. β-TrCP-mediated Wee1 destruction suppresses the phosphorylation of Cdk1 and Cdk2, which promote mitotic entry and fork progression of replication, respectively.

The activity of β-TrCP is regulated by multiple mechanisms. Phosphorylation of distinct substrates is mediated by different kinases. Since β-TrCP recognizes the phosphorylated degrons of substrates, the activities of corresponding kinases affect the substrate binding to β-TrCP. The upregulation of one phosphorylated substrate can compete with another substrate for the availability of β-TrCP (Fuchs *et al.*, 2004). The competition participants can also be pseudosubstrates that are bound but not degraded by β-TrCP, such as hnRNP-U (Davis *et al.*, 2002) and LMP1 (Tang *et al.*, 2003). In addition, the abundance of β-TrCP plays a crucial role in the regulation of SCF(β-TrCP) ligase activity, as its substrate degradation can be easily interfered by

regulating the exogenous and ectopic expression of β-TrCP (Fuchs *et al.*, 1999; Guardavaccaro *et al.*, 2003) and its dominant-negative constructs (Deshaies, 1999; Sharma *et al.*, 2015). Moreover, the self-ubiquitination and stability of β-TrCP is shown to be regulated by a bound substrate, which affect SCF(β-TrCP) ligase activity (Li *et al.*, 2004). As a D domain-contained F-box protein, β-TrCP forms dimer that promotes IκB ubiquitination (Suzuki *et al.*, 2000), consistent with the enhanced activity of dimeric F-box proteins Cdc4 and Fbw7 (Tang *et al.*, 2007; Welcker *et al.*, 2013). However, the role of β-TrCP dimerization in regulating the degradation of most substrates remains unclear.

1.1.4 Ubiquitination is counterbalanced by deubiquitinases (DUBs)

Ubiquitination is a reversible modification and can be antagonized by the deubiquitinases (DUBs), which are a large group of proteases that cleave ubiquitin off the substrate proteins (Fig 1.1). Free polyubiquitin chains can be cleaved by DUBs into monoubiquitins, while substrate-attached polyubiquitin chains can be entirely removed for recycling. DUBs can also cleave ubiquitin from the distal end of polyubiquitin chains (chain trimming) (Reyes-Turcu *et al.*, 2009).

DUBs can be subdivided into five groups according to the catalytic domain: ubiquitin-specific proteases (USPs), ubiquitin C-terminal hydrolases (UCHs), ovarian tumour proteases (OTUs), Josephins and JAB1/MPN/MOV34 metalloenzymes (JAMMs). The JAMM family members are zinc metalloproteases, while the other four families are cysteine proteases (Komander *et al.*, 2009).

Among the five families of DUBs, the USPs family is the largest one with more than 50 members. A large number of USPs are reported to associate with WD40 repeat proteins, including Usp28 (Villamil *et al.*, 2013). Our previous study showed that Usp28 deubiquitinates and stabilizes Fbw7 and results in dual regulation on Fbw7 substrates (*e.g.*, Myc, Jun, and HIF1a) (Schulein-Volk *et al.*, 2014). At low levels, Usp28 preferentially deubiquitinates Fbw7 and maintains it to promote Fbw7 substrate degradation, while the complete loss of Usp28 induces ubiquitination and destruction of Fbw7, which leads to the stabilization of Fbw7 substrates. Usp28 is also known to be phosphorylated on Ser67 and Ser714 by ATM or ATR upon DNA damage and to regulate multiple proteins in the DNA damage response pathways

(*e.g.*, 53BP1, Chk2, Claspin), which requires its catalytic activity (see 1.3) (Bassermann *et al.*, 2008; Zhang *et al.*, 2006).

1.2 Regulation of DNA damage response by the ubiquitin system

1.2.1 Overview of DNA damage response

DNA damage refers to structure alterations in DNA, which result from either cellular metabolic processes or environmental factors. During cell progresses, alkylation, oxidation, hydrolysis, and mismatch of DNA bases can induce DNA damage. Exogenous DNA damage can be generated by ionizing radiation (IR), ultraviolet (UV) radiation, Hypoxia and chemicals agents. The consequences of DNA damage include chromosomal abnormality, disruption of DNA replication and transcription. DNA double-strand breaks (DSBs) are the most destructive form of DNA damage, which can be induced by IR and chemicals like phleomycin, as well as by endogenous damage such as replication errors (Raynard *et al.*, 2008).

To preserve the genome integrity, DNA damage response (DDR) has evolved to repair DNA and prevent the transmission of abnormal DNA to daughter cells (Ciccia and Elledge, 2010; Hoeijmakers, 2001). DDR is a network of pathways that sense and transduce DNA damage signal to induce cell cycle arrest, inhibit DNA replication and transcription and promote DNA repair. Unrepaired DNA lesions results in genomic instability, cell apoptosis or senescence and thereby cause human diseases such as immunodeficiency and cancer (Hakem, 2008).

There are two major pathways to repair DSBs: homologous recombination and non-homologous end joining (NHEJ). Homologous recombination requires identical or very similar molecules of DNA elsewhere in the genome to exchange nucleotide sequences at the break sites, while NHEJ directly ligates the break ends of DNA without the need for a homologous template. The choice of DNA repair pathways is strictly regulated during distinct cell cycle phases (Chapman *et al.*, 2012). When DSBs occur before DNA replication, the first line of repair is usually NHEJ which occurs in a quick and robust manner. When DSBs arise during S phase or after DNA replication in G2 phase, DNA can be repaired by homologous recombination that

requires homologous DNA sequences and single-strand DNA (ssDNA) ends generated during DSB resection (Marechal and Zou, 2013).

Upon DSBs, phosphorylation of histone H2AX at the damage sites is required for formation of IR-induced foci (IRIF), recruitment of numerous DNA repair proteins and chromatin-remodeling complexes to DSBs sites. The mediator of DNA damage checkpoint protein 1 (Mdc1) directly binds to phosphorylated H2AX and interacts with ataxia–telangiectasia mutated (ATM). The accumulation of Mre11-Rad50-Nbs1 (MRN) mediator complex to the IRIF is required for ATM rapid localization and activation at the break sites. ATM, together with ATR (ATM and Rad3 related) and DNA-dependent protein kinase (DNA-PK) are the most upstream kinases activated during DDR and belong to the family of phosphoinositide-3-kinase-related kinases (PIKKs). Active ATM, ATR and DNA-PK at the DNA DSB sites phosphorylate multiple targets that recruit crucial DDR effector proteins, including 53BP1, BRCA1, E3 ligases RNF8 (RING finger protein 8) and RNF168, that all promote DNA repair (Hakem, 2008; Panier and Boulton, 2014).

1.2.2 The ATM and ATR signaling in DDR

The ATM signaling is primarily activated by DSBs, while ATR signaling is elicited by a broad spectrum of DNA damage events, including DSBs and various DNA lesions that disrupt replication. The generation of ssDNA during DSB resection enables ATR activation upon DSBs.

In response to DNA damage, activated ATM and ATR phosphorylate hundreds of proteins to regulate cellular response, including Chk2 and Chk1. The activation of Chk2 and Chk1 induce phosphorylation of Cdc25A at multiple sites and subsequent proteasomal degradation by the SCF(β-TrCP) ligase. The destruction of Cdc25A leads to DNA replication blockage through inefficient loading of Cdc45 to the putative replication origins (Falck *et al.*, 2002).

Another essential player for DDR is p53 transcription factor. The activated ATM, ATR, DNA–PK, Chk2, and Chk1 all promote p53 phosphorylation and activation, whereas Chk2-p53 connection is better understood. p53 is stimulated to bind DNA and to mediate transcriptional activation of its responsive genes. As a target of p53, the inhibitor of Cdks, p21 is transactivated, resulting in inhibition of Cdks and

consequent cell cycle arrest. In addition, unsuccessful DNA repair induces p53-dependent apoptosis and senescence (Harper and Elledge, 2007).

It has been suggested that the Cdc25A signaling and p53 signaling act as a two-wave model for the G1/S checkpoint. Upon DNA damage, the ATR/ATM-Chk1/2-Cdc25A pathway is rapidly activated to initiate G1/S transition arrest, while the cell cycle arrest mediated by p53 signaling occurs later for arrest maintenance (Bartek and Lukas, 2001).

1.2.3 Inhibition of DNA replication in DDR

DNA replication is the cellular process that generates two identical DNA replicas from one original DNA molecule, which occurs during S phase of cell cycle. To ensure the genome integrity in response to DNA damage, DNA replication is slowed down via regulating origin firing and replication fork progression to allow DNA repair (Iyer and Rhind, 2017).

Origin firing is the activation step of DNA replication that occurs at the replication origins where DNA is opened up and unwound to allow DNA synthesis machinery loading. First, during G1 phase of cell cycle, the origin recognition complex (Orc) binds to the origins and sequentially recruits Cdc6, Cdt1, minichromosome maintenance (Mcm) proteins (Mcm2-7) in an inactive state to form pre-replicative complexes (pre-RCs) (origin licensing). Then at the G1/S transition, Cdc7 and Cdk2 phosphorylate Mcm2 and Cdc45, respectively, which facilitate the loading of Cdc45 to the pre-RCs to form pre-initiation complexes (pre-ICs) at the origins. The pre-ICs formation results in origin unwinding to initiate DNA replication (origin firing) (Fragkos *et al.*, 2015; Walter and Newport, 2000). Subsequently, two replication forks as Y shape are established at each fired origin and they recruit DNA polymerases (Pol) to replicate the lagging and leading DNA strands (replication fork progression) (Fig 1.5) (Jones and Petermann, 2012).

The reduced replication in response to DNA damage can result from inhibition of origin firing or slowing replication fork progression (Willis and Rhind, 2009). Nevertheless, it has been shown that DNA damage slows replication via suppressing origin firing, not via reducing fork progression rate (Hughes *et al.*, 2013; Iyer and Rhind, 2017; Merrick *et al.*, 2004).

Figure 1.5

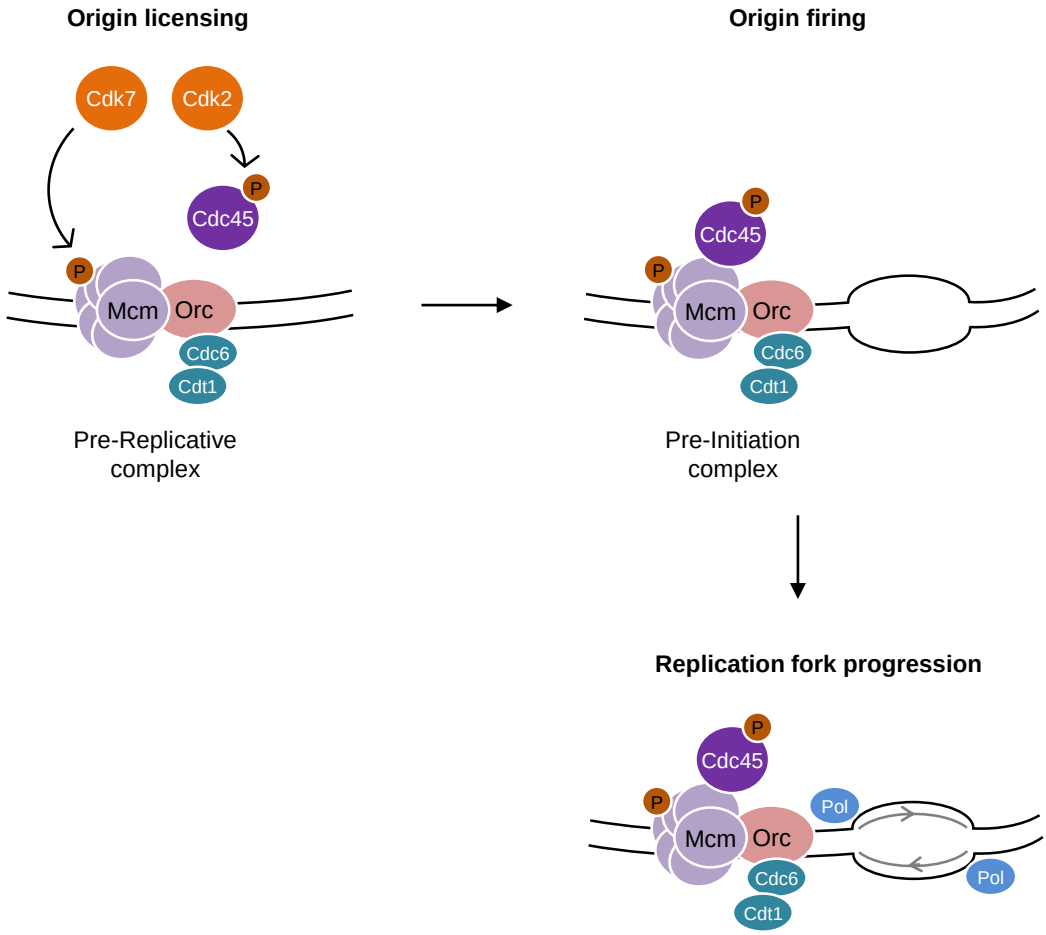

Figure 1.5. Overview of DNA replication.

During G1 phase, Orc binds to the origin sites and sequentially recruits Cdc6, Cdt1 and Mcm2-7 proteins to form pre-RCs (origin licensing). At the G1/S transition, pre-RCs are activated by Mcm2 and Cdc45 phosphorylation mediated by Cdc7 and Cdk2, respectively. This facilitates the loading of Cdc45 to pre-RCs to form pre-ICs at the origins and thereby results in origin unwinding (origin firing). At each fired origin, two replication forks as Y shape are established and DNA polymerases (Pol) are recruited to replicate the lagging and leading DNA strands (replication fork progression).

The pathways currently known for inhibition of DNA replication upon DSBs are the Cdc25A-Cdk2 and the Nbs1-BRCA1-Smc1 pathways. It has been revealed that ATM-mediated phosphorylation of Nbs1 (Nijmegen breakage syndrome protein 1), BRCA1 (Breast Cancer protein 1), BRCA2/FANCD1 (Fanconi anemia protein D1) and FANCD2 is involved in DNA damage-induced inhibition of DNA replication. The blockage of these phosphorylation events leads to radio-resistant DNA synthesis.

Moreover, the cohesin protein Smc1 (structural maintenance of chromosomes 1) is recruited to the damage sites in a phospho-NBS1- and phospho-BRCA1-dependent manner. Nbs1-, BRCA1- and Smc1-mediated homologous recombination of damaged-DNA blocks the replication fork (Andreassen *et al.*, 2006).

The Cdc25A-Cdk2 pathway for DNA replication blockade is the better investigated mechanism that inhibits origin firing upon DNA damage. As described previously, DNA damage activates ATM and ATR to phosphorylate and activate Chk2 and Chk1, resulting in phosphorylation of Cdc25A and subsequent Cdc25A degradation by the SCF(β-TrCP) ligase. As a target of Cdc25A, the inactive phosphorylated Cdk2 accumulates and inhibits Cdc45 loading at the origins of DNA replication, results in suppression of replication initiation (Fig 1.6) (Falck *et al.*, 2001; Falck *et al.*, 2002).

Figure 1.6

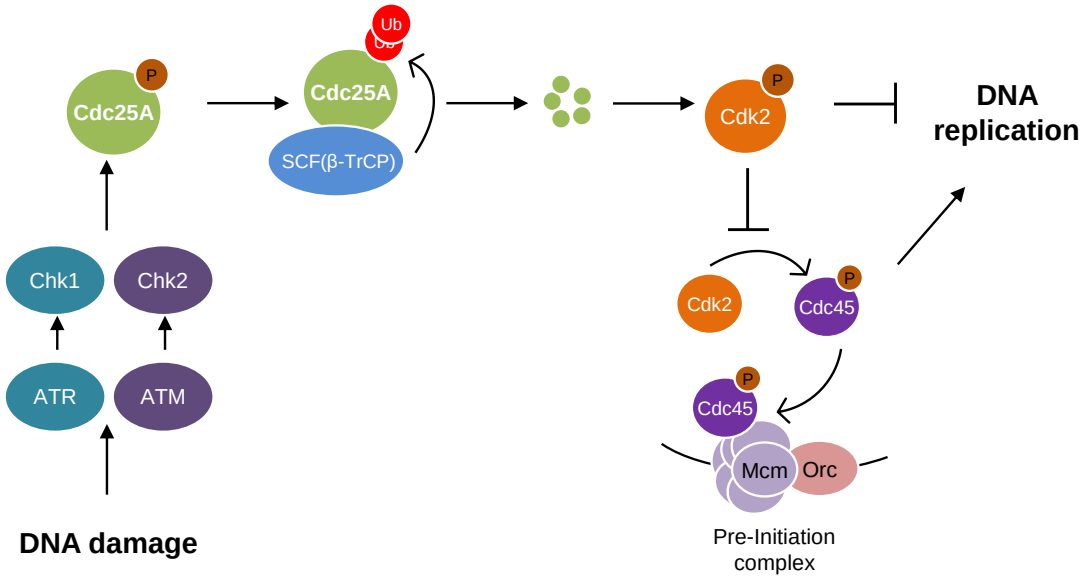

Figure 1.6. DNA damage inhibits DNA replication initiation via Cdc25A-Cdk2 pathway.

DNA damage induces activation of ATR and ATM kinases, which phosphorylate and activate Chk1 and Chk2. Cdc25A is subsequently phosphorylated by activated Chk1 and Chk2, and is degraded by the SCF(β-TrCP) ligase, resulting in accumulation of inactive phosphorylated Cdk2. A critical step of DNA replication initiation is the Cdk2-dependent loading of Cdc45 to pre-RCs to form pre-ICs. Inactive Cdk2 inhibits the formation of pre-ICs and thereby suppresses initiation of DNA replication.

On the other hand, phosphorylated Cdk2 is required for normal replication fork progression and cell recovery from replication stress (Hughes *et al.*, 2013). Cdk2 can

be phosphorylated by Wee1 to inhibit entry into S-phase, and Wee1 deletion results in decrease in the rate of replication fork (Chen and Gardner, 2004; Dominguez-Kelly *et al.*, 2011; Watanabe *et al.*, 1995; Wu *et al.*, 2001).

1.2.4 53BP1, a key DNA repair factor

p53-binding protein 1 (53BP1) is a key mediator protein of DSBs signaling. Upon DSBs, 53BP1 is rapidly recruited to the chromatin surrounding the break sites via binding to histone H2A ubiquitinated on Lys13/15 (H2AK13/15ub) and dimethylated histone H4K20 (H4K20me2). Subsequently, 53BP1 recruits additional factors to the DNA break sites to facilitate DNA repair. The interaction between 53BP1 and chromatin at the break sites promotes NHEJ-mediated DSB repair (Panier *et al.*, 2014; Zimmermann and de Lange, 2014).

53BP1 is a large protein of 1972 amino acids and contains multiple domains (Fig 1.7). Its N-terminus consists of 28 Ser/Thr-Gln (S/T-Q) sites that are targets of ATM and recruit PTIP (PAX transactivation activation domain-interacting protein) and RIF1 (RAP1-interacting factor 1) in an ATM-dependent manner. The minimal focus-forming region (FFR) is required for recruitment of 53BP1 to damaged chromatin by multiple histone marks. FFR consists of the oligomerization domain (OD), the Gly- and Arg-rich (GAR) motif, the tandem Tudor motif that interacts with histone H4K20me2, and the ubiquitination-dependent recruitment (UDR) motif that binds to H2AK15ub. The C-terminal BRCT (BRCA1 carboxy-terminal) domain of 53BP1 mediates the interaction with p53 and the chromatin modulator EXPAND1 (Panier *et al.*, 2014). In addition, 53BP1 BRCT domain interacts with the MRN complex, which recruits ATM to the damage sites, to stimulate the activity of ATM. BRCT domain of 53BP1 also contributes to the self-interaction of 53BP1. 53BP1 variant with BRCT domain-deleted shows deficiency in DNA repair (Lee *et al.*, 2010). On the other hand, there is also evidence that the BRCT domain is dispensable for the repair function of 53BP1 (Ward *et al.*, 2006).

Figure 1.7

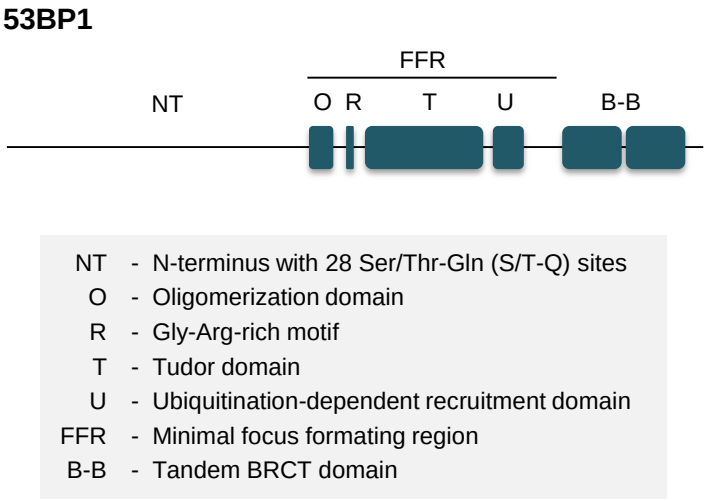

Figure 1.7. Schematic structure of 53BP1.

The N-terminus of 53BP1 contains 28 Ser/Thr-Gln (S/T-Q) sites that are targets of ATM. As the minimal region for efficient 53BP1 focus formation, the minimal focus-forming region (FFR) is composed of the oligomerization domain, the Gly-Arg-rich motif, the Tudor domain and ubiquitination-dependent recruitment domain. The C-terminus of 53BP1 contains the BRCT domain that mediates the interaction with p53, EXPAND1 and MRN complex.

The oligomerization domain of 53BP1 with the primary function to form oligomers, is shown to partially contribute to chromatin binding and promote NHEJ (Bothmer *et al.*, 2011; Zgheib *et al.*, 2009). However, the 53BP1 variant lacking OD is sufficient to mediate NHEJ at dysfunctional telomeres (Lottersberger *et al.*, 2013). Thus, the precise role of 53BP1 oligomerization in DDR remains to be studied.

It has been reported that the cellular levels of 53BP1 affect DNA damage repair. 53BP1 plays a dominant role in DNA repair choice and promotes NHEJ (Bouwman *et al.*, 2010; Bunting *et al.*, 2010). The degradation of 53BP1 in a UbcH7-dependent manner is required for DSB end resection and homologous recombination (Han *et al.*, 2014). In contrast, increasing 53BP1 levels promotes mutagenic NHEJ, resulting in an enhanced sensitivity to DNA damage (Han *et al.*, 2014; Zong *et al.*, 2015). 53BP1 has also been shown to regulate NHEJ in a RNF8- and RNF168-dependent manner. The deletion of RNF8 or RNF168 suppresses 53BP1 degradation in the nucleoplasm induced by IR, while DSB sites-bound 53BP1 is protected from destruction. IR-induced 53BP1 destruction is required for its recruitment of RIF1 that cooperates with

53BP1 to block DSB resection in G1 phase (Hu *et al.*, 2014). RNF168 mediated ubiquitination of 53BP1 with K63-linked chains is necessary for the initial recruitment of 53BP1 to DSB sites and its functions in DNA repair (Bohgaki *et al.*, 2013). TIRR (Tudor-interacting repair regulator) has been demonstrated to form complexes with 53BP1 that are required for 53BP1 stability. Upon DNA damage, the 53BP1-TIRR complex dissociates, which allows 53BP1 recruitment to DNA damage sites (Drane *et al.*, 2017; Zhang *et al.*, 2017). Additionally, a recent study demonstrated that DNA damage disrupts the interaction between 53BP1 and the nuclear structural protein Lamin A/C, which allows 53BP1 destruction in soluble nucleoplasmic fractions, but not on chromatin (Mayca Pozo *et al.*, 2017). The functions of 53BP1 destruction in the nucleoplasm in response to DNA damage remain to be investigated.

1.3 Ubiquitin system in DDR

Since many of the DDR proteins are enzymes that catalyze ubiquitination or proteins containing ubiquitin binding domains (UBDs), the ubiquitin system plays a critical regulatory role in DNA repair in both proteolytic and non-proteolytic manner.

1.3.1 Ubiquitination in DDR

Upon DNA DSBs, histone variant H2AX is phosphorylated at the break sites and recruits the adaptor protein Mdc1, followed by phosphorylation of Mdc1 by ATM. The phosphorylated Mdc1 is recognized by the RING domain of RNF8. RNF8 cooperates with the E2 enzyme Ubc13 to assemble K63 chains on histone H2AX. The ubiquitin chains on H2AX bind to RAP80 (receptor-associated protein 80), which recruits the Abraxas-BRCA1 complex. BRCA1 regulates the DNA damage checkpoint and DNA repair via promoting homologous recombination. RNF168 is also recruited to DSB sites in a RNF8-dependent manner and ubiquitinates histone H2A at K13/K15. In addition, RNF8 and RNF168 induce the proteasomal degradation of the polycomb protein L3MBTL1 and the demethylase Jumonji domain-containing protein 2A (JMJD2A), exposing dimethylated histone H4K20. The histone H2AK13/15ub and H4K20me2 recruit 53BP1 for DNA repair (Natarajan and Takeda, 2017). RNF8 and RNF168 are also shown to regulate degradation of nucleoplasmic 53BP1 to ensure 53BP1 functions in DSB repair (Hu *et al.*, 2014). The E3 ligases TRIP12 and UBR5

target RNF168 for degradation to prevent excessive spreading of histone ubiquitination from the DSB sites (Fig 1.8) (Gudjonsson *et al.*, 2012).

Figure 1.8

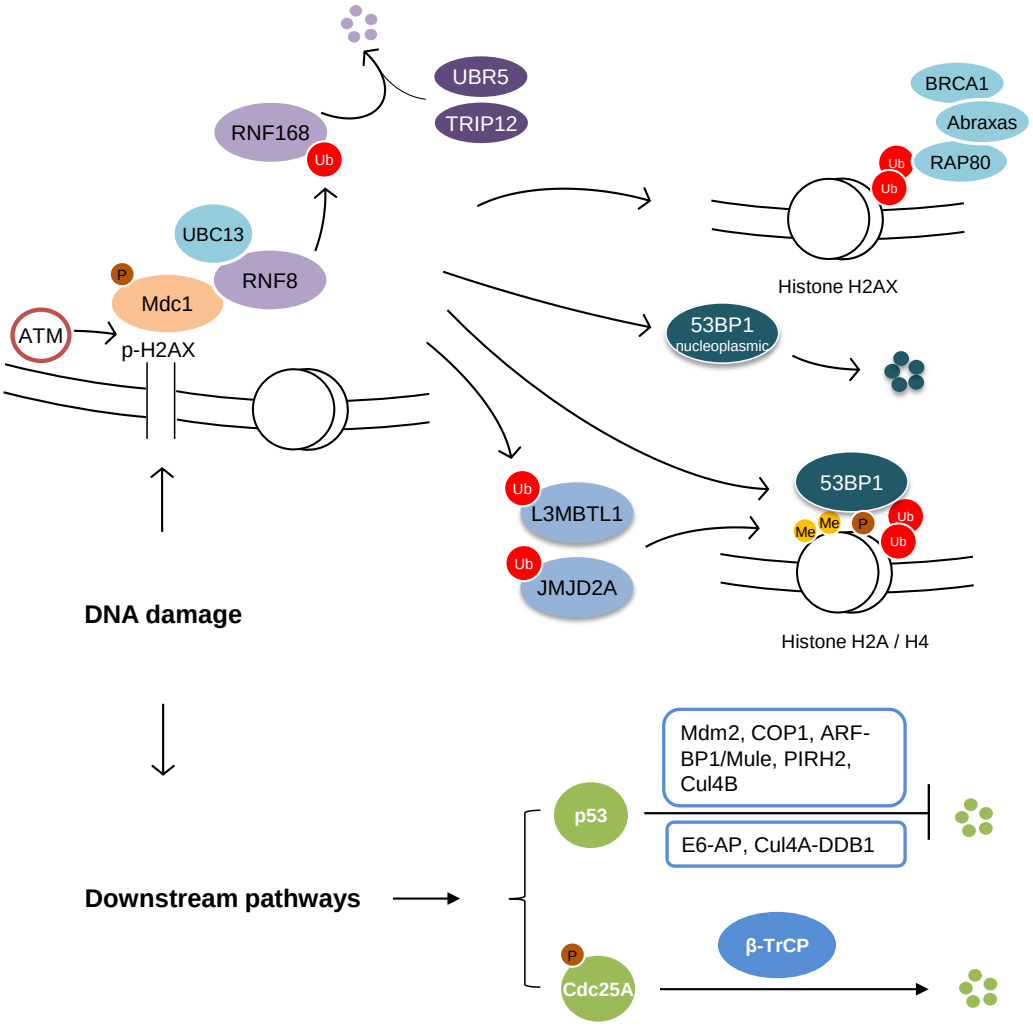

Figure 1.8. Ubiquitination in DDR.

DNA damage stimulates phosphorylation of histone H2AX which recruits Mdc1. Mdc1 is then phosphorylated by ATM and recognized by RNF8 that ubiquitinates RNF168. RNF8 and RNF168 promotes the ubiquitination of histone H2AX which recruits RAD80-Abraxas-BRCA1 complex to regulate DNA repair. Additionally, RNF168 ubiquitinates histone H2A at K13/15, while RNF168 and RNF8 mediates the degradation of L3MBTL1 and JMJD2A to expose dimethylated histone H4K20. The histone H2AK13/15ub and H4K20me2 recruit 53BP1 for DNA repair. The stability of 53BP1 is controlled by RNF8 and RNF168. Conversely, TRIP12 and UBR5 target RNF168 for degradation to prevent excessive histone ubiquitination. The downstream pathways of DDR- p53 pathway and Cdc25A pathway, are also regulated by ubiquitination. p53 is stabilized via inhibition of multiple E3 ligases upon DNA damage. Cdc25A is phosphorylated in response to DNA damage and targeted for degradation by β-TrCP.

Downstream of checkpoint kinases, the p53 signaling and Cdc25A signaling, as well as checkpoint recovery, are also regulated by the ubiquitin system. The stability of p53 has been shown to be regulated by several E3 ligases and DUBs. Mdm2 directly targets ATM/ATR-dependent phosphorylated p53 for proteasomal degradation. As a target of ATM, Mdm2 is phosphorylated and stabilized upon DNA damage, which induces accumulation of p53. p53 stability is also regulated by other E3 ligases including COP1, ARF-BP1/Mule, PIRH2, Cul4B, E6-AP and Cul4A-DDB1 (Fig 1.8) (Brinkmann *et al.*, 2015).

Upon genotoxic stress, Cdc25A is phosphorylated by Chk2 and Chk1, which are activated by ATM and ATR. The phosphorylation at S123 by Chk2 promotes Cdc25A degradation and inhibits Cdk2 activity, leading to blockage of DNA replication in response to DNA damage and controlling S-phase checkpoint (Falck *et al.*, 2001). It has also been reported that Chk1 phosphorylates multiple residues on Cdc25A and phosphorylation at S76 is essential for its further phosphorylation at S79 and S82 within the DSG motif. β-TrCP recognizes the casein kinase 1α (CK1α)-phosphorylated S82 of Cdc25A and mediates its ubiquitination and degradation (Honaker and Piwnica-Worms, 2010). Additionally, p53 activation upon DNA damage downregulates Cdc25A mRNA and protein levels (Fig 1.8) (Rother *et al.*, 2007).

DNA damage induces the activation of kinases (*e.g.*, CK1α) to stimulate phosphorylation and subsequent degradation of multiple β-TrCP substrates (*e.g.*, CReP and Set8) besides Cdc25A, resulting in regulation of biological functions (Loveless *et al.*, 2015). Mdm2 is targeted by β-TrCP for ubiquitination and destruction upon DNA damage (Inuzuka *et al.*, 2010). During cell recovery, β-TrCP-mediated degradation of Claspin prevents further activation of Chk1 during G2/M phase, while Wee1 destruction restores the activities of Cdk1 and Cdk2 for mitotic entry and replication fork progression (Fig 1.4) (Freire *et al.*, 2006).

1.3.2 Deubiquitination in DDR

As the reverse process of ubiquitination, deubiquitination by DUBs is involved in all DDR pathways to regulate cellular response (Table 1). The DUBs Brcc36, Usp3, Poh1 and Usp44 have been reported to antagonize histone ubiquitination, which thereby interfere with the recruitment of 53BP1 and other repair factors at the damage sites. Usp34 and Otub1 modulate RNF168 levels and the activity of Ubc13-

RNF168 complex (Citterio, 2015). The histone ubiquitination induced by DNA damage is negatively regulated by Usp16 and Usp3 (Shanbhag *et al.*, 2010; Sharma *et al.*, 2014).

The regulation of p53 by DUBs is either via direct deubiquitination, or through modulation of its regulators or binding partners. Reported p53 DUBs include Usp7, Usp4, Usp2A, Usp10, Usp42, Usp29, Uch-L1, NOXA, Otubain 1, Usp9X, Usp18 and Usp28 (Hu *et al.*, 2014).

Usp28 has been shown to be phosphorylated by ATM or ATR and to be an ATM pathway effector upon IR. 53BP1 is stabilized by Usp28 in response to DNA damage, resulting in control of cellular response via ATM-Chk2-p53 pathway in human lung cancer NCI-H460 cells (Zhang *et al.*, 2006). Cuella-Martin *et al.* showed that 53BP1 and Usp28 cooperate to stimulate the transcription-regulating activities of p53 upon DNA damage (Cuella-Martin *et al.*, 2016). Interestingly, another report suggests that although Usp28 is recruited to DSBs sites in a 53BP1-dependent manner, Usp28 deletion has minor effect on 53BP1 stability and DNA damage response (Knobel *et al.*, 2014). The reasons underlying these conflicting results remain to be investigated. Independently of 53BP1, Usp28 controls the destruction of Myc oncoprotein in response to DNA damage via dissociation of Usp28 from Fbw7 (Popov *et al.*, 2007). Furthermore, Usp28 antagonizes Claspin destruction by APC/C, leading to Chk1 activation in response to DNA damage (Bassermann *et al.*, 2008).

Table 1

Dubs	Targets	Regulation
Brcc36, Usp3, Poh1, Usp44	Histones	Inhibit the recruitment of 53BP1 and other repair factors to the DNA damage sites
Usp16 Usp3	Histones	Counteract histone ubiquitination induced by DNA damage
Usp34 Otub1	RNF168	Stabilizes RNF168 Inhibits RNF168 activity
Usp7, Usp4, Usp2A, Usp10, Usp42, Usp29, Uch-L1,	p53, or its regulators and binding partners	Regulate p53 pathway in DDR

NOXA, Otubain 1, Usp9X, Usp18 and Usp28		
Usp28	53BP1 Myc Claspin	Has minor effects or controls DDR via ATM-Chk2-p53 pathway Promotes Myc degradation Activates Chk1

1.4 Objectives of the thesis

DNA damage occurs frequently during cell processes and cells are programmed to inhibit DNA replication to allow DNA repair. DNA repair is essential for genome integrity and stability. Therefore, it is important to understand how DNA damage induces blockade of DNA replication for repair. 53BP1 is a key regulator and mediator protein for DNA damage response and is known to interact with Usp28. However, the role of Usp28 on 53BP1 and cellular response upon DNA damage remains debatable.

In this thesis, a novel mechanism for rapid DNA replication suppression upon DNA damage is revealed, which involves 53BP1- and Usp28-dependent activation of the SCF(β-TrCP) ubiquitin ligase to regulate Cdc25A-Cdk2 pathway. Additionally, the dimerization of β-TrCP, which can be controlled by non-proteolytic ubiquitination and deubiquitination by Usp28, is established as a critical process for regulating β-TrCP activity in response to DNA damage. This might provide a novel mechanism for rapid SCF ubiquitin ligase activation upon DNA damage via deubiquitination and dimerization of the F-box proteins. It also gives a new insight into DNA damage-induced nucleoplasmic destruction of 53BP1 oligomers, which releases and activates β-TrCP.

2 Materials

Chemicals were purchased from Sigma-Aldrich, Roth, Invitrogen, Merck, Thermo Scientific, New England Biolabs (NEB). All reagents were prepared with ddH2O unless otherwise indicated.

2.1 Mammalian cell lines

Cell lines	Description
HeLa	Human cervix carcinoma cell line (ATCC)
HCT116	Human colon carcinoma cell line (ATCC)
U2OS	Human osteosarcoma cell line
KPC	Murine pancreatic cancer cell line
Phoenix	Second-generation retrovirus producer lines based on the 293T cell line
HEK293T	Human Embryo Kidney cell line (ATCC)
MEFs	Mouse embryonic fibroblasts immortalized by the expression of shRNA targeting p19ARF (Schulein-Volk *et al.*, 2014)

2.2 Bacterial strains

DH5α	NEB® 5-alpha Competent E. coli (High Efficiency) (C2987H)
	NEB® 5-alpha Subcloning efficiency (C2988J)

2.3 Cell culture medium and supplements

2.3.1 Medium and antibiotics for mammalian cell culture

HeLa, HCT116, U2OS, KPC, Phoenix, MEFs	DMEM full medium: DMEM with 4.5 g/L glucose, L-glutamine, sodium pyruvate, and sodium bicarbonate (Sigma). 10% (v/v) FBS (Invitrogen, inactivated for 30 min heating at 56°C before usage) 1% (v/v) Penicillin / Streptomycin (Sigma) 1X MEM Non-Essential Amino Acid Solution (Sigma) 0.0004% 2-Mercaptoethanol (Invitrogen)
HEK293T	DMEM full medium: DMEM with 4.5 g/L glucose, L-glutamine, sodium pyruvate, and sodium bicarbonate (Sigma). 10% (v/v) FBS (Invitrogen, inactivated for 30 min heating at 56°C before usage) 1% (v/v) Penicillin / Streptomycin (Sigma)
Freezing medium	90% FBS, 10% DMSO
Antibiotics	The corresponding antibiotics with the indicated concentrations were applied to select the infected cells. Blasticidin (InvivoGen) 5 µg/ml Puromycin (InvivoGen) 1 µg/ml G418 (InvivoGen) 1 mg/ml (for Neomycin selection)

2.3.2 Medium and antibiotics for bacterial cell culture

LB-medium	10 g/L Tryptone 5 g/L Yeast extract 10 g/L NaCl autoclaved

LB-agar	LB-medium with 15 g/L agar was autoclaved, then cooled to approx. 55°C, corresponding antibiotics were applied and 12 ml of the medium mix was poured into a 10 cm dish.
SOC-medium	20 g/L Tryptone, 5 g/L Yeast Extract, 4.8 g/L $MgSO_4$, 3.603 g/L dextrose, 0.5 g/L NaCl, 0.186 g/L KCl, autoclaved
Antibiotics	Specific antibiotics were added to LB-medium and LB-agar plates according to the resistance of bacteria: Ampicillin 100 µg/ml Kanamycin 30 µg/ml

2.3.3 Reagents for cell treatments

Cells were treated with the chemicals for specified times and then proceeded for analysis.

Chemicals	**Stock concentration**	**Working concentration**
Cycloheximide (CHX, Sigma)	50 mg/ml in Ethanol	50 µg/ml
MG132 (Calbiochem)	20 mM in Ethanol	10 µM
Phleomycin (Invivo Gen)	20 mg/ml	20 µg/ml
Crystal violet solution		0.6% (w/v) Crystal violet, 20% (v/v) Ethanol.
Nocodazole	40 µg/ml in DMSO	40 ng/ml

2.4 Reagents

2.4.1 For cell culture, transfection and infection

$CaCl_2$ solution	2.5 M $CaCl_2$ in ddH_2O, filtered
DMEM empty medium	DMEM full medium without FBS and antibiotics
1X HBS	25 mM HEPEs, 140 mM NaCl, 0.75 mM Na_2HPO_4, pH 7.05, filtered
Opti-MEM	Opti-MEM® I Reduced Serum Medium
PBS	8 g/L NaCl, 0.2 g/L KCl, 1.44 g/L Na_2HPO_4, 0.24 g/L KH_2PO_4, pH 7.4, autoclaved
PEI (Polyethylenimine)	1.2 µg/µl PEI in ddH_2O, filtered
Polybrene	4 mg/ml Polybrene

2.4.2 For cell lysis and pulldown assays

Biotin elution buffer	10X Buffer BE Strep-Tactin® Elution Buffer with Biotin (IBA)
Cytoplasmic lysis buffer	5 mM PIPEs, pH 8.0, 0.85 mM KCl, 0.1% Triton X-100
Denaturing lysis buffer	10 mM Tris, pH 8.0 1 mM EDTA 2% SDS 10 mM DTT

Deubiquitination buffer	50 mM HEPEs, pH 7.5, 100 mM NaCl, 5% Glycerol, 5 mM MgCl2, 1 mM ATP, 1 mM DTT
Flag peptide	5 mg/ml 3X FLAG® Peptide (Sigma) in TBS
Ni-NTA wash buffer	30 mM Imidazole in PBS
Ni-NTA beads	PureCube Ni-NTA Agarose (Biozym)
Protein A beads	Pierce™ Protein A Agarose (Thermo Fisher Scientific)
Protein G beads	Protein G Sepharose (Sigma)
RIPA lysis buffer	50 mM Tris, pH 8.0 150 mM NaCl 0.1% SDS 1% Triton X-100
Strep-Tactin beads	Strep-Tactin Sepharose 50% suspension (IBA)
TE buffer	10 mM Tris-HCl, pH 8.0, 1 mM EDTA
TNT lysis buffer	50 mM Tris, pH 8.0 150-500 mM NaCl
Urea buffer	8 M Urea in PBS, 10 mM Imidazole

2.4.3 For ChIP

Blocking solution for beads	5 mg/ml BSA in PBS
ChIP dilution buffer	50 mM Tris, pH 8.0, 167 mM NaCl,

	0.11% Na-deoxycholate, 1.1% Triton X-100, Protease and phosphatase inhibitors freshly added
ChIP wash buffer I	Nuclei lysis buffer was diluted 10X with ChIP dilution buffer.
Cytoplasmic lysis buffer	5 mM PIPEs, pH 8.0, 0.85 mM KCl, 1% Triton X-100, Protease and phosphatase inhibitors freshly added
Direct elution buffer	10 mM Tris, pH 8.0, 300 mM NaCl, 5 mM EDTA 1% SDS
Formaldehyde	37% Formaldehyde (Sigma)
Glycine solution	2 M Glycine in ddH_2O
HighPrep PCR beads	HighPrep™ PCR-Reagenz (Biozym)
MNase	(Thermo Scientific)
MNase buffer	(Thermo Scientific)
Nuclei lysis buffer	50 mM Tris, pH 8.0, 10 mM EDTA, 1% SDS, Protease and phosphatase inhibitors freshly added
PicoGreen reagent	Quant-iT PicoGreen dsDNA reagent (Thermo Fisher Scientific)
Protein A magnetic beads	NEB
RIPA high salt buffer II	50 mM Tris, pH 8.0, 500 mM NaCl, 1 mM EDTA, 0.1% SDS 0.1% Na-deoxycholate, 1% Triton X-100
RIPA LiCl buffer III	50 mM Tris, pH 8.0,

	500 mM $LiCl_2$, 1 mM EDTA, 0.7% Na-deoxycholate, 1% Triton X-100

2.4.4 For immunoblotting

Ammonium persulfate (10%, APS)	0.5 g APS were dissolved in 5 ml ddH_2O, stored at -20°C
Antibody dilution buffer	5% BSA in TBST
Blocking solution for PVDF membrane	5% (w/v) nonfat dry milk in TBST
Bis-Tris	1.25 M Bis-Tris, pH 6.8
Bis-Tris separation gel	8-12% (v/v) Acrylamide 0.35 M Bis-Tris 0.1% (v/v) APS 0.075% (v/v) TEMED
Bis-Tris stacking gel	4% (v/v) Acrylamide 0.2 M Bis-Tris 0.125% (v/v) APS 0.0375% (v/v) TEMED
Developing solution A and B	Immobilon Western HRP Substrate (Millipore)
MOPS running buffer (20 X)	1 M MOPS, 1 M Tris, 20 mM EDTA, 2% SDS
MOPS running buffer (ready to use)	5% MOPS running buffer (20X), 1 mM sodium bisulfite
NuPAGE sample buffer (20 x)	250 mM Tris, pH 8.0, 4% SDS,

	25% (v/v) Glycerol, 0.01% Bromophenol blue, 0.1M DTT
Protein marker	PageRuler™ Prestained Protein Ladder (Thermo Scientific)
PVDF transfer membrane	Amersham™ Hybond® P Western blotting membranes, PVDF (Sigma)
Stripping buffer	60 mM Tris, pH 6.8, 0.7% 2-Mercaptoethanol, 2% SDS
Transfer buffer (10X)	144 g/L Glycine, 30.2 g/L Tris base
Transfer buffer (ready to use)	10% Transfer buffer (10X), 20% Methanol
TBS (20 x)	500 mM Tris base, 2.8 M NaCl, pH 7.4
TBS-T	1 x TBS, 0.2% Tween-20

2.4.5 For immunofluorescent staining

Blocking solution	4% BSA in TBS-T.
$CuSO_4$ solution	100 mM $CuSO_4$
EdU	10 mM EdU
Formaldehyde	2% formaldehyde in PBS, pH 6.9
Na-Ascorbate solution	1 M Na-Ascorbate
Na-Phosphate reaction buffer	100 mM Na-Phosphate, pH 7.0
Duolink PLA reagents	Duolink® In Situ Red Starter Kit Mouse/Rabbit (Sigma)

Sulfo-Cyanin-3-azide	0.2 mM Sulfo-Cyanin-3-azide in ddH_2O (Lumiprobe)

2.4.6 For FACS analysis

1% BSA / PBS-T	0.5% (v/v) Tween 20, 1% (w/v) BSA in PBS
BrdU	30 mM BrdU in ddH2O
2N HCl/ Triton solution	1.67 ml HCl in 8.28 ml ddH_2O, 0.5% Triton X-100
1% BSA / PBS	1% (v/v) BSA in PBS
PI solution	20 µg/ml PI, 100 µg/ml RNase A in PBS
0.1 M Sodium Tetraborate	0.1 M Sodium Tetraborate, pH 8.5

2.4.7 For PCR

M-MLV Reverse Transcriptase	Promega
Phusion HF DNA polymerase	Thermo Scientific
SYBR-Green qPCR Master Mix	Thermo Scientific

2.4.8 For recombinant DNA analysis

Agarose gel	1-2% (w/v) agarose in 1X TAE buffer, 1X GelGreen (VWR)

DNA loading buffer (6X)	10 mM Tris-HCl (pH 7.6), 0.03% Bromophenol blue, 60% Glycerol 60 mM EDTA
DNA marker	Gene Ruler 1 kb Plus DNA ladder (Thermo Scientific)
GTE buffer	25 mM Tris, pH 8.0, 50 mM Glucose, 10 mM EDTA
NaOH/SDS lysis solution	200mM NaOH, 1% SDS
Potassium acetate solution	3 M potassium acetate, pH 5.2
TAE buffer (50X)	2 M Tris, pH 8.0, 5.7% acetic acid, 50 mM EDTA
T4 DNA ligase	Thermo Scientific
T4 DNA ligase buffer (10X)	Thermo Scientific

2.4.9 For DNA and RNA isolation

TRI RNA Isolation reagent	TRI Reagent (Sigma)
Phenol/Chloroform reagent	Phenol : Chloroform : Isoamyl Alcohol 25:24:1, Saturated with 10mM Tris, pH 8.0, 1 mM EDTA (Sigma)

2.4.10 Supplements

Isopropanol	(Sigma)

Protease K	10 mg/ml Protease K in ddH2O
RNase A	10 mg/ml RNase A (Thermo Scientific)
Protease inhibitor	Protease inhibitor cocktail (Sigma, P8340), used 1:500
Phosphatase inhibitor	Phosphatase Inhibitor Cocktail 3 (Sigma), used 1:500

2.5 Kits

GenElute™ Gel Extraction Kit	Sigma
GenElute™ HP Plasmid Miniprep Kit	Sigma
GenElute™ HP Plasmid Midiprep Kit	Sigma
GenElute HP Plasmid Maxiprep Kit	Sigma
MinElute PCR Purification Kit	Qiagen
Monarch® DNA Gel Extraction Kit	NEB
NEBNext® Ultra™ II DNA Library Prep Kit for Illumina®	NEB
NEBNext® Multiplex Oligos for Illumina® (Index Primer Set 1)	NEB
NEBNext® Multiplex Oligos for Illumina® (Index Primer Set 2)	NEB

2.6 Antibodies

2.6.1 Primary antibodies

Antigen	Application	Supplier, ordering no.
53BP1	IB	Cell Signaling, 4937
	IB, IP, IF	Novus, NB100-304
β-actin	IB	Sigma, AC-15/A5441

β-TrCP	IB, IP, IF, ChIP	Cell Signaling, 4394
Bim	IB	Cell Signaling, 2933
Bmi1	IB	Cell Signaling, 5856
Cdc25A	IB	Cell Signaling, 3652
	IB	Santa Cruz, sc-7389
Cdc25B	IB	Cell Signaling, 9525
Cdc45	IB, IP	Cell Signaling, 11881
Cdk1/Cdc2 p34	IB, IP	Santa Cruz, sc-54
Cdk2(M2)	IB	Santa Cruz, sc-163
Chk1	IB	Bethyl, A300-298A
Chk2	IB	Cell Signaling, 2662
EZH2	IB	Bethyl, A304-197A
FLAG	IB, IP	Sigma, F3165
	IB, IP	Cell Signaling, 2368
HA	IB, IP, IF	Cell Signaling, 3724
	IB, IP, IF	Cell Signaling, 2367
Histone H3	IB, IF	Abcam, ab1791
IκB-α	IB	Santa Cruz, sc-371
Mcl1 (S-19)	IB	Santa Cruz, sc-819
Mcm7	IB	Bethyl, A302-585A-M
p53	IB	Cell Signaling, 2524
p21	IB	Santa Cruz, sc-397
phospho-Cdk (Thr14/Tyr15)-R	IB	Santa Cruz, sc-28435-R
phospho-Cdk2 (Tyr 15)	IB	Abcam, EPR2233Y
phospho-Chk1 (Ser345)	IB	Cell Signaling, 2348
phospho-Chk2 (Thr68)	IB	Cell Signaling, 2661

phospho-H2AX (Ser139)	IB	Millipore, 07-164
Usp28	IB, IF	Sigma, HPA006778
Vinculin	IB	Sigma, SAB4200080

2.6.2 Secondary antibodies

Antigen	Application	Supplier, ordering no.
anti-Rabbit IgG-HRP	IB	Cell Signaling, 7074
anti-mouse IgG-HRP	IB	Cell Signaling, 7076
Alexa Fluor® 488 anti-Rabbit IgG	IF	Cell Signaling, 4412
Alexa Fluor® 488 anti-Mouse IgG	IF	Cell Signaling, 4408
Alexa Fluor® 555 anti-Rabbit IgG	IF	Cell Signaling, 4413
Alexa Fluor® 555 anti-Mouse IgG	IF	Cell Signaling, 4409
Alexa Fluor® 488 anti-BrdU antibody	FACS	Biolegend, 364106

2.7 Oligonucleotides

2.7.1 Primers

Primers applied in this study were synthesized by Sigma-Aldrich.

Primers for qPCR were designed with PrimerBank online tool spanning an intron to avoid unwanted amplification of genomic DNA.

fw = forward, rev = reverse

Cloning	
53BP1-NT-Strep-MfeI-fw	ACGTCAATTGCATCTGCTTGGTCTCATCCTC AATTTGAAAAAGACCCTACTGGAAGTCAGTT GGATTC
53BP1-NT-XhoI-rev	ACGTACCTCGAGTCAGCTATGGAGCGACTC TGTATCATC
53BP1-FFR-Strep- BamHI-fw (53BP1-CT-Strep- BamHI-fw)	ACGTACGGATCCTCTGCTTGGTCTCATCCTC AATTTGAAAAACAGGGAGAAGAAGAGTTTGA TATG
53BP1-FFR- EcoRI-rev	ACGTACGAATTCTCATTCACCGGTGTTGTCT CCACTCTC
53BP1-BRCT-Strep- BamHI-fw	ACGTACGGATCCTCTGCTTGGTCTCATCCTC AATTTGAAAAACCCTCTGCCCTGGAAGAGCA G
53BP1-BRCT-XhoI-rev (53BP1-CT, FL)	ACGTACCTCGAGTTAGTGAGAAACATAATCG TGTTT
53BP1-CTΔOD-Strep- BamHI-fw	ACGTACGGATCCTCTGCTTGGTCTCATCCTC AATTTGAAAAAGAAAGAAAAGTAACTGAGGA GACTGAAGAGCCAATT
53BP1-FL-XhoI-fw	ACGTACCTCGAGATGTCTGCTTGGTCTCATC CTCAATTTGAAAAAGACCCTACTGGAAGTCA GTT
β-TrCP2-HindIII-fw	ACGTAAGCTTATGGAGCCCGACTCGGTG
β-TrCP2-EcoRI-rev	ACGTACGAATTCTTATCTAGAGATGAAAGTG AATGTTCTGGA
β-TrCP2-CT-HindIII-fw	ACGTACAAGCTTATGATAGAATCTAACTGGC GGTGTGG
β-TrCP2-NT-EcoRI-rev	ACGTACGAATTCTTAAGTCTCTATATCCTGG ATAATCTTTGGG
β-TrCP2-BamHI-fw	ACGTGGATCCATGGAGCCCGACTCGGTG
β-TrCP2-K430R-fw	GGGCCTATGATGGGAGAATTAAAGTTTGGG
β-TrCP2-K430R-rev	CCCAAACTTTAATTCTCCCATCATAGGCCC
β-TrCP2-ΔD-fw	CAAGTGGAATTTGTGGAACATGAAGAATCAC GAATGTGTCATTATCAG

β-TrCP2-ΔD-rev	CTGATAATGACACATTCGTGATTCTTCATGTTCCACAAATTCCACTTG
Cdc25A-Strep-BamHI-fw	ACGTACGGATCCATGTCTGCTTGGTCTCATCCTCAATTTGAAAAAGAACTGGGCCCGGAGCCCCC
Cdc25A-EcoRI-rev	ACGTACGAATTCTCAGAGCTTCTTCAGACGACTGTACATCTCCC
qPCR	
mCdc25A 1-fw	AGCCACTTTGTCCGATGAGG
mCdc25A 1-rev	GCAACGATCGGCAAGGTTTG
mCdc25A 2-fw	CAAACCTTGCCGATCGTTGC
mCdc25A 2-rev	TCTGCTCTCTTCAACACCGC
ChIP-qPCR	
CENPP-fw	TAGGTCGGCGTAAGAGAGGA
CENPP-rev	TCCCTGGCTGTCTAAGCAGT
CCAR-fw	CGAAGCCTTCTTTCCTGATG
CCAR-rev	ATATGGTCCCTCCCTCGTCT
POLG-fw	TCAATTGATGGTTGGCAAGA
POLG-rev	CAACGGAAGGCAACATTTTT
RBM42-fw	CTCCAGGTTTGAGCAGGAAG
RBM42-rev	GGCATTGTGTTCCCTGACTT
TXNIP1-fw	AGAGCGCAACAACCATTTTC
TXNIP1-rev	CGATCTCCACAAGCACTCCT
ETV5-fw	AATTCTCAGCCTTCCCCATT
ETV5-rev	ATGAAGCGGGTTTCTTTCGT
gRNA	
Usp28-1-fw	CACCGGAGTTGATGGTTGGCCAGTT
Usp28-1-rev	AAACAACTGGCCAACCATCAACTCC

53BP1-1-fw	CACCGCAGGATTTTCTTTGTGCGTC
53BP1-1-rev	AAACGACGCACAAAGAAAATCCTGC
53BP1-2-fw	CACCGAACGAGGAGACGGTAATAGT
53BP1-2-rev	AAACACTATTACCGTCTCCTCGTTC
53BP1-3-fw	CACCGCACATGTGGTTCCATCAGTC
53BP1-3-rev	AAACGACTGATGGAACCACATGTGC
β-TrCP1-fw	CACCGACGAGTTTATGTGCCCATGT
β-TrCP1-rev	AAACACATGGGCACATAAACTCGTC

2.7.2 Gene fragments

Gene	Supplier
MGC Human TP53BP1 Sequence-Verified cDNA	Dharmacon/GE Healthcare
β-TrCP-KR of N-terminus	Dharmacon/GE Healthcare
53BP1-CTKR	Dharmacon/GE Healthcare

2.7.3 RNA oligonucleotides

Silencer Select pre-designed siRNA oligonucleotides against 53BP1 were purchased from Thermo Fisher Scientific, s14315 targeting exon12, s14313 targeting exon 17 (targeting all the isoforms). The ON-TAGETplus Non-targeting pool was applied as a control siRNA.

2.8 Plasmids

2.8.1 Empty vectors

Vector	Application / Resistance
pcDNA3.1	Transient expression
pFLAG	Transient expression
pRRL-Puro	Lentiviral expression, puromycin resistance
pWZL	Retroviral expression, blasticidin resistance
pBabe	Retroviral expression, puromycin resistance

2.8.2 Vectors for lentivirus and retrovirus production

Vector	Description
psPAX2	2nd generation lentiviral packaging plasmid
pMD2.G	Lenti-viral envelope vector
Eco receptor	Ecotropic retrovirus receptor

2.8.3 Plasmids available in the lab of AG. Dr. Nikita Popov’s group

Vector	Description
pFLAG-β-TrCP2	Transient expression for Flag-tagged human β-TrCP2
pFLAG-β-TrCP2-K430R	Transient expression for Flag-tagged human β-TrCP2 with K430R mutation
pFLAG-β-TrCP2-R413A	Transient expression for Flag-tagged human β-TrCP2 with R413A mutation

pcDNA3-HA-β-TrCP2	Transient expression for HA-tagged human β-TrCP2
pcDNA3-HA-Usp28	Transient expression for HA-tagged human Usp28
pcDNA3-HA-Usp28-C171A	Transient expression for HA-tagged human Usp28 with C171A mutation
pcDNA3-His6Ubiquitin	Transient expression for hexa-histidine (His6)-tagged ubiquitin
pWZL-HA-β-TrCP2	Stable retroviral expression for HA-tagged human β-TrCP2
pWZL-HA-Usp28	Stable retroviral expression for HA-tagged human Usp28
pWZL-HA-Usp28-C171A	Stable retroviral expression for HA-tagged human Usp28 with C171A mutation

2.8.4 Plasmids generated for this study

Vector	**Description**
pFLAG-β-TrCP2-ΔD	Transient expression for Flag-tagged human β-TrCP2 with LI61EE mutation
pFLAG-β-TrCP2-KR	Transient expression for Flag-tagged human β-TrCP2 with all K replaced by R
pFLAG-β-TrCP2-KRΔD	Transient expression for Flag-tagged human β-TrCP2 with all K replaced by R and LI61EE mutation
pFLAG-β-TrCP2-CT	Transient expression for Flag-tagged human β-TrCP2 with C-terminus (AA 185-508)
pFLAG-β-TrCP2-NT	Transient expression for Flag-tagged human β-TrCP2 with N-terminus (AA 1-184)
pcDNA3-HA-Strep-β-TrCP2	Transient expression for HA- and Strep-tagged human β-TrCP2
pcDNA-HA-MT-Cdc25A	Transient expression for HA- and Myc-tagged human Cdc25A

pcDNA3-HA-Strep-53BP1	Transient expression for HA- and Strep-tagged human 53BP1
pcDNA3-HA-Strep-53BP1-NT	Transient expression for HA- and Strep-tagged human 53BP1 with N-terminus (AA 1-1219)
pcDNA3-HA-Strep-53BP1-CT	Transient expression for HA- and Strep-tagged human 53BP1 with C-terminus (AA 1220-1972)
pcDNA3-HA-Strep-53BP1-FFR	Transient expression for HA- and Strep-tagged human 53BP1 with FFR domain (AA 1220-1711)
pcDNA3-HA-Strep-53BP1-BRCT	Transient expression for HA- and Strep-tagged human 53BP1 with BRCT domain (AA 1712-1972)
pcDNA3-HA-Strep-53BP1-CTΔOD	Transient expression for HA- and Strep-tagged human 53BP1 C-terminus with oligomerization deleted (AA 1266-1972)
pBabe-HA-β-TrCP2	Stable retroviral expression for HA-tagged human β-TrCP2
pBabe-HA-β-TrCP2-ΔF	Stable retroviral expression for HA-tagged human β-TrCP2 with F-box (AA 95-133) deleted
pWZL-HA-β-TrCP2-K430R	Stable retroviral expression for HA-tagged human β-TrCP2 with K430R mutation
pWZL-HA-Strep-53BP1-CT	Stable retroviral expression HA- and Strep-tagged human 53BP1 C-terminus
pWZL-HA-Strep-53BP1-CTKR	Stable retroviral expression HA- and Strep-tagged human 53BP1 C-terminus with all K to R except K1667 and K1669 (AA 1220-1972)
pWZL-HA-Strep-53BP1-CTΔOD	Stable retroviral expression for HA- and Strep-tagged human 53BP1 C-terminus with oligomerization deleted (AA 1266-1972)

2.9 Consumables

Consumables, like cell culture dishes, tubes and other disposable plastics were purchased from the companies Becton Dickinson, Eppendorf, Greiner, VWR, Nunc, Sarstedt.

2.10 Equipment

Equipment	Supplier
Automated Electrophoresis	
Chemiluminescence imaging	Bio-Rad ChemiDoc™ MP Imaging System
Cell culture incubator	Thermo Scientific, HERA cell 150i
Cell Counter	Luna™ Automated Cell Counter
Centrifuges	Eppendorf 5417R, Eppendorf 5424, VWR PCR plate spinner.
Deep-sequencer	Genome Analyzer IIx (Illumina)
Flow Cytometer	BD FACS Canto II Flow Cytometer 338962
Heating block	Accu block digital dry bath, Eppendorf Thermomixer C
Illumina NextSeq instrument	(Core Unit Sys Med, University of Würzburg)
Incubator shaker	
pH meter	Schott Lab850
Photometer	Bio Photometer D30
Microscopes	Motic AE31
PCR thermal cycler	Bio-Rad T100™ Thermal Cycler
Power supply	VWR
Quantitative RT-PCR machine	Bio-Rad CFX Connect Real-Time system
SDS-PAGE system	Bio-Rad
TECAN infinite M200 PRO	TECAN infinite M200 PRO
Transilluminator	Transilluminator DR-45M

Ultrasonifier	UP50H Ultrasonic Processor
Vortex mixer	
Water bath	VWR VWB12
Immunoblot transfer chamber	BioSTEP
Whatman filter paper	

2.11 Software and online programs

Programs	**Supplier**
Acrobat™	Adobe Inc.
ApE plasmid editor	by M. Wayne Davis
BD FACSDiva	BD Biosciences
Bio-Rad CFX Manager 3.1	Bio-Rad
Crispr gRNA design tool	http://crispr.mit.edu/
FlowJo 2	FlowJo, LLC
Image Lab 5.0 software	Bio-rad
Integrated Genome Browser	(Nicol et al., 2009)
NIS-Elements BR 3.0	Nikon
Office 365	Microsoft Inc.
R 3.1.1	R foundation
UCSC Genome Bioinformatics	http://genome.ucsc.edu
PimerX	http://www.bioinformatics.org/primerx/
Primer bank	https://pga.mgh.harvard.edu/primerbank/
PyMOL Molecular Graphics System	Version 1.8 Schrödinger, LLC.

3 Methods

3.1 Cell biology methods

3.1.1 Cell culture

All eukaryotic cell lines were cultured in a cell incubator at 37°C, 5% CO_2 and 95% relative humidity.

Passaging cells

Cells were passaged every two to three days for maintaining cell lines. To split cells, cells were washed with PBS following removal of medium, and then trypsinized to detach cells from the culture dish. The appropriate culture medium with 10% FBS is added to neutralize trypsin. Cells were resuspended and centrifuged at 800 x g for 3 min. The cell pellet was resuspended in fresh medium and an appropriate fraction of the cell suspension was plated to a new dish with fresh medium. To seed cells at a specific cell number, the cell number was detected with Luna automated cell counter or a Neubauer counting chamber.

Freezing cells

For long-term storage, cells were stored in liquid nitrogen. Cells were trypsinized and transferred into a 15 ml tube with 10 ml PBS. Cells were spun down followed by removal of supernatant. Cell pellet was resuspended in the freezing medium and the cell suspension was transferred to cryo vials. First the cryo vials were stored in a Quick-Freeze container to freeze slowly until -80°C. After at least 2h, the cryo vials were transferred to liquid nitrogen storage tanks.

Thawing cells

Frozen cells were rapidly thawed in a 37°C water bath. Cell suspension was then transferred into a PBS-filled 15 ml tube and centrifuged at 800 x g for 3 min. Cell pellet was then resuspended in fresh full medium and plated into a dish.

3.1.2 Transient transfection of plasmid DNA

For transient over-expression of plasmid DNA, one of the following methods was applied to transfect cells, which depends on the cell lines. Cells were seeded at an appropriate density in a 6-well plate. After overnight culture, transfection medium was added to the cells. The amount of reagent was for one well of a 6-well plate.

PEI transfection

The transfection solution A and B were prepared as follows.

Solution A	6 µg target DNA, 200 µl DMEM medium
Solution B	10 µl PEI (1.2 µg/µl), 200 µl DMEM medium

After 5 min RT incubation, the solution A and B were mixed and incubated for 5 min at RT. The reaction mix was then added dropwise to cells. After O/N incubation, cells were washed with PBS and fresh full medium was added. Cells were collected for analysis 24 h or 48 h after transfection.

Calcium phosphate transfection

The cell medium was replaced freshly before transfection. 6 µg target DNA was mixed with 200 µl HBS followed by addition of 12 µl 2.5 M $CaCl_2$. The mixture was incubated for 20 min at RT and then added to cells. After O/N incubation, cells were washed with PBS and fresh medium was added. Cells were harvested for analysis 24 h or 48 h after transfection.

3.1.3 Infection for generating stable cell lines

To create cells stably expressing target protein, ether retroviral or lentiviral infection was applied. The receptor cells and the virus producing cells were seeded at an appropriate density. After O/N culture, the medium was replaced freshly and the transfection mixture was applied. The amount of reagent was for receptor cells in one well of a 6-well plate.

Retroviral infection

Phoenix cells were used to produce retrovirus. Phoenix cells in a 6 cm dish was transfected with 8 µg target DNA and 4 µl Helper plasmid in PEI solution according to PEI transfection protocol. For human receptor cells, cells in a 6-well plate were transfected with 6 µg Eco receptor in PEI solution. After overnight incubation, cells were washed with PBS and fresh full medium was added to cells. The virus containing supernatants of phoenix cells were collected 48 h and 72h after transfection.

The medium of receptor cells was removed and 1 ml fresh full medium was added. The virus containing supernatants were filtered with 0.45 µm filter and added to the receptor cells. After addition of 3.5 µl polybrene, cells were incubated with virus for 24 h, following by replacement of fresh full medium. On the next day, cells were split into 10 cm dish and the corresponding selection antibiotic was added.

Mouse receptor cells were directly infected by virus produced by phoenix cells without transfection of Eco receptor.

Lentiviral infection

HEK293T cells in 10 cm dish were transfected with PEI solution. The following solutions were prepared and incubated 5 min at RT.

Solution A	10 µg lentiviral expression plasmid, 10 µg psPAX2, 2.5 µg pMD2.G, 700µl OptiDMEM
Solution B	3.5 ml OptiDMEM, 150 µl PEI

Solution A and B were mixed and incubated 20 min at RT. After replacement of 6 ml fresh medium, the reaction mix was added dropwise to HEK293T cells. The virus containing supernatants of HEK293T cells were collected 48 h and 72 h after transfection. The supernatants were filtered with 0.45 µm filters and applied to receptor cells in the same manner as for retroviral infection without Eco receptor transfection.

3.1.4 Transfection of siRNA

siRNAs from Dharmacon were transfected according to the siRNA transfection protocol recommended by Dharmacon. Cells were seeded in a 12-well plate with full

medium without antibiotics in appropriate density and cultured O/N. The following transfection solutions were prepared and incubated 5 min at RT.

Solution A	1.25 µl siRNAs (5 µM), 98.75 µl Opti-MEM
Solution B	4 µl DharmaTransfect1 reagent + 96 µl Opti-MEM

The solution A and B were mixed and incubated 20 min at RT. The mixture was then added dropwise to cells. After O/N incubation, the medium was changed to fresh full medium. Cells were collected for analysis 48 h after transfection.

3.1.5 Treatment

Irradiation of cells were performed with Faxitron CP160 cabinet X-ray system or a Siemens linear accelerator. Chemical treatments were listed as below.

Table 3.1

Compound	Work conc.	Incubation time (if not specifically indicated)
Phleomycin (Phleo)	20 µg/ml	4 h
Cycloheximide (CHX)	50 µg/ml	
MG132	10 µM	4 h
Nocodazole	40 ng/ml	4 h or 8 h after IR

3.1.6 Colony formation assay

The crystal violet staining was applied to visualize cell densities and detect the ability of cell proliferation.

Cells were irradiated by graded single doses (0 - 8 Gy) with a 6 MV Siemens linear accelerator (Siemens) at a dose rate of 2 Gy/min. Cells were then immediately re-plated with the same cell number into a new 6-well plate and cultured for 7 to 14 days. Afterwards, cells were fixed and stained with the crystal violet solution for 15 min at RT. Excess dye was washed away with PBS and the plates were air dried. Colonies

containing at least 50 cells were counted as survivors. Four replicates were done for each dosage, and at least three independent experiments were repeated.

3.1.7 BrdU-PI co-staining for flow cytometry

Bromodeoxyuridine (BrdU) is an analog of thymidine, which is incorporated into the newly synthesized DNA of replicating cells. BrdU-incorporated cells can be identified with anti-BrdU antibodies. Propidium iodide (PI) is a fluorescent intercalating agent that can label DNA content. PI staining of DNA by FACS (fluorescence-activated cell sorting) was applied to detect DNA content and analyze cell cycle distribution.

Cells treated with or without IR were immediately exposed to 40 ng/ml Nocodazole to prevent mitotic exit. 30 µM BrdU was added 30 min prior to collection. At the indicated timepoints, cells were trypsinized and spun down for 5 min at 800 x g. After washing with cold PBS, cells were centrifuged again. Cell pellets were then resuspended in 300 µl PBS and fixed by adding 700 µl chilled 100% EtOH while vortexing.

After at least O/N storage at -20°C, cells were spun down for 5 min at 800 x g and the supernatant was removed. To denature DNA, 1 ml 2 M HCl / 0.5% Triton X-100 was added to cells and incubated for 30 min at RT. Following centrifuging, cells were resuspended in 1 ml 0.1 M $Na_2B_4O_7$ (pH 8.5) for neutralization.

Cells were again spun down and washed with 100 µl 1% BSA / PBS. Following 1 h incubation with 5 µl Alexa Fluor® 488 anti-BrdU antibody in 50 µl 1% BSA / PBS-T at RT (protected from light), cells were washed with 100 µl 1% BSA / PBS and the pellets were resuspended in 350 µl PI solution. After 30 min incubation at RT in the dark, cell suspensions were diluted with PBS and transferred into FACS tubes for flow cytometry detection. The BrdU- or PI-negative and double negative control samples were applied for compensation parameter setting. The BrdU-positive cells and cell cycle distribution were analyzed with FlowJo2 software.

3.1.8 Immunofluorescent staining

To analyze the levels and subcellular localization of proteins, cells were plated on glass cover slips at appropriate density. After O/N culture, cells were washed with

PBS and fixed with 2% PFA for 15 min at RT. Then cells were washed with PBS for 3 times and the cover slips were used immediately or stored in PBS at 4°C.

Cells were permeabilized by 0.3% Triton X-100 in PBS for 10 min at RT, followed by 1 h incubation in blocking solution. Cells were then incubated with primary antibody (1:100 – 1:500) in blocking solution for 2 h at RT. After 3 times washing with PBS, cells were incubated with fluorescence-labeled secondary antibody (1:200) in blocking solution in dark for 1 h.

Following 3 times of PBS washing, the cover slips were mounted with mounting medium (Duolink® In Situ Mounting Medium with DAPI, Sigma) onto slides and sealed with nail polish. After 15 min incubation at RT protected from light, the slides were analyzed with a fluorescence microscope and could be stored at -20°C in dark.

3.1.9 EdU labeling assay

5-ethynyl-2'-deoxyuridine (EdU) is a nucleoside analog to thymidine and an alternative for BrdU to measure active DNA synthesis. The detection of EdU is based on a click reaction between an azide and an alkyne, which is a copper catalyzed reaction. EdU contains alkynes which can react with the azide-containing fluorescent dye and the reaction can be visualized with a fluorescence microscope.

Cells on cover slips treated with or without IR were immediately exposed to 40 ng/ml Nocodazole. 20 µM EdU was added 10 min prior to fixation. Cells were fixed with 2% PFA for 15 min at RT. Following 3 times PBS washing, cells were permeabilized in 0.3% Triton X-100 / PBS for 10 min at RT and then incubated with 100 mM Tris (pH 7.0) for 5 min. The click reaction mixture was prepared with following compounds.

Table 3.2

Compound	**Final conc.**
100 mM NaPhosphate reaction buffer, pH 7.0	100 mM
Sulfo-Cy3-azide	0.4 µM
$CuSO_4$ solution	2 mM

1 M NaAscorbate solution	100 mM

Cells were incubated with the reaction mixture for 30 min at RT and washes 3 times with PBS for 15min. Afterwards, the cover slips were mounted with DAPI mounting medium (Sigma) onto slides and sealed with nail polish. After 15 min incubation at RT, samples were analyzed with a fluorescence microscope. The EdU positive cells were counted from at least 200 cells and quantified with three independent experiments with Fiji software.

3.1.10 Proximity ligation assay (PLA)

Proximity ligation assay (PLA) was applied to detect and visualize protein-protein interactions and localization. In this assay, two primary antibodies with different species recognize the target proteins. Species-specific secondary antibodies (PLA probes) bind to the primary antibodies. When the target proteins are in close proximity (<40 nm), the specific DNA strands on PLA probes interact through two DNA oligonucleotides added subsequently. The two oligonucleotides forms DNA circles by ligation and the circles are amplified with a polymerase to generate high concentration of fluorescence.

Cells on cover slips were processed with Duolink® In Situ Red Starter Kit Mouse / Rabbit (Sigma) according to the manufacturer's protocol. The permeabilization and fixation were processed as described in the immunofluorescent staining protocol (see 3.1.8). The PLA probes were diluted in blocking solution.

3.2 Molecular biology methods

3.2.1 RNA Isolation

RNA isolation from cells was performed with TRI RNA Isolation reagent (Sigma). Cells collected from a 6 cm dish were lysed in 1 ml TRI reagent for 5 min at RT. With addition of 200 µl chloroform, the mixture was vortexed for 15 s and incubated at RT for 10 min. Followed centrifugation at 14,000 rpm, 4°C for 10 min, the mix was separated into three phases. The upper phase containing RNA was transferred into a fresh tube and 500 µl isopropanol was added to precipitate RNA. After centrifugation

at 14,000rpm, 4°C for 10 min, the RNA precipitate was washed with 75% EtOH, air-dried, and then dissolved in 50 µl RNase free ddH2O for further analysis.

3.2.2 cDNA synthesis

To analyze the expression of specific genes or generate new DNA for target genes, complementary DNA (cDNA) was synthesized from total RNA via reverse transcription with random primers.

To this end, 2 µg total RNA was diluted to 20 µl with nuclease-free water and incubated for 2 min at 65°C to denature RNA. After cooling down, 30 µl cDNA synthesis mix listed below was added to the denatured RNA.

Table 3.3. cDNA synthesis mix:

30µl Reaction	Component
10 µl	5X M-MLV reverse transcriptase reaction buffer (Promega)
1.25 µl	10 mM dNTPs (Sigma)
2 µl	Random primers (500 µM Stock, Sigma)
1 µl	RiboLock RNase Inhibitor (40 U/µl, Thermo)
1 µl	M-MLV reverse transcriptase (200 U/µl, Promega)
To 30 µl	Nuclease-free water

The mixture was incubated in the thermocycler with the following conditions.

Table 3.4

Temp	Time
25°C	10 min
37°C	60 min
70°C	15 min
4°C	Hold

The concentration of cDNA product was measured with Nanodrop. In PCR reaction for cloning, 50 ng cDNA was used. In qPCR reaction for mRNA analysis, cDNA was diluted 1:5 with nuclease-free water and 1 µl was added per qPCR reaction.

3.2.3 Polymerase chain reaction (PCR)

PCR for DNA cloning

To generate DNA fragments with restriction sites, the target DNA was amplified from existed plasmid DNA or cDNA with specific primers. This method can insert tags and restriction sites to the target DNA, and create DNA variants with deletions and insertions. The reaction mix was set up with the following components (Table 3.5) and incubated under PCR thermocycling conditions for cloning (Table 3.6).

Table 3.5

Component	25 µl Reaction
5X Phusion HF or GC Buffer	5 µl
10 mM dNTPs	0.5 µl
10 mM dNTPs	0.5 µl
10 µM Forward Primer	1.25 µl
10 µM Reverse Primer	1.25 µl
Template DNA	50 ng
DMSO (optional)	(0.75 µl)
Phusion DNA Polymerase	0.5 µl
Nuclease-free water	to 25 µl

Table 3.6. PCR thermocycling conditions for cloning

Step	Temp	Time
Initial Denaturation	98°C	30 s

25-35 Cycles	98°C 50-62°C 72°C	30 s 20 s 30 s / kb
Final Extension	72°C	10 min
Hold	4°C	

The reaction mix was loaded with 6X loading buffer to agarose gel, followed by gel extraction (see 3.2.7 and 3.2.8).

PCR for site-directed mutagenesis

For generate mutant plasmid DNA, primers with the desired mutation was applied for PCR with the wildtype plasmid DNA as templates. The PCR procedures were the same as for cloning. After PCR, the reaction mix with addition of 2 µl DpnI and the desired buffer was incubated at 37°C O/N to digest template DNA. The product was then diluted 1:5 in ddH2O for transformation to competent bacteria.

Quantitative real-time PCR (qPCR)

Quantitative real-time PCR was applied to analyze mRNA abundance using cDNA (see 3.2.2) and DNA enrichments from ChIP (see 3.3.12). During DNA amplification by qPCR, as a double-strand DNA (dsDNA) -binding fluorescent dye, SYBR-Green intercalates nonspecifically into dsDNA, allowing DNA quantification in real time. The qPCR reaction mix as below (Table 3.7) was incubated under the thermocycling conditions for qPCR (Table 3.8).

Table 3.7

Component	10 µl Reaction
cDNA (see 3.2.2) or DNA from ChIP (see 3.3.12) diluted in Nuclease-free water	5 µl
SYBR-Green Mix (Thermo Scientific)	2.5 µl
10 µM Forward Primer	0.25 µl
10 µM Reverse Primer	0.25 µl
Nuclease-free water	2 µl

Table 3.8. PCR thermocycling conditions for qPCR

Step	Temp	Time
Initial denaturation	95°C	15 min
40-45 Cycles	95°C 60°C 72°C	30 s 20 s 15 s/kb
Final extension	72°C	10 min
Melting curve	95°C	1 min
	60°C	30 s
	95°C	30 s

The threshold cycle (CT) value from qPCR results indicates the cycle number at which the fluorescence signal was significantly above the background fluorescence. The enrichment fold of samples was calculated relative to mS16 as a housekeeping gene for mRNA analysis, or relative to IgG samples for ChIP.

For mRNA analysis,

$\Delta CT = CT_{target} - CT_{mS16}$

$\Delta\Delta CT = \Delta CT_{IR} - \Delta CT_{control}$

Enrichment fold = $2^{-\Delta\Delta CT}$

For ChIP DNA analysis,

$\Delta CT = CT_{IgG} - CT_{target}$

Enrichment fold = $2^{\Delta CT}$

CT value indicates the average CT value of triplicates in qPCR measurement. The standard deviation (SD) was calculated to show error bars.

$$SD = \sqrt{\frac{\sum(x-\overline{x})^2}{(n-1)}}$$

3.2.4 Bacteria transformation

To generate and amplified recombinant plasmid DNA, transformation into competent bacteria was performed with PCR products, DNA ligation mix or DNA plasmids as target DNA for expression. Competent bacteria were thawed on ice for 5 min, followed by addition of the target DNA and incubation on ice for 30 min. After heat shock at 42 °C for 30 s, the bacteria were cooled down on ice for 5 min and incubated at 37°C for 1 h with addition of 100 µl SOC-medium. To generate colonies, the bacteria suspension was then plated on LB-agar plates with corresponding selection antibiotics for O/N culture at 37°C. The colonies were picked up and cultured in LB-medium with antibiotics for amplification and further analysis.

3.2.5 Plasmid isolation from bacteria

Minipreparation (Miniprep)

To analyze the colonies generated from transformation with alkaline lysis, the bacteria were incubated in 2 ml LB-medium with antibiotics O/N at 37°C. The suspensions were spun down at 12,000 rpm for 3 min. The bacteria pellets were resuspended in 100 µl GTE buffer containing 0.5 µl RNase A, followed by lysis with 200 µl of NaOH/SDS lysis solution for 3 min at RT. The lysis was stopped by addition of 150 µl potassium acetate solution. The mixtures were then spun down at 14,000 rpm, 4°C for 10 min. The supernatants were transferred into a fresh tube and mixed with 500 µl isopropanol (Sigma). After centrifugation again, the DNA pellets were washed with 70% EtOH, air dried and dissolved in 30 µl TE buffer.

To amplify small amounts of plasmids for transfection and infection, the bacteria with target plasmids were incubated in 5 ml LB-medium and the plasmids were isolated with Miniprep kit (Sigma) according to manufacturer's protocol.

Minipreparation (Midiprep) and Maxipreparation (Maxiprep)

For isolation of plasmid DNA for large amounts, 200 ml and 400 ml LB-medium with bacteria were processed with Midiprep kit and Maxiprep kit (Sigma) according to the manufacturer's protocol. The purified plasmids were eluted in TE buffer from columns and adjusted to 1 µg/µl with Nanodrop detection.

3.2.6 Restriction digest of DNA

To prepare DNA for cloning and analyze DNA isolated from colonies, restriction digest of DNA was performed with restriction enzymes from Fermentas and Thermo Scientific. The digestion mix was set up with the recommended restriction buffers and enzyme amounts in the following table and incubated for 2 h at the recommended temperature.

Digestion mix:

1 µg DNA

0.5 µl restriction enzyme 1

0.5 µl restriction enzyme 2

1 µl 10X reaction buffer

ddH2O to 10µl

For specific digestion reaction, the amounts of DNA, enzymes, total volume and digestion time were optimized.

3.2.7 DNA gel electrophoresis

1-2% agarose gel was used to separate DNA fragments by gel electrophoresis. Agarose was boiled in TAE buffer and 1 µg/µl GelGreen was added after it cooled to approx. 50°C. Following the mix formed a solid gel in a gel chamber with combs, the digested DNA was loaded into the pockets of the gel with 6X DNA loading buffer. The DNA ladder was loaded next to the samples as a marker for the DNA fragments size. The DNA fragments stained with GelGreen were separated in the gel at 130 V for 1 h and visualized on a UV transilluminator.

3.2.8 DNA extraction

To extract DNA fragments and PCR products from agarose gels, the DNA bands in the gels were cut out and extracted with Gel Extraction Kit (Sigma) according to the manufacturer's protocol.

3.2.9 DNA ligation

To connect the insert DNA into a compatibly digested vector, DNA ligation was performed with the T4 DNA ligase (Thermo Scientific). The ligation mix listed below was incubated for 3 h at 22°C or O/N at 16°C and transformed into competent bacteria. The ratio of vector and insert amounts was adjusted.

Ligation mix:

50 ng digested vector

150ng insert DNA fragment

1 µl T4 DNA ligase

1 µl 10X T4 ligation buffer

ddH2O to 10 µl

3.2.10 Nucleic acid quantification

Nanodrop measurement

The concentration of DNA and RNA was measured with the Bio Photometer. 1-2 µl DNA or RNA was applied to measure the absorbance at 260 nm. The purity was judged by the ratio of absorbance at 260 and 280 nm, while ~ 1.8 for DNA and ~2.0 for RNA was generally accepted as pure.

PicoGreen measurement

dsDNA concentrations of ChIP products and DNA libraries were determined with Quant-iT PicoGreen dsDNA reagent (Invitrogen). As a fluorescent probe that binds to dsDNA, the fluorescence of PicoGreen at a wavelength of 485/535nm was measured according to the manufacturer's protocol.

3.3 Biochemical methods

3.3.1 Cell lysis

For extraction of total proteins, cells were trypsinized and spun down at 800 x g for 5 min. Cell pellets were washed with PBS and centrifuged again. Following removal of supernatant, cells were resuspended in RIPA buffer with proteinase and phosphatase inhibitors and incubated on ice for 30 min with occasionally vortexing. The suspension was then spun down at maxi-speed for 10 min at 4°C. The supernatant was transferred to a fresh tube. The protein concentration was measured with the BCA assay.

3.3.2 Subcellular fractionation

To study the subcellular location of proteins, fractionation procedure was applied to separate cytoplasm, nucleoplasm and chromatin. Cells were lysed in cytoplasmic buffer I on ice for 10 min and then spun down at 800 x g 4°C for 5 min. The supernatant I was transferred into a fresh tube, while the pellet was resuspended in TNT150 for 20 min on ice. The suspension was again centrifuged at 2,000 x g 4°C for 10 min to get the supernatant II as soluble nuclear fraction. The pellet was then resuspended in RIPA buffer on ice for 30 min and the suspension was analyzed as chromatin nuclear fraction. The soluble and chromatin nuclear fractions of proteins were investigated with immunoblotting.

3.3.3 Bicinchoninic acid assay (BCA) assay

Protein concentration of cell lysates were quantified with BCA assay. 1 µl cell lysate was mixed with 200 µl BCA reagents (buffer A and B, 50:1) and added into a well of a flat bottom 96-well transparent plate. The reaction mixtures were incubated at 37°C for 30 min. The absorbance was measured at a wavelength of 550 nm on the plate reader. The protein concentration was quantified with reference to the standard curve with a series of BSA dilutions.

3.3.4 SDS Polyacrylamide gel electrophoresis (SDS-PAGE)

SDS-PAGE was applied to separate proteins in Bis-Tris polyacrylamide gels by electrophoresis according to molecular weights. A Bis-Tris polyacrylamide gel contained an 8-12% stacking bottom gel and a 4% resolving upper gel. Protein lysates were boiled in sample buffer for 10 min at 95°C. Equal amounts of proteins were loaded on Bis-Tris polyacrylamide gels in SDS-PAGE chambers (Bio-Rad), together with PageRuler Prestained Protein Ladder as a molecular weight marker. MOPS running buffer containing sodium bisulfite was filled into the chambers and proteins were separated by electrophoresis at 135 V.

3.3.5 Protein transfer

Following separation of proteins by SDS-PAGE, proteins were transferred onto a PVDF membrane for immunoblot. The PVDF membrane was first activated in methanol and then soaked in transfer buffer with sponges, the gel and filter papers. The transfer sandwich was assembled sequentially as sponge- filter papers - gel - filter papers - sponge. Wet transfer was performed for the sandwich in a transfer cassette filled with transfer buffer at 125 V 4 ˚C for 2 h.

3.3.6 Immunoblot

The PVDF membranes with proteins were blocked for 1 h in blocking solution. Then primary antibody in blocking solution was applied for O/N incubation at 4°C. After three times washing with TBS-T (15 min / time), membranes were incubated with secondary antibody in blocking solution (1: 3,000) for 2 h at RT, followed by three times TBS-T washing (15 min / time). With incubation of Immobilon Western HRP Substrate (Millipore), membranes were detected by the LAS-4000 imager (Bio-Rad). Protein signals were quantified and relative to the signals of loading controls (Vinculin, β-actin, or Cdk2) using Image Lab 5.0 software.

Stripping

To remove the antibodies bound to proteins on PVDF membranes, the membranes were incubated at 55°C for 20 min in stripping buffer. After thoroughly washing under

flowing ddH2O and with TBS-T, membranes were then processed with the immunoblot procedures again with antibodies of target proteins.

3.3.7 Immunoprecipitation

To investigate the protein-protein interaction, immunoprecipitation for ectopic and endogenous proteins were performed under non-denaturing or denaturing conditions.

Non-denaturing immunoprecipitation

HeLa cells expressing target proteins were lysed in TNT150-500 buffer with protease and phosphatase inhibitors. For chromatin associated proteins, the lysate was treated with Benzonase and then sonified for 30 s with 50% amplitude and 50% cycles. After incubation for 30 min on ice, cell lysates were centrifuged at maxi speed 4°C for 10 min. 5% of supernatant was taken as input. For TNT500 lysate, TNT without salt was added to the remained supernatant to dilute NaCl till 300 mM. The supernatant was transferred into a fresh tube with 10 µl washed Protein A beads or Protein G beads and the antibody against target protein. The mixture was rotated at 4°C for at least 4 h. Afterwards, beads were separated by centrifuging, washed and rotated with fresh lysis buffer (TNT150-300) for two times at 4°C, 30 min / time. Cells without the target protein expression were applied as control pull downs.

For Strep-tag pull down assay, Streptavidin beads were used instead of Protein A and G beads without addition of antibodies. Cells without Strep-tagged proteins or Streptavidin beads pre-incubated with 5X Biotin elution buffer were applied as control pull downs.

To elute proteins that bound to beads, 10 µl of Flag peptide in 40 µl lysis buffer was added to beads for Flag-tag pull down. For Strep-tag pull down, 10 µl of 10X Biotin elution buffer in 40 µl lysis buffer was added to beads. Samples were rotated at 4°C for 2 h and spun down to take the supernatant as eluates.

The input, beads or eluates were boiled in sample buffer at 95°C for 10 min. The supernatants were subjected for SDS-PAGE and immunoblot analysis.

Denaturing immunoprecipitation

To precipitate proteins without interaction partners, the denaturing immunoprecipitation was performed. Cells were lysed in denaturing lysis buffer and boiled at 95°C for 10 min. 5 µl lysate was taken as input, while the remained lysate were added to TNT lysis buffer and processed as described in the protocol for Non-denaturing immunoprecipitation.

Sequential pulldown

In this study, the sequential pull down was performed to analyze whether dimerized proteins were ubiquitinated. The lysates of cells overexpressing Strep-HA-tagged β-TrCP and Flag-tagged β-TrCP were separated- 5% as input for immunoblot, 15% for Flag-tag IP, 80% for Strep-tag pull down. The beads from Strep-tag pull down were eluted in denaturing lysis buffer and boiled at 95°C for 10 min. 5% of the eluates were taken for immunoblot, while the remains were then applied for Flag-tag immunoprecipitation. The input, the eluates from Strep-tag pull down, the beads from Flag-tag immunoprecipitation were boiled in sample buffer at 95°C for 10 min and subjected for SDS-PAGE and immunoblot analysis.

3.3.8 Protein purification

The protein purification of Usp28 WT and C171A was accomplished by Theresa Klemm. Human Usp28 catalytic domain (hUsp28cat, AA149-707) was cloned into pCDF-22 vector with the SLIC method (Li and Elledge, 2007) for expression of N-terminally thioredoxin-His-tagged hUsp28cat. The mutant C171A was then introduced by mutagenic PCR. The proteins were expressed in *E.coli* Rosetta 2 (DE3) cells and purified. The trx-His-tag was cleaved off and the pure protein was flash-frozen in liquid nitrogen followed by storage at -80°C.

3.3.9 Mass spectrometry analysis

Mass spectrometry analysis for ectopic β-TrCP2 was performed as previously described (Barenz *et al.*, 2013) with minor modifications by Dr. Thomas Ruppert.

3.3.10 Ubiquitination assay

His-Ub pulldown assay

To detect the Histidine-tagged ubiquitin (His-Ub) conjugation on proteins, HeLa cells transiently expressing His-Ub and the target proteins were collected and resuspended in 100 µl PBS, while 5 µl was kept as input. The cell suspension was lysed in 1 ml Urea buffer for 10 min at RT, followed by centrifuging at maxi speed for 10 min. The supernatant was transferred to a fresh tube with 20 µl of washed Ni-NTA beads (50%) and the samples were then rotated at RT for at least 4 h. Afterwards, beads were separated by centrifuging and washed with Ni-NTA wash buffer for 5 min rotating. The input and beads were boiled in sample buffer at 95°C for 10 min and spun down. The supernatants were proceeded for SDS-PAGE and immunoblot analysis.

In vivo deubiquitination assay

To detect deubiquitination of β-TrCP *in vivo*, cells overexpressing HA-tagged ubiquitin and Flag-tagged β-TrCP with WT- or C171A-Usp28 were applied for Flag-tag immunoprecipitation under the similar conditions as in non-denaturing immunoprecipitation protocol (see 3.3.7) with RIPA buffer replacing TNT150-300 buffer.

In vitro deubiquitination assay

To investigate deubiquitination of β-TrCP by Usp28 *in vitro*, cells overexpressing HA-tagged ubiquitin and Flag-tagged β-TrCP were used for Flag-tag non-denaturing immunoprecipitation with TNT150 buffer. After O/N incubation with cell lysates and the Flag-tag antibody, beads were washed with TNT150 buffer for 30 min, followed by washing with deubiquitination buffer for 30 min. The proteins bound to beads were eluted by Flag-peptide in deubiquitination buffer. The eluates were incubated with 1 µg Usp28-WT or -CA proteins at 30°C for 2 h. The reaction mix was then proceeded for immunoblot.

3.3.11 Structure model generation

The model of a dimeric β-TrCP1-Skp1 complex was created via superposing the crystal structure of the β-TrCP1-Skp1 complex (Wu *et al.*, 2003) and the dimeric β-TrCP1 with the small-angle X-ray scattering (SAXS)-based model of the homologous dimeric Cdc4-Skp1 complex (kindly provided by Frank Sicheri, Toronto) (Tang *et al.*, 2007). Superpositions and illustrations were done by Dr. Sonja Lorenz with the PyMOL Molecular Graphics System, Version 1.8 Schrödinger, LLC.

3.3.12 Chromatin immunoprecipitation (ChIP)

Chromatin immunoprecipitation (ChIP) was performed to investigate the interaction between proteins and DNA. Briefly, the chromatin was cross-linked with proteins and then isolated and fragmented, followed by immunoprecipitation with antibodies against target proteins. The enrichment of DNA bound to target proteins was measured by q PCR with primers for a certain DNA sequence of interest on chromatins.

Fixation and chromatin isolation

For one ChIP, subconfluent cells in 15 cm dish were fixed in 1% formaldehyde for 15 min at RT with gentle shaking, followed by addition of 125 mM Glycine to quench formaldehyde for 5 min at RT. The subsequent procedures were performed at 4°C or on ice. Cells were washed three times with chilled PBS and scraped off the dishes with PBS. The cell suspension was spun down at 800 x g for 5 min. The cell pellet was resuspended in 3 ml cytoplasmic lysis buffer with inhibitors and incubated on ice for 10 min. After centrifugation at 800 x g for 5 min, the nuclei were separated as pellets.

Nuclei digestion and shearing

To obtain DNA fragments between 200 - 800 bp, the nuclei were washed with MNase buffer and incubated with 1.8 µl MNase in 200 µl MNase buffer at 37°C for 18 min with shaking at 800 rpm. With addition of 20 µl EDTA, the digested nuclei were centrifugated at 13,000 rpm for 1 min, followed by resuspension in 200 µl Nuclear lysis buffer with inhibitors and incubation on ice for 10 min. To shear the nuclei, the

nuclei suspensions were sonified for 7 – 8 min at 50% amplitude and 50% cycles (30 s pulse, 1 min break) and incubated on ice for 10 min. After spinning down at 14,000 rpm for 10 min, 5 µl of the supernatant containing chromatin was taken as input and the remains were diluted 10 times with ChIP dilution buffer.

Chromatin size control

To control DNA fragments size, 10 µl non-diluted nuclei supernatant was mixed with 490 µl TE buffer, 160 mM NaCl and 20 µg/ml RNAse A and incubated at 37°C for 1h followed by 6 h or O/N at 65°C with shaking to reverse crosslink. Afterwards, 5 mM EDTA and 200 µg/ml Proteinase K was added and incubated at 45°C for 2 h. The DNA fragments were then isolated with Phenol/Chloroform extraction and precipitated with 100% EtOH and 3 M Na-acetate. The DNA pellet was washed with 80% EtOH and air dried, dissolved in 20 µl TE buffer. The DNA fragments were loaded with 6X loading buffer on 1.5% agarose gel and were separated to check the sizes.

Chromatin immunoprecipitation

The remained chromatin from one 15 cm dish was divided into 2 tubes for IgG- and target protein-IP. 2 µg IgG or antibody against target protein was added to chromatin and the samples were rotated O/N at 4°C.

On the next day, 5 µl Protein A or G magnetic beads for each sample were washed and incubated with blocking solution for 30 min on ice. A magnetic rack was applied to separate beads from solutions. The chromatin with antibody was spun down at 14,000 rpm for 10 min, the supernatant was transfer to the beads and incubated for 6 h at 4°C with rotating. Afterwards, the beads were washed 3 times with ChIP wash buffer I, RIPA high salt buffer II and RIPA LiCl2 buffer III, once with TE buffer. For each washing step, the beads were incubated on ice for 5 min.

DNA elution, reverse-crosslinking and purification

The input and beads were incubated with 1 µl RNAse A in 200 µl direct elution buffer for 1 h at 37°C, followed by O/N incubation at 65°C with intensive shaking to elute DNA and reverse crosslinking. The supernatant with eluted DNA was then transferred to a fresh tube with addition of 1.5 µl proteinase K and incubated at 45°C for 2 h.

The DNA was purified using MinElute PCR Purification Kit (Qiagen) according to manufacturer's protocol. DNA was eluted from the column with 40 µl elution buffer.

To identify the enrichment of DNA at specific genomic sites, qPCR was performed with 0.5 µl of DNA per reaction (see 3.2.3).

3.3.13 Next-generation sequencing

ChIP-Sequencing (ChIP-Seq)

For ChIP-Sequencing, ChIP procedures were performed as described in 3.3.12 and all the material were amplified 4 times. The DNA was eluted in 40 µl TE buffer and the concentration was determined with Quant-iT PicoGreen dsDNA reagent (Thermo Fisher Scientific).

ChIP-Seq DNA library preparation

ChIP-Seq DNA libraries were prepared with NEBNext® Ultra™ II DNA Library Prep Kit for Illumina following manufacturer's protocol with minor modifications. After DNA cleanup without size selection using HighPrep PCR beads, DNA were first enriched with 5 PCR cycles and purified again with HighPrep PCR beads. The purified DNA was loaded on 1.5% agarose gels and extracted with Monarch® DNA Gel Extraction Kit for size-selection (200-500 bp). The DNA libraries were then amplified with additional 5 PCR cycles and the concentration was detected with PicoGreen dsDNA reagent. The sequencing for the DNA libraries was performed on Illumina NextSeq 500 instrument (Core Unit Sys Med, University of Würzburg).

ChIP-Seq data analysis

All bioinformatical analyses of ChIP-Sequencing data were performed by Dr. Nikita Popov. The sequencing reads were aligned to the human genome hg19 with STAR aligner (Dobin *et al.*, 2013).

Independent ChIP-qPCR assays were performed to validate the individual peaks identified by ChIP-Sequencing with the primers listed in 2.7.1.

4 Results

4.1 Usp28 controls cell recovery from DNA damage

Previous studies showed that Usp28 controls DNA damage response via regulating 53BP1 stability to facilitate Chk2-p53-PUMA pathway (Zhang *et al.*, 2006), while another publication suggested that Usp28 has minor effects on DNA repair (Knobel *et al.*, 2014). These conflicting data leads us to investigate the role of Usp28 in regulating DDR using immortalized MEFs, which were isolated from Usp28-/- mice and analyzed in previous researches (Diefenbacher *et al.*, 2014; Schulein-Volk *et al.*, 2014). Usp28+/+ and Usp28-/- MEFs were treated with IR (Fig 4.1A) or phleomycin (a chemical which can generate DSBs) (Fig 4.1B), followed by re-plating with the same cell numbers for colony formation. Crystal violet staining for the colonies showed that DNA damage impaired the proliferation of both wildtype (WT) and Usp28 knockout (KO) cells. We quantified a series of colony formation assays with different IR doses and the results revealed that comparing to WT cells, Usp28 KO cells displayed enhanced long-term survival in response to either treatment (Fig 4.1A). This is in line with the observations in lung carcinoma H460 cells that Usp28 knockdown cells are more resistant to IR treatment (Zhang *et al.*, 2006). More efficient cell recovery from IR treatment was also observed via colony formation assays of HeLa Usp28-null cells, generated with CRISPR-mediated gene editing by Ravi Babu Kollampally (Fig 4.1C).

IR treatment didn't change Usp28 protein levels in MEFs and had no effect on subcellular localization of Usp28, shown by the immunofluorescence staining and immunoblot (Fig 4.1D, E). As a sensitive molecular marker for DNA damage (Banath *et al.*, 2010; Mah *et al.*, 2010), histone H2AX phosphorylation upon IR was determined via immunofluorescence staining and immunoblot with the antibody against phospho-Ser139-H2AX. The protein levels and foci of phospho-H2AX induced by IR treatment were similar in Usp28 WT and KO cells (Fig 4.1D, E).

Figure 4.1

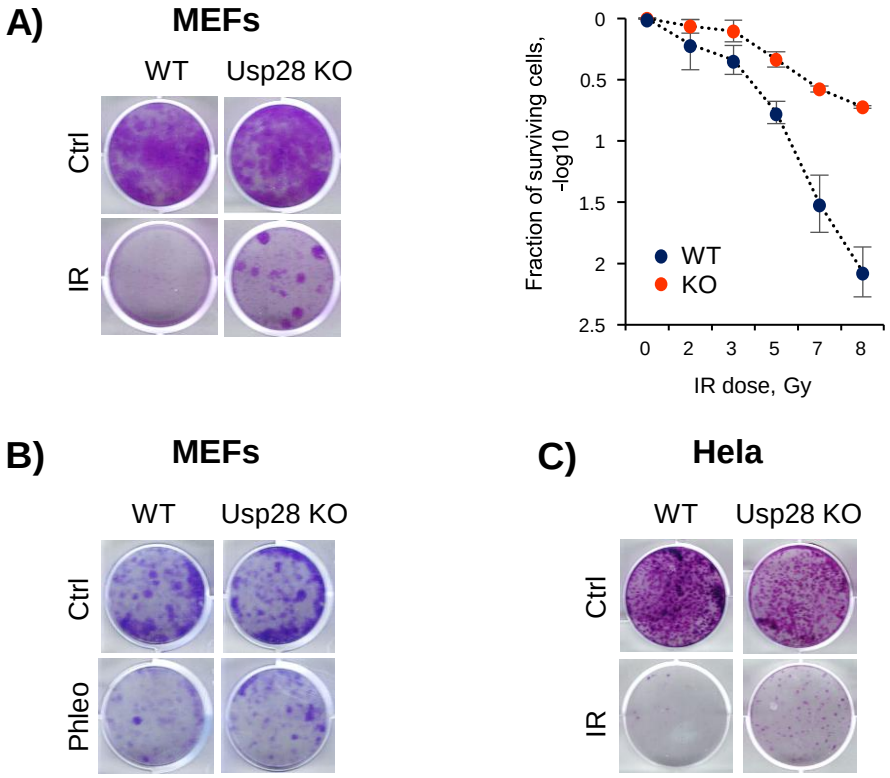

Figure 4.1. Usp28 controls cell recovery from DNA damage[1]

A) A representative colony formation assay of Usp28+/+ and Usp28-/- MEFs upon IR showing enhanced cell survival of Usp28-/- cells. Cells were treated with or without IR, re-plated with the same cell numbers and stained with crystal violet after 7 to 10 days culture. A series of assays with different IR doses were quantified. Error bars represent SD of three biological replicates.

B) C) Colony formation assays for phleomycin-treated Usp28 WT and KO MEFs (B), IR –treated HeLa Usp28 WT and KO cells (C). Cells were treated with phleomycin or IR and analyzed as in (A).

[1]This figure was included in a similar form in the manuscript (Xu *et al.*, in preparation) (see also following pages).

Figure 4.1

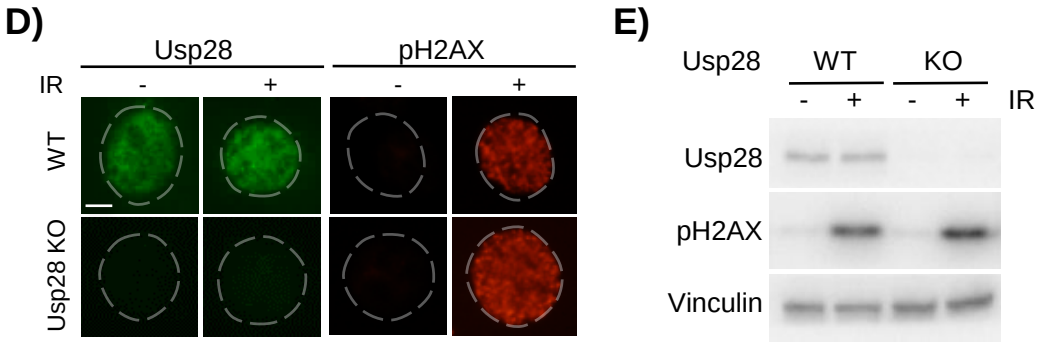

Figure 4.1. Usp28 controls cell recovery from DNA damage[1]

D) Immunofluorescent staining of phospho-Ser139-H2AX and Usp28 before and after IR in Usp28+/+ and Usp28-/- MEFs. Cells were stained with primary antibodies against phospho-Ser139-H2AX and Usp28 which were raised in different species, followed by incubation with corresponding secondary antibodies conjugated to individual fluorescent labels. Scale bar = 20μm.

E) Immunoblotting of phospho-Ser139-H2AX and Usp28 upon IR in WT and Usp28 KO MEFs.

4.2 Usp28 loss compromises DNA replication arrest and Cdc25A degradation induced by DNA damage

4.2.1 Usp28 deletion compromises DNA damage-induced DNA replication arrest

If Usp28 regulates DNA damage response through p53 pathway as suggested by previous studies (Meitinger *et al.*, 2016; Zhang *et al.*, 2006), Usp28-null cells should have lower induction of p53 that would enhance cell resistance to DNA damage. To investigate this, we examined the protein levels of p53 and p21, which is induced by p53 activation (Isaacs *et al.*, 1997), after IR treatment with immunoblotting. Surprisingly, IR-simulated induction of p53 and p21 in Usp28 KO cells were not compromised comparing to that in WT cells (Fig 4.2.1A), suggesting that the stabilization and activation of p53 in response to DNA damage were not impaired by Usp28 loss. These results indicate that Usp28 can regulate cellular response to DNA damage independently of p53.

Figure 4.2.1

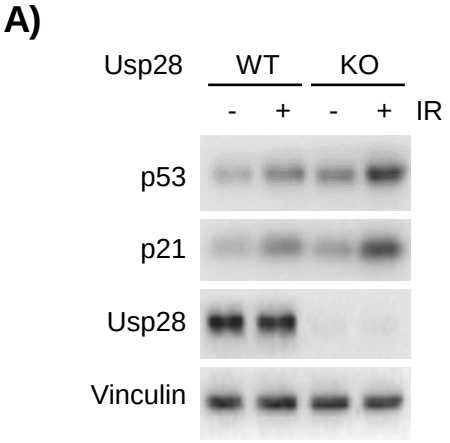

Figure 4.2.1. Usp28 deletion compromises DNA damage-induced DNA replication arrest[1].

A) Immunoblots of p53 and p21 revealing that the induction of p53 and p21 upon IR treatment was not attenuated in Usp28 KO MEFs.

In addition to p53 pathway modulation, DNA damage induces degradation of Cdc25A phosphatase, suppressing Cdk2 dephosphorylation and leading to rapid blockade of DNA replication (Falck *et al.*, 2001; Falck *et al.*, 2002). To analyze this pathway, we first performed BrdU-PI co-staining assays for WT and Usp28 KO MEFs after IR. BrdU was incorporated into DNA during active DNA synthesis and measured by FACS, while PI staining was applied to determine the DNA contents and the cell populations in distinct cell cycle phases. Cells were treated with IR or left untreated, followed by addition of nocodazole, and collected at the indicated timepoints with 30 min incubation of BrdU prior to collection. Quantification of four independent experiments showed that the fractions of BrdU-positive cells (Fig 4.2.1B, cells in the dashed boxes) were significantly downregulated in WT cells at 4 h and 8 h after IR, suggesting impaired DNA replication. However, this suppression was compromised in Usp28 KO cells. In addition, IR induced G1 phase arrest in WT cells, which was weakened in Usp28 KO cells. Supportively, as an alternative for BrdU, EdU labeling assays based on fluorescent staining showed persistent EdU incorporation in Usp28-null cells upon IR, whereas it was downregulated in WT cells (Fig 4.2.1C). These results suggest that Usp28 loss compromises DNA replication arrest in response to DNA damage, indicating the possible involvement of Cdc25A which can regulate DNA replication upon DNA damage.

Figure 4.2.1

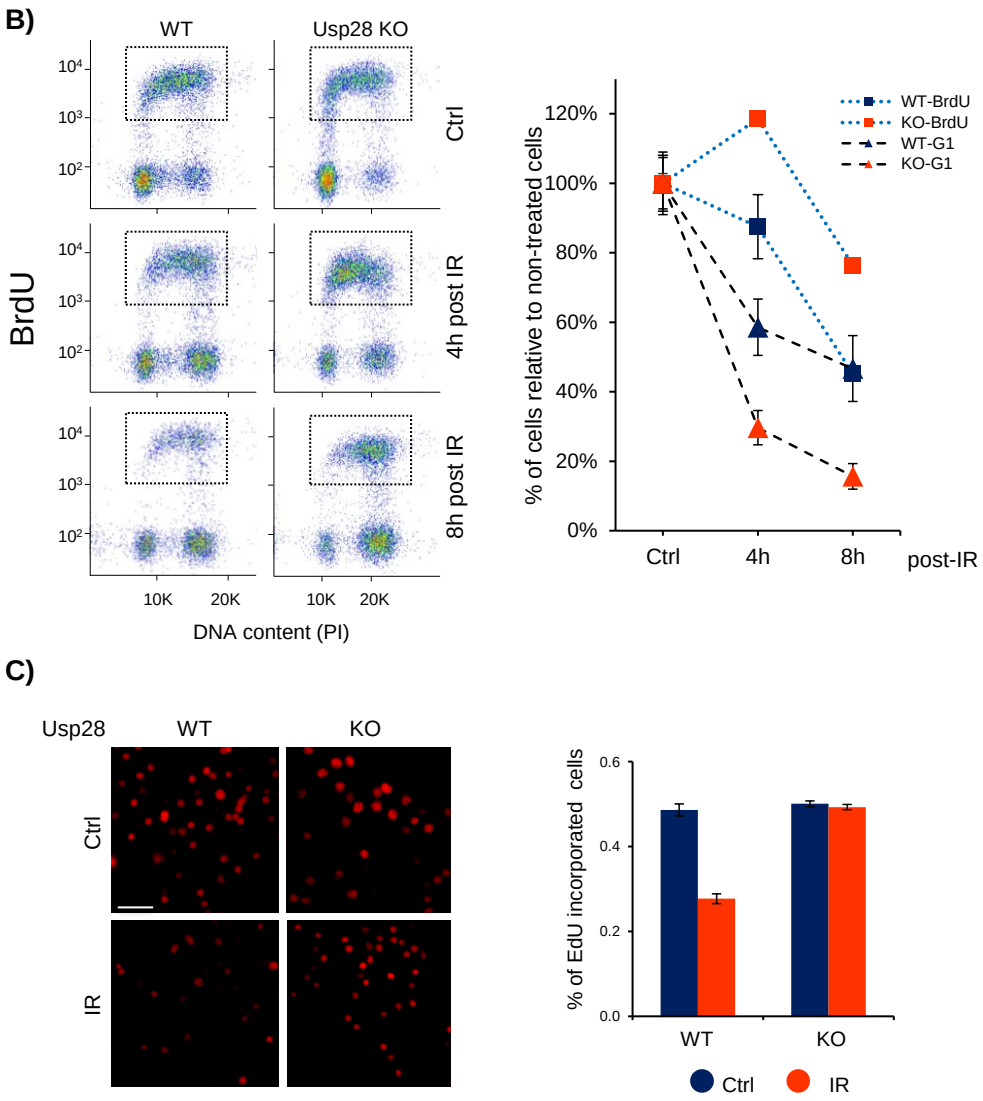

Figure 4.2.1. Usp28 deletion compromises DNA damage-induced DNA replication arrest[1].

B) BrdU/PI-FACS analysis for WT and Usp28 KO MEFs upon IR. Cells were treated with or without IR and exposed to Nocodazole immediately after IR. After 30 min incubation of BrdU, cells were collected at indicated timepoints and analyzed by FACS. The left panel showed the representative profile of FACS data and the right panel showed the quantification with 4 independent experiments. The fractions of BrdU-positive cells and cells in G1 phase were relative to those of non-treated cells. Error bar = SD.

C) Representative images for EdU incorporation in Usp28 WT and KO MEFs upon IR treatment. Cells were treated with IR and incubated with EdU for 10 min prior to fixation. EdU labeling assays were performed and visualized under a fluorescence microscope. At least 200 cells were counted for each independent experiment and three biological replicates were quantified for error bars (SD). Scale bar = 200 μm.

4.2.2 Usp28 loss impairs Cdc25A degradation induced by DNA damage

To investigate whether DNA damage-induced Cdc25A degradation accounts for the distinct regulation of DNA replication in WT and Usp28 KO cells, we detected the protein levels of Cdc25A upon IR in MEFs with immunoblotting. Concomitant with the arrest of DNA replication, IR and phleomycin induced rapid degradation of Cdc25A in WT MEFs, which was blocked by Usp28 loss (Fig 4.2.2A, C); this defect was accompanied by the persistent DNA synthesis (Fig 4.2.1B, C). In addition, we generated HCT116 and HeLa cells with a nearly complete Usp28 loss by stable expression of shRNA against Usp28. In these cells and HeLa Usp28 KO cells generated by CRISPR gene editing, Cdc25A destruction upon DNA damage was also attenuated as in MEFs (Fig 4.2.2D, E).

The levels of phosphorylated Chk2 and Chk1 upon IR were virtually identical in Usp28 WT and KO MEFs, suggesting similar levels of Cdc25A phosphorylation (Fig 4.2.2A). In line with Cdc25A levels, its target- Thr14/Tyr15- phosphorylated Cdk2 and Cdk1 were induced upon IR in WT cells, but not in Usp28-null cells (Fig 4.2.2B). Notably, the phosphorylated and total Cdk1 and Cdk2 levels at steady state were enhanced by Usp28 deletion (Fig 4.2.2B). The high basal levels of pCdk2 in Usp28 KO cells might contribute to the enhanced replication fork progression and cell recovery from DNA damage (see the discussion in section 5.5). Previous reports demonstrated that Cdc45 loading to pre-RCs is a critical Cdk2-dependent step for initiation of DNA replication and Cdc45 dissociates from Mcm7 upon DNA damage (Falck *et al.*, 2002; Fragkos *et al.*, 2015; Liu *et al.*, 2006). To analyze this, immunoprecipitation of endogenous Cdc45 after IR treatment from Benzonase-treated lysates of Usp28+/+ and Usp28-/- MEFs was performed and analyzed with immunoblotting for Mcm7 and histone H3. The results revealed the dissociation of Cdc45 from Mcm7 upon IR in WT cells, as well as downregulation of Cdc45 binding to histone H3 (Fig 4.2.2F), in line with induction of inactive phospho-Cdk2 (Fig 4.2.2B). These effects were blocked in Usp28-null cells that showed unaltered phospho-Cdk2 levels in response to IR. These data indicate that the persistent DNA replication upon DNA damage in Usp28-deleted cells results from the regulation of Cdc25A-Cdk2 pathway.

Figure 4.2.2

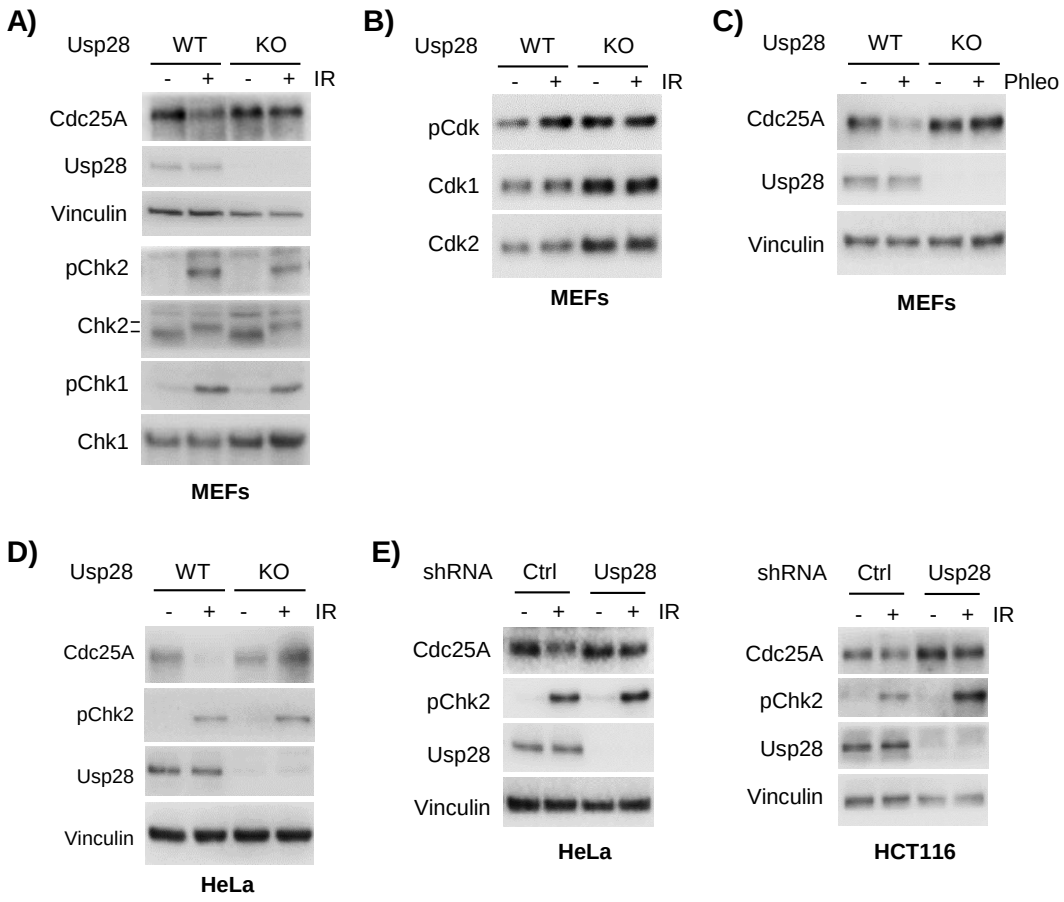

Figure 4.2.2. Usp28 loss impairs Cdc25A degradation induced by DNA damage[1].

A) B) C) Protein levels of Cdc25A, total and phosphorylated Chk1, Chk2, Cdk1 and Cdk2 in Usp28+/+ and Usp28-/-MEFs upon IR (A, B) and phleomycin (C) treatment.

D) E) Protein levels of Cdc25A and phosphorylated Chk2 in WT and Usp28 KO HeLa cells (D), as well as in control and Usp28 knockdown HeLa and HCT116 cells (E).

Cdc25A has been shown to be degraded by the ubiquitin-proteasome system (Busino *et al.*, 2003; Honaker *et al.*, 2010; Jin *et al.*, 2003). To determine whether the attenuated Cdc25A destruction upon IR in Usp28-null cells is mediated by proteasome, MEFs were treated with MG132, a cell-permeable proteasome inhibitor which effectively blocks the proteolytic activity of the 26S proteasome (Lee and Goldberg, 1996), before or after IR. Immunoblotting showed that MG132 treatment equalized the protein levels of Cdc25A in WT and Usp28 KO MEFs. The destruction of Cdc25A upon IR treatment in WT cells was also blocked by proteasome inhibition (Fig 4.2.2G).

Figure 4.2.2

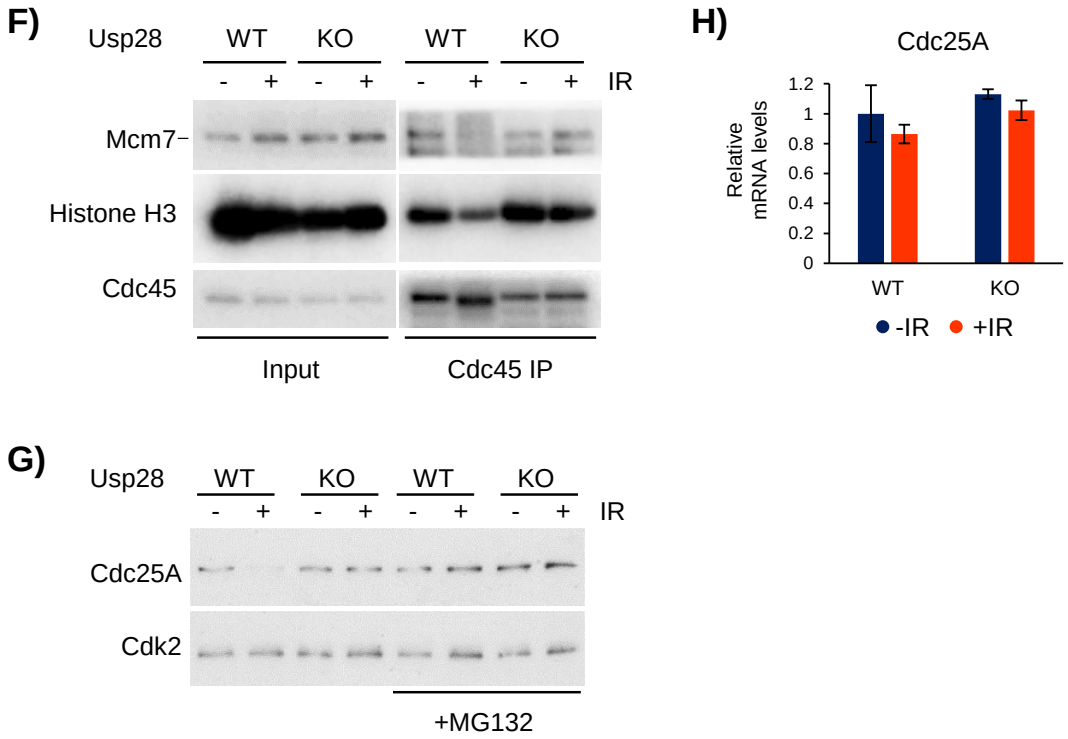

Figure 4.2.2. Usp28 loss impairs Cdc25A degradation induced by DNA damage[1].

F) Immunoprecipitation of Cdc45 showed dissociation of Cdc45 from Mcm7 and histone H3 upon IR in WT cells but not in Usp28 KO MEFs. Usp28+/+ and Usp28-/-MEFs were treated with or without IR, collected for non-denaturing immunoprecipitation with Cdc45 antibody and analyzed with immunoblotting.

G) Immunoblots showing that MG132 treatment rescued the decrease of Cdc25A levels upon IR in WT cells and equalized Cdc25A levels in WT and Usp28 KO MEFs. Cells were treated with EtOH or MG132 for 4 h before or after IR and collected for immunoblotting.

H) RT-qPCR analysis showed identical minor downregulation of Cdc25A mRNA levels in Usp28+/+ and Usp28-/- MEFs upon IR. Cells were treated with or without IR and collected for RNA isolation, followed by reverse transcription into cDNA and analysis with RT-qPCR. Error bars = SD.

Since the mRNA expression of Cdc25A can affect its protein levels, we detected Cdc25A mRNA levels in WT and Usp28 KO MEFs upon IR. Unlike protein levels, the slight downregulation of Cdc25A mRNA levels after IR were identical in Usp28+/+ and Usp28-/- MEFs (Fig 4.2.2H), suggesting the transcription of Cdc25A was not responsible for the distinct regulations of Cdc25A protein levels upon DNA damage. Taken together, these results suggest that Usp28 deletion compromises proteasomal

degradation of Cdc25A upon DNA damage, which results in attenuated DNA replication blockade.

4.3 Usp28 stimulates the activity of SCF(β-TrCP) ligase

4.3.1 Usp28 promotes the degradation of β-TrCP substrates

Previous studies established that Cdc25A is ubiquitinated and degraded by SCF(β-TrCP) ubiquitin ligase (Busino *et al.*, 2003; Jin *et al.*, 2003), and our data showed that the destruction of Cdc25A was impaired by Usp28 loss, indicating the possibility that Usp28 promotes β-TrCP-mediated substrate degradation. In fact, the protein levels of Cdc25A, as well as additional β-TrCP substrates including Bmi1, BimEL, IκB and Mcl1 (Banerjee Mustafi *et al.*, 2017; Dehan *et al.*, 2009; Ding *et al.*, 2007; Winston *et al.*, 1999), were higher in Usp28 KO MEFs and knockdown HCT116 and HeLa cells (Fig 4.3.1A). To determine the stability of these substrates, cells were treated with cycloheximide that inhibits protein synthesis, and were collected at indicated timepoints for immunoblotting. The results showed that Cdc25A and other β-TrCP substrates were rapidly turned over in WT cells, while the downregulations occurred slower in Usp28 KO MEFs (Fig 4.3.1B, C). Thus, β-TrCP substrates were more stable in Usp28-null cells.

As Cdc25A destruction upon DNA damage was compromised in Usp28-deficient cells, we detected the protein levels of other β-TrCP substrates after IR. Like Cdc25A, BimEL and Bmi1 were degraded in WT cells upon IR and this effect was attenuated by Usp28 deletion (Fig 4.3.1D). The phosphorylation of BimEL is mediated by Rsk1/2 and Erk1/2 kinases that are independent of checkpoint kinases (Dehan *et al.*, 2009). This suggests that Usp28 loss attenuates DNA damage-induced β-TrCP substrate degradation independently of checkpoint kinases-mediated substrate degron phosphorylation.

Additionally, we performed transient transfection assays to analyze the effect of Usp28 on β-TrCP-dependent substrate degradation. HeLa cells were transfected with plasmids encoding Cdc25A and either empty vector or plasmids encoding β-TrCP and Usp28, followed by harvesting after 24 h for immunoblotting. As expected, exogenous β-TrCP promoted the turnover of Cdc25A, which was stimulated by ectopic Usp28 (Fig 4.3.1E). Usp28 overexpression also promoted β-TrCP-mediated

degradation of endogenous BimEL and Bmi1 (Fig 4.3.1F). Distinct from Chk1/2-dependent phosphorylation of Cdc25A, the degrons of BimEL and Bmi1 are phosphorylated by different kinases (RsK1/2 and Erk1/2 for BimEL and CK1α for Bmi1) (Banerjee Mustafi *et al.*, 2017; Busino *et al.*, 2003; Dehan *et al.*, 2009; Jin *et al.*, 2003; Nacerddine *et al.*, 2012). The similar effects of Usp28 on different β-TrCP substrates indicate that Usp28 most likely regulates β-TrCP activity directly, as opposed to specifically modulating individual substrates.

Figure 4.3.1

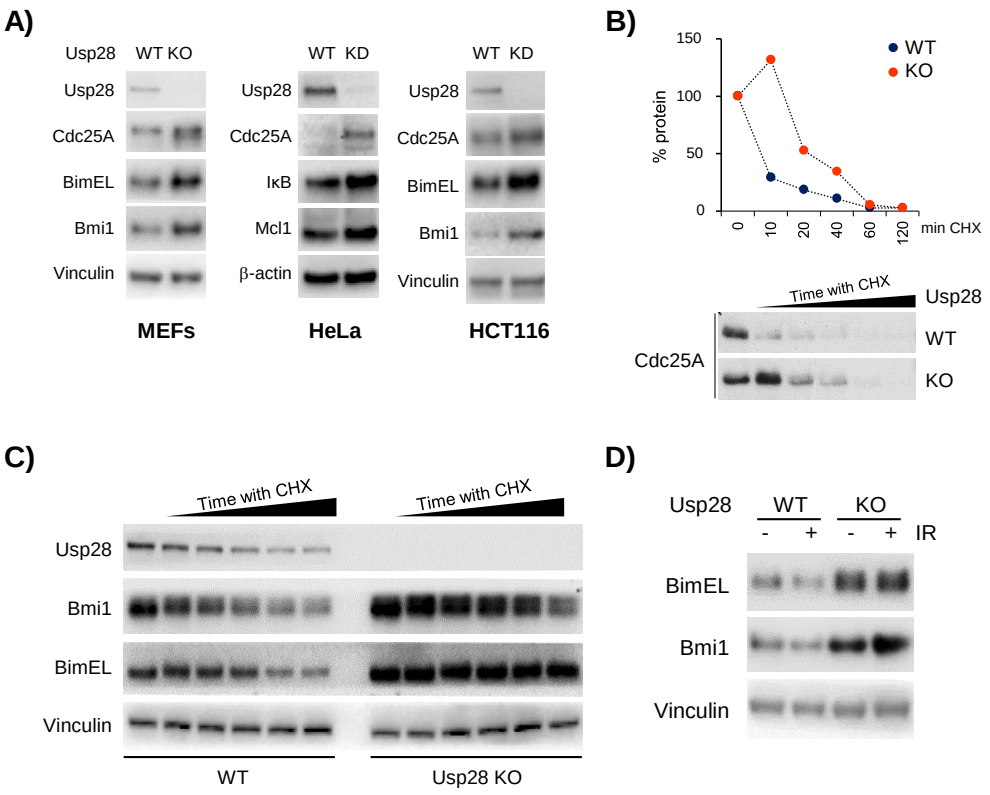

Figure 4.3.1. Usp28 promotes the degradation of β-TrCP substrates[1].

A) Immunoblots showing higher steady state levels of β-TrCP substrates in Usp28-/- MEFs, Usp28 knockdown HeLa and HCT116 cells.

B) Cycloheximide (CHX) chase assays demonstrating enhanced stability of Cdc25A in Usp28 KO MEFs. Cells were treated with CHX for the indicated time and collected for immunoblotting. The abundance of Cdc25A proteins was quantified, normalized against that of vinculin and relative to that in non-treated cells.

C) CHX chase assays for β-TrCP substrate stability in Usp28 WT and KO MEFs.

D) Immunoblots showing that Usp28 deletion suppressed IR-induced degradation of BimEL and Bmi1 in MEFs.

Figure 4.3.1

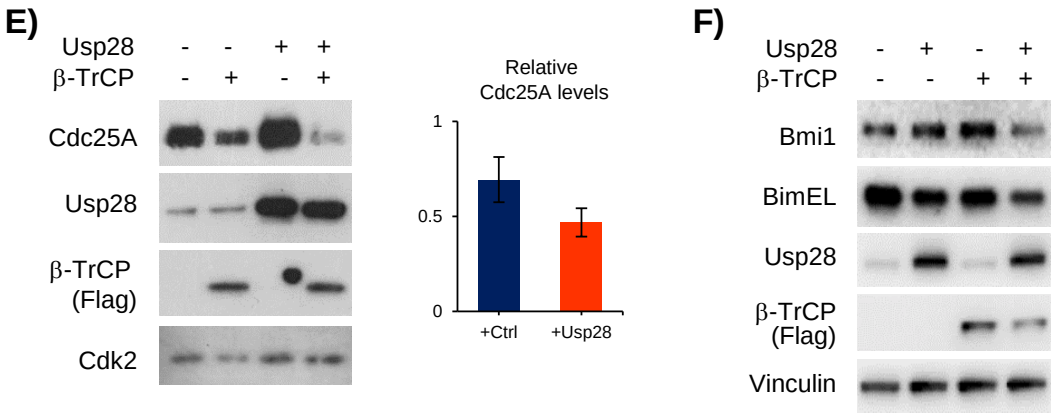

Figure 4.3.1. Usp28 promotes the degradation of β-TrCP substrates[1].

E) F) Immunoblots showed that overexpression of Usp28 promotes β-TrCP-dependent degradation of exogenous Cdc25A (E) and endogenous BimEL, Bmi1 (F). Cells transiently transfected with corresponding plasmids were lysed and analyzed with immunoblotting. Five independent experiments were quantified and Cdc25A protein abundance was normalized against loading control and relative to that of samples without ectopic β-TrCP, error bars = SD.

4.3.2 Usp28 binds to β-TrCP

To access the interaction between Usp28 and β-TrCP, we precipitated endogenous β-TrCP and observed binding of Usp28 in the immunoblot analysis (Fig 4.3.2A). In addition, we generated HeLa cells stably expressing HA-tagged β-TrCP by retroviral infection. Immunofluorescent staining for endogenous Usp28 and stably expressed HA-tagged β-TrCP in HeLa cells showed that they both localized in the nucleus (Fig 4.3.2B, left panels). Moreover, we performed proximity ligation assays (PLA) that can visualize protein-protein interactions and localizations via fluorescent signals. HeLa control and HA-tagged β-TrCP stably expressing cells were applied for PLA with the antibodies against HA-tag and Usp28. PLA signals in HA-β-TrCP expressing cells revealed the association between β-TrCP and endogenous Usp28 (Fig 4.3.2B, right panel).

Figure 4.3.2

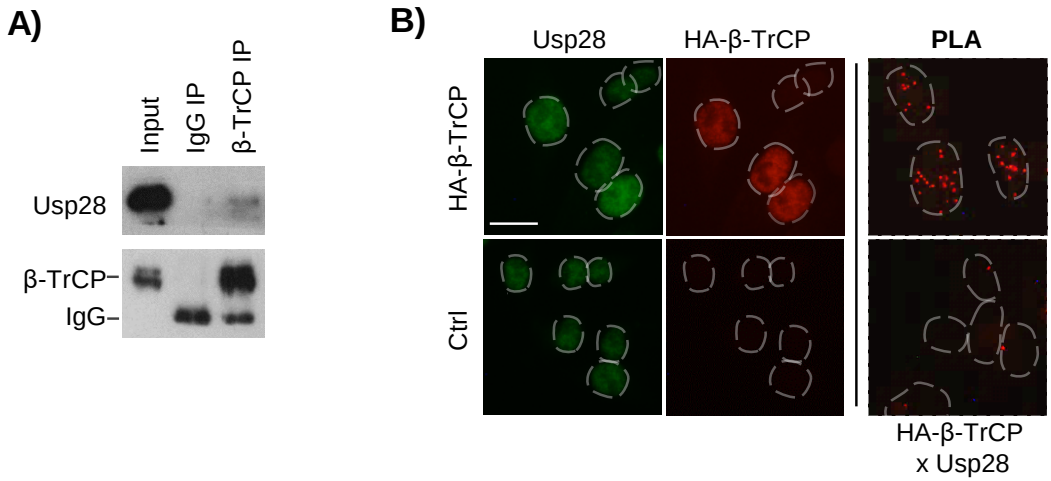

Figure 4.3.2. Usp28 binds to β-TrCP[1].

A) Immunoprecipitation of endogenous β-TrCP showing the interaction with Usp28.

B) PLA assays (right) with antibodies against HA-tag and Usp28 in HeLa cells stably expressing HA-β-TrCP documented the interaction between HA-β-TrCP and Usp28, revealed by the increasing signals comparing to those in control cells. IF staining (left) showed the nuclear localization of β-TrCP and endogenous Usp28. Scale bar = 20 μm.

β-TrCP consists of the D-domain and F-box domain in the N-terminus and the WD40 repeats that mediates substrate binding in the C-terminus. To map the Usp28 binding regions on β-TrCP, we generated recombinant β-TrCP2 plasmids with C-terminus (CT, AA 185-508) or N-terminus (NT, AA 1-184). HeLa cells were transfected with Flag-tagged β-TrCP2 full length or fragments and harvested for Flag-tag immunoprecipitation. The immunoblots for Flag-tag IP showed that Usp28 interacted with the WD40 repeats of β-TrCP (Fig 4.3.2C). Previous study demonstrated that substrates bind to β-TrCP via WD40 domain, in which Arg413 of β-TrCP2 (corresponding to Arg474 of β-TrCP1) contacts the phosphorylated residues of the DSG motif in substrates (Wu *et al.*, 2003). Thus, we detected the interaction between Usp28 and the Arg413 mutant of β-TrCP2 (R413A-β-TrCP). R413A-β-TrCP bound to Usp28 at the similar levels as WT-β-TrCP (Fig 4.3.2D), suggesting that the interaction between Usp28 and β-TrCP is distinct from typical substrates binding.

Figure 4.3.2

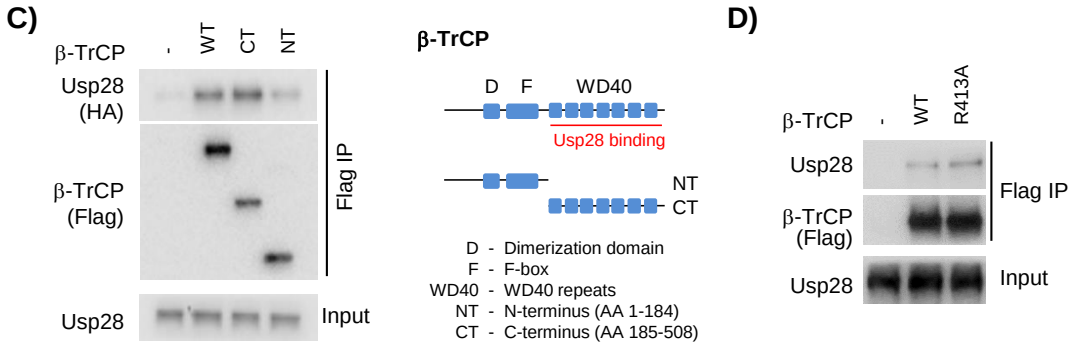

Figure 4.3.2. Usp28 binds to β-TrCP[1].

C) Immunoprecipitation of Flag-tagged β-TrCP WT and variants showed Usp28 binding to the WD40 repeats of β-TrCP. Cells were transiently transfected with corresponding plasmids and collected for IP. The schematic displayed the domains of β-TrCP.

D) Immunoprecipitation of Flag-tagged β-TrCP documenting that Arg413 mutation did not affect Usp28 binding to β-TrCP.

4.3.3 Usp28 deubiquitinates β-TrCP

Previous studies showed that the catalytic activity of Usp28 is necessary for regulating the abundance of multiple DNA damage signaling proteins and the activity of Fbw7 (Schulein-Volk *et al.*, 2014; Zhang *et al.*, 2006). To investigate whether the catalytic activity of Usp28 is required for promoting β-TrCP activity, WT and the catalytic-inactive C171A mutant Usp28 (Usp28-CA) were stably expressed in Usp28 KO MEFs via retroviral infection (Popov *et al.*, 2007). The reconstitution of WT-Usp28 downregulated the protein levels of Cdc25A, whereas the expression of C171A-Usp28 didn't (Fig 4.3.3A). This suggests that the stimulation of β-TrCP activity by Usp28 requires its catalytic activity.

Figure 4.3.3

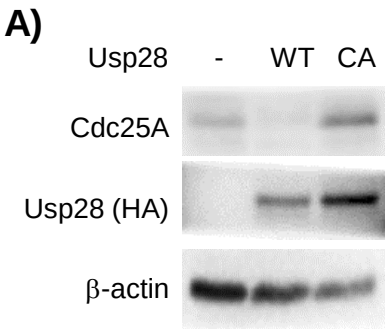

Figure 4.3.3. Usp28 deubiquitinates β-TrCP[1].

A) Immunoblots showing reduced protein levels of Cdc25A in Usp28-/- MEFs with stably expression of WT but not catalytic-inactive C171A (CA) Usp28. Usp28-/- MEFs were infected by retrovirus expressing WT- or C171A-Usp28 and collected for immunoblots.

To analyze if Usp28 can deubiquitinate β-TrCP, *in vivo* deubiquitination assay was performed. HeLa cells were transiently transfected with HA-tagged ubiquitin, Flag-tagged β-TrCP and WT- or CA-Usp28 and treated with or without IR before harvesting. Immunoprecipitation for Flag-tagged β-TrCP with cell lysates in RIPA buffer was performed, followed by immunoblotting with a HA antibody to detect ubiquitinated β-TrCP. In the absence of exogenous Usp28, β-TrCP showed a strong ubiquitination signal. Ectopic WT-Usp28 significantly downregulated β-TrCP ubiquitination, while catalytic-inactive Usp28 didn't (Fig 4.3.3B). Importantly, β-TrCP was deubiquitinated after IR in the absence of exogenous Usp28, while this effect was blocked by overexpression of C171A-Usp28 (Fig 4.3.3B). This suggests that endogenous Usp28 is responsible for IR-induced β-TrCP deubiquitination. In addition, denaturing immunoprecipitation of endogenous β-TrCP from MEFs were performed and analyzed by immunoblotting with a ubiquitin antibody to detect ubiquitinated β-TrCP. β-TrCP was deubiquitinated in Usp28-proficient cells upon IR treatment, while this effect was attenuated in Usp28 KO cells (Fig 4.3.3C), supporting the results of overexpressed β-TrCP (Fig 4.3.3B). Moreover, we performed *in vitro* deubiquitination assay – Flag-tagged β-TrCP proteins modified with HA-tagged ubiquitin were transiently expressed in HeLa cells and isolated by Flag-tag immunoprecipitation, followed by reaction with Usp28- WT or -CA proteins purified from *E.coli* Rosetta 2 (DE3) cells. Consistent with the results of *in vivo* assay, WT-Usp28 but not the

catalytic-inactive Usp28 deubiquitinated β-TrCP *in vitro* (Fig 4.3.3D).

Figure 4.3.3

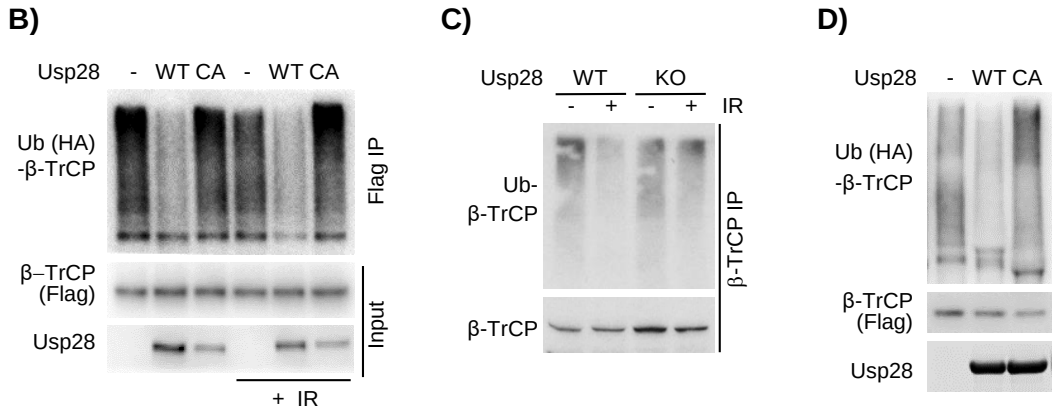

Figure 4.3.3. Usp28 deubiquitinates β-TrCP[1].

B) *In vivo* deubiquitination assay for β-TrCP by Usp28-WT or -CA upon IR treatment. HeLa cells were transfected with HA-tagged ubiquitin, Flag-tagged β-TrCP and corresponding Usp28 plasmids and treated with or without IR before harvesting. Flag-tagged β-TrCP was precipitated in RIPA buffer and analyzed by immunoblotting.

C) Denaturing IP for β-TrCP showing IR-induced deubiquitination of endogenous β-TrCP in Usp28+/+ but not Usp28-/- MEFs. Cells were treated with IR and collected for denaturing IP with β-TrCP antibody, followed by immunoblotting with ubiquitin antibody.

D) *In vitro* deubiquitination assays for β-TrCP by Usp28-WT or -CA. Flag-tagged β-TrCP and HA-tagged ubiquitin were transiently expressed in HeLa cells and isolated by Flag-tag immunoprecipitation, followed by reaction with WT/CA-Usp28 proteins purified from *E.coli* Rosetta 2 (DE3) cells and immunoblot analysis with HA antibody.

Since protein ubiquitination can result in proteolytic and non-proteolytic regulation, we asked whether deubiquitination of β-TrCP by Usp28 affects β-TrCP stability. Cycloheximide chase assays for MEFs showed similar turnover rates of β-TrCP in WT and Usp28 KO cells, suggesting the deubiquitination of β-TrCP by Usp28 regulates β-TrCP activity in a non-proteolytic manner without affecting its stability.

Figure 4.3.3

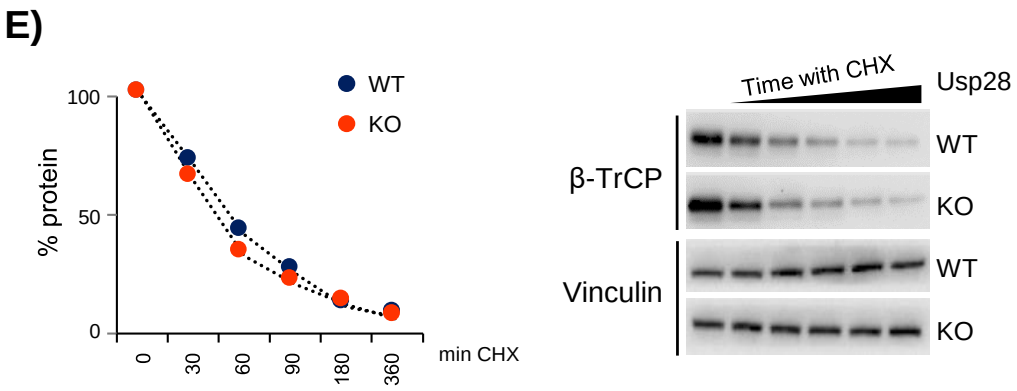

Figure 4.3.3. Usp28 deubiquitinates β-TrCP[1].

E) Cycloheximide chase assays documented identical β-TrCP stability in Usp28 WT and KO MEFs. Cells were treated with cycloheximide for indicated time and harvested for immunoblots. The abundance of β-TrCP proteins was quantified, normalized against that of vinculin and relative to that in non-treated cells.

4.4 Usp28 promotes dimerization of β-TrCP

The question then arose was how deubiquitination by Usp28 promotes β-TrCP activity. It has been demonstrated that in addition to regulate substrate recruitment, self-ubiquitination of E3 ligases correlates with their self-association and regulates their activities (Fuchs *et al.*, 1999; Li *et al.*, 2004; Petroski and Deshaies, 2005). Previous studies reported that the dimer-deficient Fbw7 and Cdc4 with the mutation in the dimerization interface have higher levels of self-ubiquitination (Min *et al.*, 2012; Tang *et al.*, 2007). Conversely, dimerization of Fbw7 and Cdc4 enhances their activity in mediating ubiquitination and degradation of multiple substrates (Tang *et al.*, 2007; Welcker *et al.*, 2013). Similarly, it has been shown that β-TrCP dimerization is necessary for the ubiquitination of IκB (Suzuki *et al.*, 2000). We reasoned, therefore, that the deficiency of deubiquitinating β-TrCP in Usp28-null cells inhibits β-TrCP dimerization, which results in suppressed activity in substrate degradation.

4.4.1 β-TrCP dimerization is required for its activity and is promoted by Usp28

To investigate the role of dimerization in β-TrCP function, we generated dimer-deficient β-TrCP (ΔD) with mutations in the dimerization interface of β-TrCP D-domain (LI at 61, 62 were replaced with EE). The corresponding mutant in the D-domain of Cdc4 was shown to be dimer-deficient previously (Tang *et al.*, 2007). To detect the dimerization ability of ΔD-β-TrCP, HA-tagged β-TrCP and Flag-tagged β-TrCP WT or ΔD were transiently expressed in HeLa cells, followed by Flag-tag immunoprecipitation. ΔD-β-TrCP showed strongly impaired binding to HA-tagged β-TrCP, confirming that ΔD-β-TrCP is dimer-deficient (Fig 4.4.1A). His-Ub pulldown assays from HeLa cells transiently expressing His-tagged ubiquitin and WT- or ΔD-β-TrCP demonstrated that the self-ubiquitination of dimer-deficient β-TrCP was strongly accumulated (Fig 4.4.1B), supporting the former studies on Fbw7 and Cdc4 (Min *et al.*, 2012; Tang *et al.*, 2007).

Figure 4.4.1

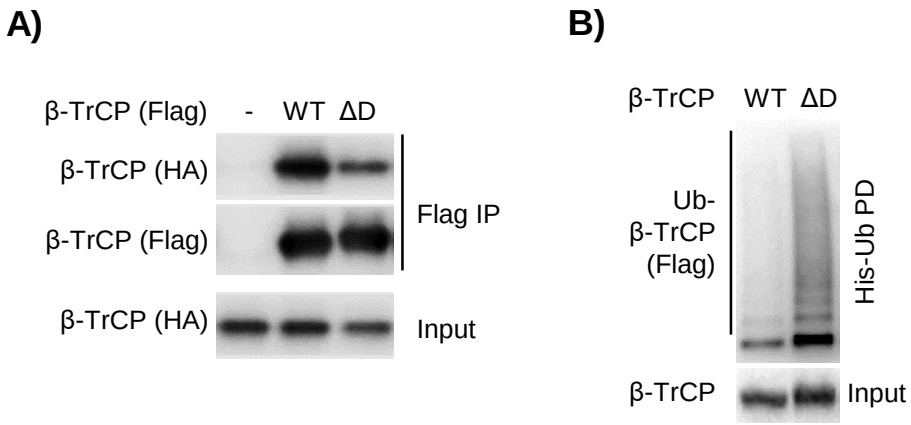

Figure 4.4.1. β-TrCP dimerization is required for its activity and is promoted by Usp28[1].

A) Immunoprecipitation of Flag-tagged β-TrCP demonstrated that ΔD-β-TrCP was dimer-deficient. HeLa cells were transiently transfected with HA-tagged β-TrCP and Flag-tagged β-TrCP-WT or -ΔD, followed by Flag-tag immunoprecipitation and immunoblot analysis.

B) His-Ub pull down assay for ectopic β-TrCP revealing elevated self-ubiquitination of the dimer-deficient β-TrCP. Cells expressing His-Ub and Flag-tagged β-TrCP-WT or -ΔD were collected and pulled down by Ni-NTA beads, followed by immunoblotting.

Figure 4.4.1

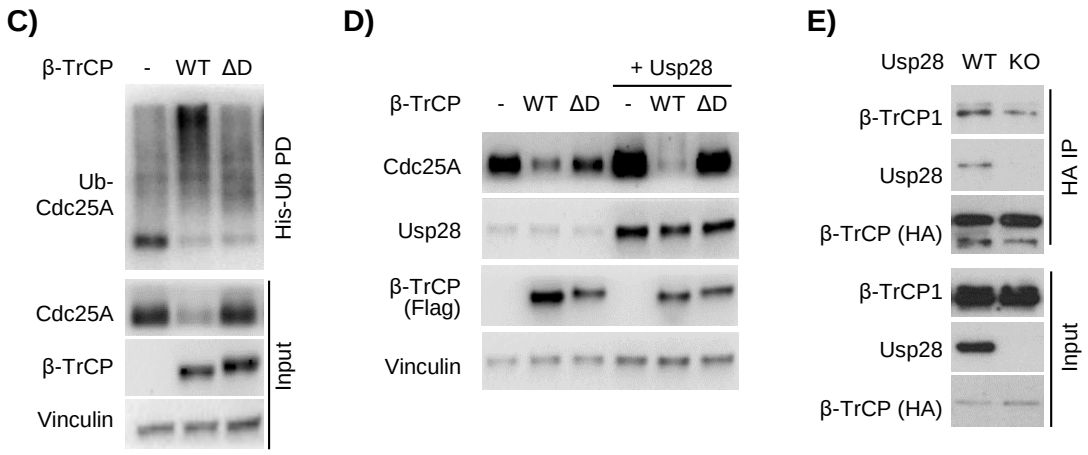

Figure 4.4.1. β-TrCP dimerization is required for its activity and is promoted by Usp28[1].

C) His-Ub pull down assay for exogenous Cdc25A after transient transfection showing that Cdc25A was ubiquitinated and degraded by WT but not dimer-deficient β-TrCP.

D) Cdc25A degradation by β-TrCP in the absence or presence of Usp28. HeLa cells were transient transfected with the plasmids encoding Cdc25A, corresponding β-TrCP and Usp28 and analyzed with immunoblotting.

E) Immunoprecipitation of stably expressed HA-tagged β-TrCP documenting the impaired binding to endogenous β-TrCP in Usp28-/- MEFs.

To analyze the activity of the dimer-deficient β-TrCP, we performed His-Ub pulldown assays for ectopic Cdc25A in the presence of WT- or ΔD-β-TrCP. The results demonstrated that Cdc25A was strongly ubiquitinated and degraded by WT-β-TrCP, while ΔD-β-TrCP showed significantly impaired activity (Fig 4.4.1C), in line with a previous study which reported that dimeric β-TrCP promotes the ubiquitination of IκB (Suzuki *et al.*, 2000). As shown previously, ectopic Usp28 promotes WT-β-TrCP-mediated degradation of Cdc25A in transient transfection assays (Fig 4.4.1D). However, the activity of ΔD-β-TrCP was not enhanced by Usp28 (Fig 4.4.1D). To investigate the effect of Usp28 on β-TrCP dimerization, we immunoprecipitated stably expressed HA-tagged β-TrCP from HeLa WT and Usp28 KO cells. The binding of endogenous β-TrCP to HA-tagged β-TrCP was suppressed by Usp28 loss, indicating that Usp28 promotes β-TrCP dimerization (Fig 4.4.1E). This can explain why Usp28 didn't enhance the activity of ΔD-β-TrCP, as ΔD-β-TrCP couldn't form dimer after

Usp28-mediated deubiquitination. These results support the hypothesis that Usp28 promotes dimerization of β-TrCP to stimulate its activity.

4.4.2 Ubiquitination of β-TrCP directly modulates its activity

β-TrCP is known to be self-ubiquitinated (Li *et al.*, 2004), but it remains unclear which lysines in β-TrCP are ubiquitin acceptor sites. To determine whether β-TrCP activity is directly regulated via ubiquitination, we created a mutant of β-TrCP with all lysines replaced by arginines (β-TrCP-KR), as the same type of mutant was previously applied to analyze ubiquitination-mediated regulation of protein activity and degradation (Batonnet *et al.*, 2004; Jaenicke *et al.*, 2016; Li *et al.*, 2009). His-Ub pulldown assays showed absence of ubiquitination signal for β-TrCP-KR, confirming that β-TrCP-KR is ubiquitination-deficient (Fig 4.4.2A).

Comparing to β-TrCP-WT, β-TrCP-KR showed enhanced activity in mediating Cdc25A ubiquitination and degradation, revealed by His-Ub pulldown assays (Fig 4.4.2B, C). Furthermore, we introduced the mutations within the dimerization interface (L61E and I62E) into β-TrCP-KR to generate the dimer-deficient β-TrCP-KR (β-TrCP-KRΔD). The activity of β-TrCP-KRΔD in Cdc25A degradation was suppressed comparing to that of either WT- or KR-β-TrCP (Fig 4.4.2C), suggesting that the higher activity of non-ubiquitinated β-TrCP was due to an enhanced dimerization. Moreover, Cdc25A degradation by β-TrCP-KR was not stimulated by Usp28, likely because Usp28 is unable to deubiquitinate β-TrCP-KR (Fig 4.4.2C). These data indicate that Usp28 promotes the activity of β-TrCP by direct deubiquitination.

Since monomeric β-TrCP was highly ubiquitinated, we asked whether ubiquitinated β-TrCP can dimerize. To investigate this, we performed sequential pulldown experiments from cells overexpressing Strep-HA-β-TrCP, Flag-tagged β-TrCP and HA-tagged ubiquitin. Strep-tagged pulldowns for β-TrCP were performed and the beads were eluted under denaturing conditions. Cell lysates and Strep-tag pulldown eluates were used for Flag-tagged β-TrCP immunoprecipitation. In this assay, efficient binding of Strep-HA-β-TrCP was observed in Flag-tagged β-TrCP IP from cell lysates. However, the Flag-tag IP with the eluates from Strep-tag pulldowns showed only unmodified Strep-HA-β-TrCP binding, demonstrating that β-TrCP ubiquitination interferes with its dimerization (Fig 4.4.2D).

Figure 4.4.2

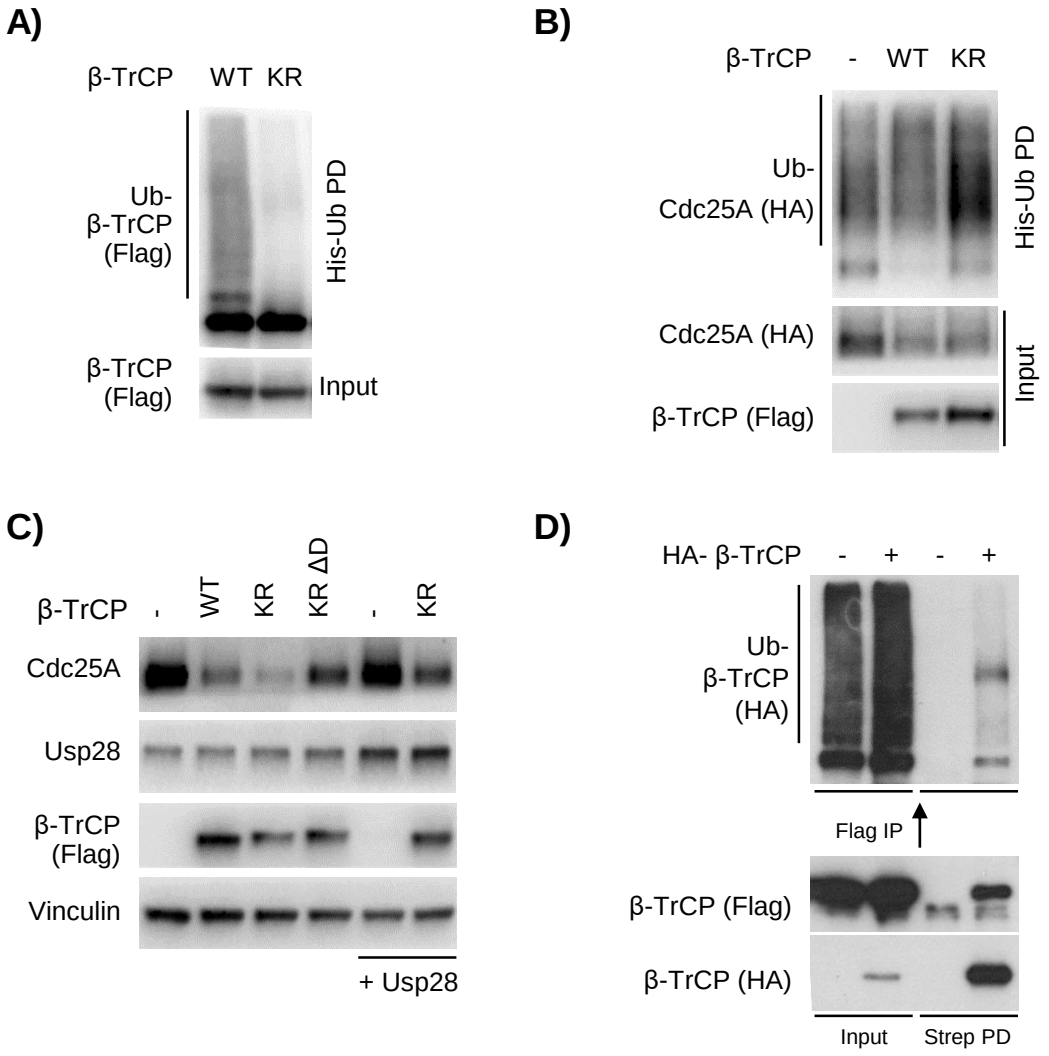

Figure 4.4.2. Ubiquitination of β-TrCP directly modulates its activity[1].

A) His-Ub pulldown assay showing ubiquitination-deficiency of KR-β-TrCP in transient transfection.

B) The ubiquitination levels of ectopic Cdc25A was promoted by KR mutation in β-TrCP in His-Ub pulldown assay. Cells were transfected with Cdc25A, His-Ub and the corresponding β-TrCP alleles and treated with MG132 for 4 h, followed by His-Ub pulldown.

C) Ectopic Cdc25A degradation by β-TrCP-WT and corresponding variants with or without co-expression of Usp28.

D) Sequential pulldown assays showing that the dimeric β-TrCP were unmodified. Cells overexpressing Strep-HA-β-TrCP, Flag-β-TrCP and HA-Ub were collected for Flag-tag IP from cell lysates and the eluates from Strep-tag pulldowns, followed by immunoblot analysis.

4.4.3 Site-specific ubiquitination at Lys430 inhibits β-TrCP activity

To determine the ubiquitin acceptor sites in β-TrCP, mass spectrometry analysis for ectopic affinity-purified β-TrCP2 was performed by Dr. Thomas Ruppert. A single ubiquitin acceptor in β-TrCP2 at Lys430 was identified, as the MS/MS spectrum of the tryptic peptide corresponding to AA 422-432 of β-TrCP2 showed a mass increase corresponding to the Gly-Gly moiety (114 Da) at K430 (Fig 4.4.3A, B).

Figure 4.4.3

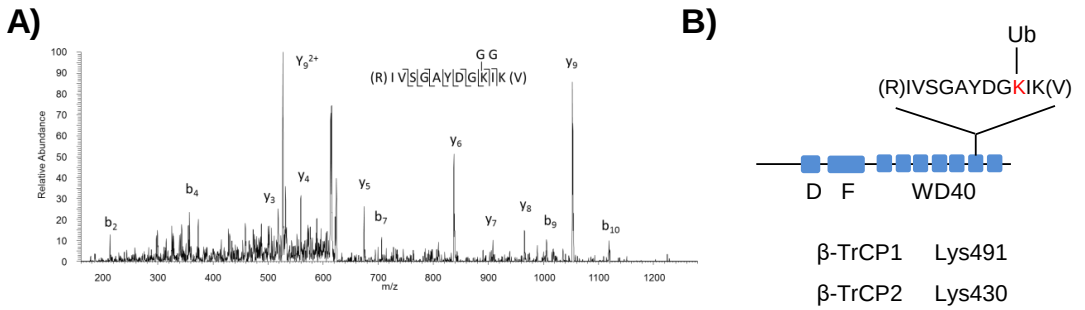

Figure 4.4.3. Site-specific ubiquitination at Lys430 inhibits β-TrCP activity[1].

A) The MS/MS spectrum of the tryptic peptide corresponding to AA 422-432 of human β-TrCP2 (IVSGAYDGKIK), showing a mass increase at K430, suggesting that a single ubiquitin acceptor at K430 was identified.

B) The schematic structure of β-TrCP displayed the location of Lys430.

We generated the mutation of K430 to arginine (β-TrCP-K430R) to inhibit the ubiquitination at this site, which was applied to investigate whether this site-specific ubiquitination affect β-TrCP function. We first performed His-Ub pulldown assays to detect Cdc25A ubiquitination by β-TrCP-K430R from transiently transfected cells after MG132 treatment. β-TrCP-K430R showed higher activity in mediating Cdc25A ubiquitination (Fig 4.4.3C), as well as in promoting Cdc25A degradation (Fig 4.4.3D). In line with this, comparing to β-TrCP-WT, ectopic β-TrCP-K430R was more active in mediating Cdc25A degradation in Usp28 KO cells (Fig 4.4.3E).

Supporting the idea that ubiquitination inhibits dimerization of β-TrCP, immunoprecipitation of HA-tagged β-TrCP-WT or -K430R from stably expressing cells revealed that β-TrCP-K430R had higher ability in dimerizing with endogenous β-TrCP1 (Fig 4.4.3F). Taken together, blockade of β-TrCP ubiquitination at K430

mimicked the effects of Usp28, indicating that this site-specific ubiquitination is a direct target of Usp28 and inhibits β-TrCP dimerization.

Figure 4.4.3

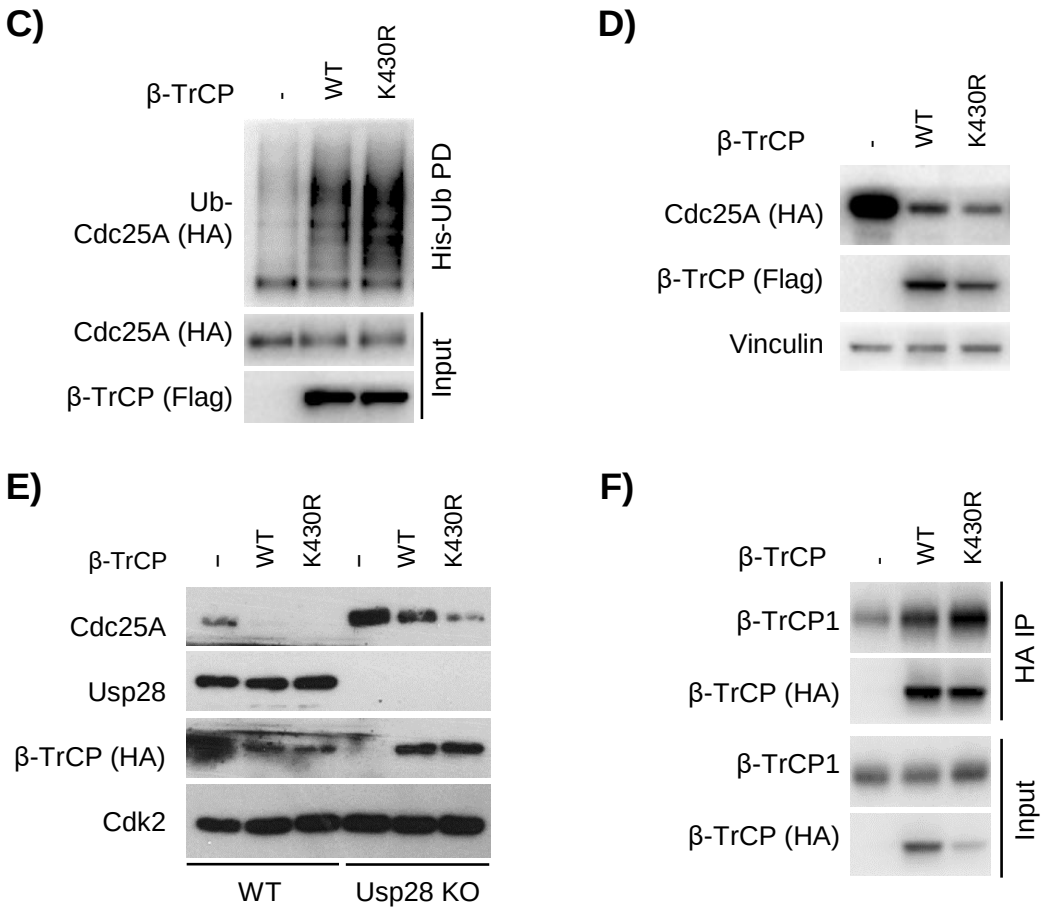

Figure 4.4.3. Site-specific ubiquitination at Lys430 inhibits β-TrCP activity[1].

C) His-Ub pulldown after MG132 treatment showing the higher levels of ectopic Cdc25A ubiquitination mediated by β-TrCP-K430R in transient transfection assay. Cells transiently expressing corresponding plasmids were treated with MG132 for 4 h and collected for His-Ub pulldown.

D) Ectopic Cdc25A degradation by β-TrCP-WT and -K430R revealing the enhanced activity of K430R-β-TrCP.

E) Ectopic Cdc25A protein levels in WT and Usp28 KO HeLa cells transiently expressing WT- or K430R-β-TrCP.

F) Immunoprecipitation of stably expressed HA-β-TrCP -WT or -K430R showing better interaction of K430R-β-TrCP with endogenous β-TrCP1.

4.4.4 Ubiquitination at Lys430 interferes with β-TrCP dimerization

Tang *et al.* have established the structure of β-TrCP1 D-domain and generated the model of the homologous dimeric Cdc4-Skp1 complex based on small-angle X-ray scatter (SAXS) measurements (Tang *et al.*, 2007). Via superposing the β-TrCP1 D-domain structure and the crystal structure of the β-TrCP1-Skp1 complex (Wu *et al.*, 2003) with the model of the homologous dimeric Cdc4-Skp1 complex (Tang *et al.*, 2007), a structure mode of the dimeric β-TrCP1-Skp1 complex was generated by Dr. Sonja Lorenz (Fig 4.4.4A, B). Intriguingly, this model shows that K491 of β-TrCP1 (corresponding to K430 of β-TrCP2) localizes in the region where the two propeller domains of β-TrCP dimer subunits are close in proximity. Therefore, we hypothesized that ubiquitin chain conjugated to this site might disrupt the orientation of the propeller domains and inhibit the formation of β-TrCP dimers, supporting the experimentally observation that K430R-β-TrCP2 showed enhanced ability to dimerize (Fig 4.4.3F).

Figure 4.4.4

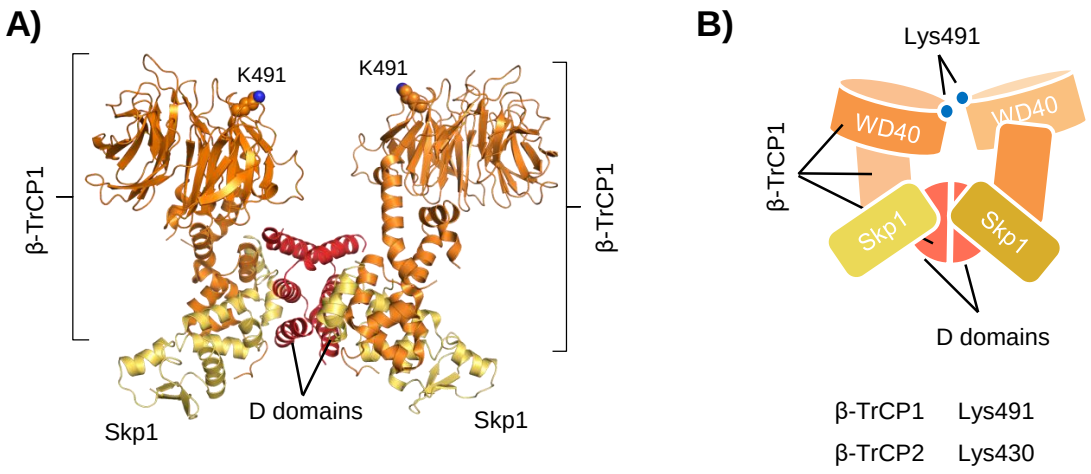

Figure 4.4.4. Ubiquitination at Lys430 interferes with β-TrCP dimerization[1].

A) Crystal structure model of dimeric β-TrCP1-Skp1 complex with the location of Lys491 in β-TrCP1, corresponding to Lys430 in β-TrCP2.

B) A simplified model of dimeric β-TrCP-Skp1 complex.

4.5 Usp28 and β-TrCP promote 53BP1 degradation upon DNA damage

4.5.1 Usp28 promotes β-TrCP-dependent 53BP1 degradation

A previous study by Zhang *et al.* showed that Usp28 is a 53BP1-interaction protein and stabilizes 53BP1 in response to DNA damage (Zhang *et al.*, 2006), whereas Knobel *et al.* demonstrated that Usp28 deletion had minor effect on 53BP1 stability (Knobel *et al.*, 2014). As 53BP1 is a key mediator protein of DSB repair (Adams and Carpenter, 2006; Noon and Goodarzi, 2011), we first determined 53BP1 protein levels upon IR in Usp28-/- MEFs, Usp28 knockout HeLa and knockdown HCT116 cells. IR treatment induced rapid degradation of 53BP1 in WT cells, as shown in previous studies (Fig 4.5.1A) (Hu *et al.*, 2014; Mayca Pozo *et al.*, 2017). Surprisingly, this downregulation of 53BP1 was suppressed in all these cell lines lacking Usp28 (Fig 4.5.1A), similar to Cdc25A and other β-TrCP substrates. Accordingly, we asked whether 53BP1 is degraded in a β-TrCP-dependent manner.

To test this idea, β-TrCP1 knockout HCT116 cells using CRISPR technology were generated by Lyudmyla Taranets. In fact, β-TrCP1 knockout cells had higher levels of 53BP1 and other β-TrCP substrates like Bmi1 at steady states (Fig 4.5.1B). Furthermore, we generated F-box deleted β-TrCP variant (β-TrCP-ΔF, AA 95-133 deleted, Fig 4.5.1C), which has been shown to be a dominant-negative allele in previous studies (Latres *et al.*, 1999; Sharma *et al.*, 2015). In transient transfection assays, ectopic WT-β-TrCP promotes the destruction of endogenous 53BP1, while ΔF-β-TrCP didn't (Fig 4.5.1D). Consistently, the stable expression of β-TrCP-ΔF via retroviral infection in HeLa and KPC cells upregulated 53BP1 and Cd25A levels and attenuated IR-induced degradation of 53BP1 (Fig 4.5.1E, F). Taken together, these data suggest that Usp28 promotes 53BP1 degradation in a β-TrCP-dependent manner.

Figure 4.5.1

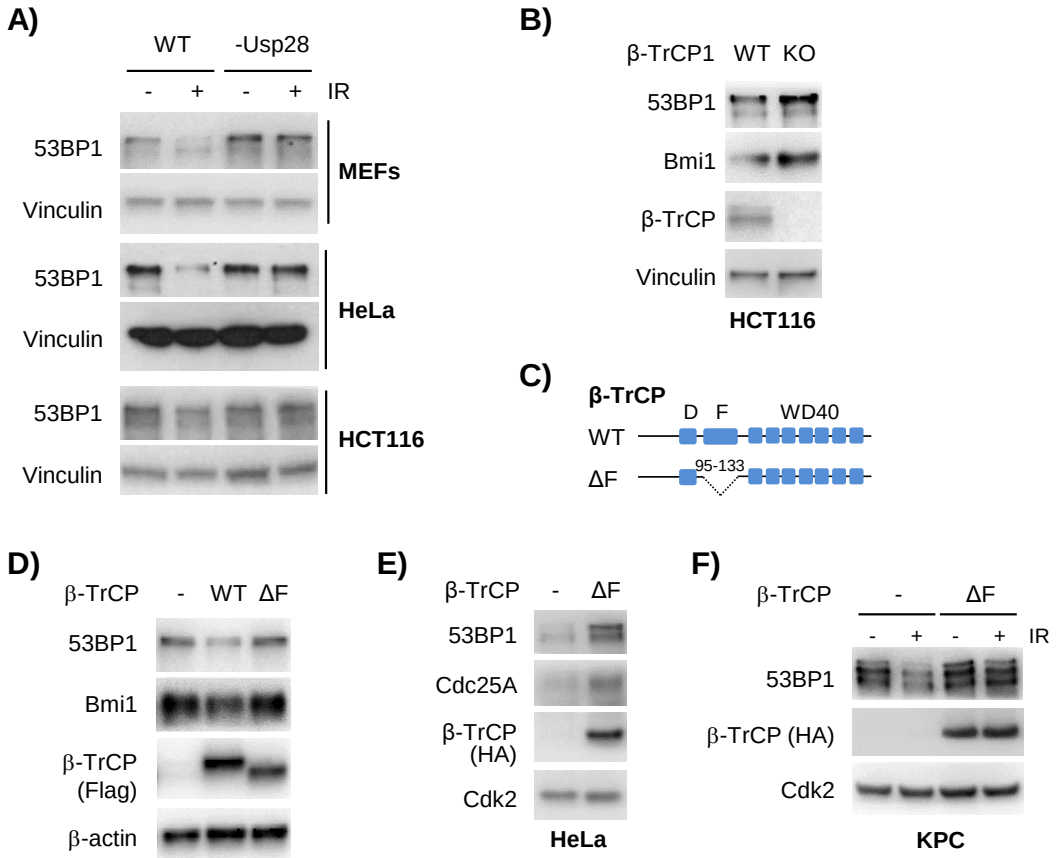

Figure 4.5.1 Usp28 promotes β-TrCP-dependent 53BP1 degradation[1].

A) Immunoblots showing that 53BP1 degradation induced by IR was attenuated in Usp28-/- MEFs, Usp28 knockout HeLa and knockdown HCT116 cells.

B) Protein levels of 53BP1 and Bmi1 were upregulated in β-TrCP1 KO HCT116 cells.

C) The schematic showed the deletion of F-box in β-TrCP-ΔF allele.

D) Protein levels of endogenous 53BP1 and Bmi1 were downregulated by ectopic β-TrCP-WT but not β-TrCP-ΔF in transient transfection assays.

E) Immunoblots demonstrated elevated levels of 53BP1 and Cdc25A at steady state in HeLa cells stably expressing HA-tagged β-TrCP-ΔF.

F) Immunoblot analysis showing that 53BP1 degradation upon IR treatment was attenuated in KPC cells stably expressing β-TrCP-ΔF.

Figure 4.5.2

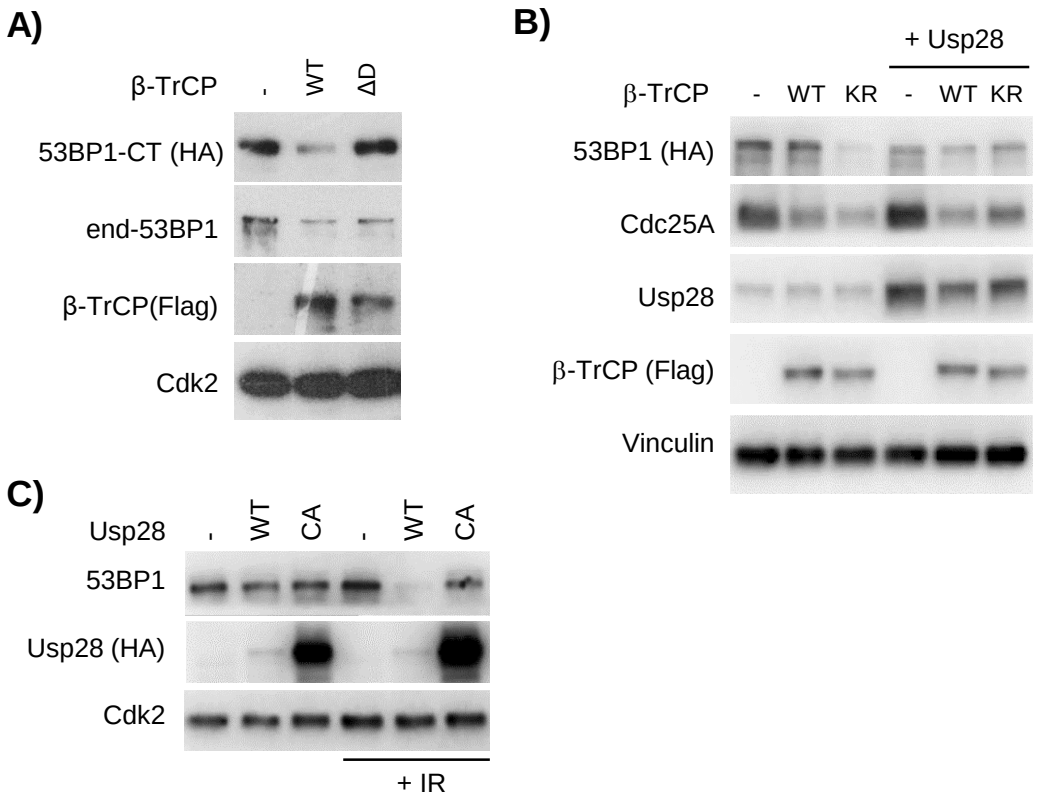

Figure 4.5.2. Usp28 stimulates β-TrCP-dependent degradation of 53BP1 [1].

A) Immunoblots showing impaired activity of dimer-deficient β-TrCP in degrading ectopic 53BP1-CT and endogenous 53BP1 in transient transfection assays.

B) Ectopic Cdc25A and full-length 53BP1 degradation by β-TrCP-WT or -KR in the absence and presence of Usp28 in transient transfection assays.

C) Immunoblots showing downregulated protein levels of 53BP1 in Usp28 KO MEFs reconstituted with WT- but not CA-Usp28, especially upon IR treatment.

4.5.2 Usp28 stimulates β-TrCP-dependent degradation of 53BP1

To analyze whether 53BP1 degradation is regulated by β-TrCP, the dimer-deficient β-TrCP was applied in transient transfection assays. The results showed that WT but not dimer-deficient β-TrCP downregulated the levels of ectopic 53BP1-CT and endogenous 53BP1 (Fig 4.5.2A). As well as Cdc25A, β-TrCP-KR promoted 53BP1 degradation more efficiently than β-TrCP-WT (Fig 4.5.2B). Ectopic Usp28 stimulated 53BP1 destruction by β-TrCP-WT, but not by β-TrCP-KR (Fig 4.5.2B). Additionally,

stably expressed WT but not catalytical-inactive Usp28 in Usp28-/- MEFs downregulated 53BP1 levels, especially upon IR treatment (Fig 4.5.2C), similar to the effects on Cdc25A (Fig 4.3.3A). These results indicate that Usp28 promotes β-TrCP-dependent destruction of 53BP1.

4.5.3 53BP1 BRCT domain interacts with the WD40 repeats of β-TrCP

To study the interaction between 53BP1 and β-TrCP, we used immunoprecipitation of endogenous 53BP1 in HeLa cells. This assay confirmed the binding of 53BP1 to β-TrCP (Fig 4.5.3A). Moreover, PLA assay for HeLa control cells and cells stably expressing HA-β-TrCP was performed with antibodies against HA-tag and 53BP1. The experiments showed more prominent PLA signals in HA-β-TrCP expressing cells, suggesting the protein association between endogenous 53BP1 and HA-β-TrCP (Fig 4.5.3B).

Figure 4.5.3

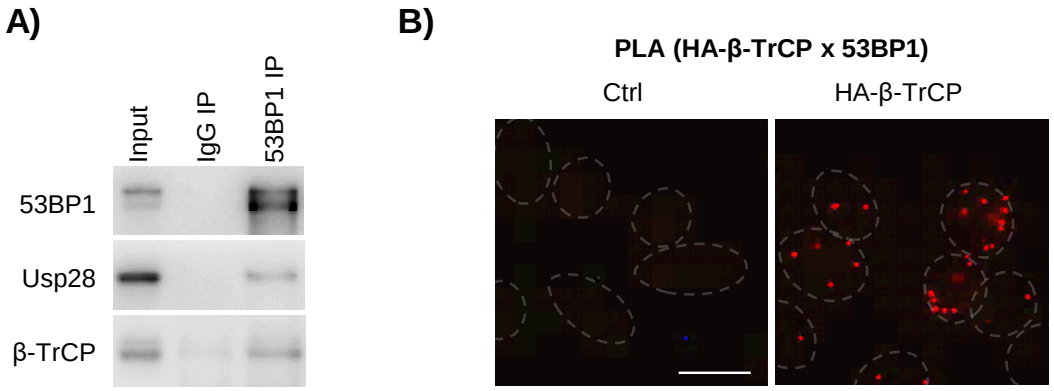

Figure 4.5.3. 53BP1 BRCT domain interacts with the WD40 repeats of β-TrCP[1].

A) Immunoprecipitation of endogenous 53BP1 in HeLa cells documenting its binding to β-TrCP.

B) PLA assay revealed the association between endogenous 53BP1 and HA-tagged β-TrCP with more prominent PLA signals in HA-β-TrCP stably expressing HeLa cells. Scale bar = 20 μm.

Figure 4.5.3

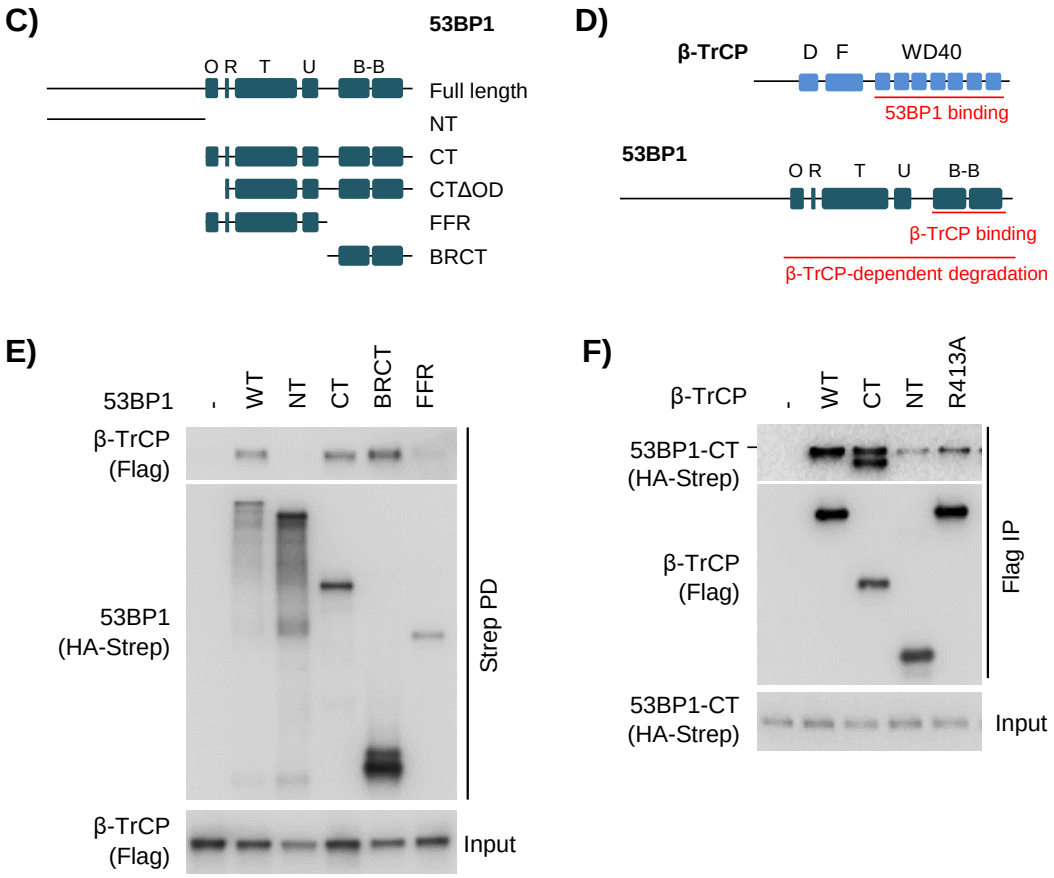

Figure 4.5.3. Usp28 promotes β-TrCP-dependent degradation of 53BP1[1].

C) Schematic structure of 53BP1 full length and variants.

D) Schematic summary for interaction between 53BP1 and β-TrCP.

E) Strep-tag pulldowns of HA-Strep-tagged 53BP1 full length and variants showing that its BRCT domain interacted with β-TrCP in transient transfection assay.

F) Immunoprecipitation of Flag-tagged β-TrCP WT and variants from transiently transfected cells demonstrating that the WD40 repeats of β-TrCP bound to 53BP1 and R413A mutation in β-TrCP inhibited 53BP1 binding.

Since 53BP1 degradation is dependent on β-TrCP, it raised the possibility of 53BP1 being a substrate of β-TrCP. However, 53BP1 does not have the consensus binding motif with the sequence of $DSG(X)_{2+n}S$, which can be recognized by β-TrCP (Cardozo and Pagano, 2004). To map the β-TrCP binding sites in 53BP1, we generated several deletion variants of 53BP1 shown in the schematic (Fig 4.5.3C). HA-Strep-tagged 53BP1 WT and variants were transiently expressed with Flag-

tagged β-TrCP in HeLa cells and pulled down by Streptavidin beads. This assay revealed that 53BP1 WT, CT and BRCT domain bound to β-TrCP, suggesting that BRCT domain is the minimal interacting domain with β-TrCP (Fig 4.5.3D, E). In turn, immunoprecipitation of Flag-tagged β-TrCP variants showed that 53BP1 bound to the WD40 repeats (CT) of β-TrCP (Fig 4.5.3D, F), supporting the previous data which demonstrated that the substrate adapters of the ubiquitin ligase APC/C interact with 53BP1 through their WD40 repeats (Kucharski *et al.*, 2017). Moreover, mutation of Arg413 in β-TrCP significantly impaired 53BP1 binding (Fig 4.5.3F), indicating that 53BP1 interacts with the common interface of β-TrCP for substrate binding.

4.5.4 53BP1 oligomerization is required for its β-TrCP-dependent destruction

Since the C-terminal half of 53BP1 contains the minimal region for efficient 53BP1 focus formation and for β-TrCP binding and is commonly used in the analysis of 53BP1 function (Iwabuchi *et al.*, 2003; Zhang *et al.*, 2006), we selected 53BP1-CT with AA 1220-1972 for the next steps of our study. 53BP1 is known to form oligomers and previous data showed that the oligomerization domain of 53BP1 is required for efficient recognition of DNA DSBs (Zgheib *et al.*, 2009). To determine whether 53BP1 oligomerization affects the interaction between 53BP1 and β-TrCP, a variant of 53BP1-CT without oligomerization domain (AA 1266-1972, 53BP1-CTΔOD) was stably expressed in MEFs via retroviral infection. Strep-tag pulldowns for 53BP1-CTWT or -CTΔOD confirmed the defect in oligomerization of 53BP1-CTΔOD, as evident from the absence of endogenous 53BP1 binding (Fig 4.5.4A). IR-induced degradation of endogenous 53BP1 and stably expressed 53BP1-CT in MEFs was inhibited by the deletion of oligomerization domain (Fig 4.5.4B), suggesting that oligomerization is required for 53BP1 destruction. However, this oligomerization region does not contain lysine residues which target the protein for ubiquitination and degradation, also has no degrons similar to the consensus binding motif as β-TrCP substrates. Additionally, comparing to 53BP1-CTWT, the association of 53BP1-CTΔOD with β-TrCP was significantly attenuated (Fig 4.5.4A). Therefore, these results indicate that 53BP1 oligomers are the target for β-TrCP-dependent degradation.

In transient transfection assays, Strep-tag pulldowns for 53BP1-CT showed that in the presence of ectopic β-TrCP, the binding of 53BP1-CT to endogenous 53BP1 was diminished upon overexpression of Usp28, suggesting that Usp28 stimulated the degradation of 53BP1 oligomers (Fig 4.5.4C). Taken together, these results indicate that Usp28 promotes β-TrCP-dependent destruction of 53BP1 oligomers.

Figure 4.5.4

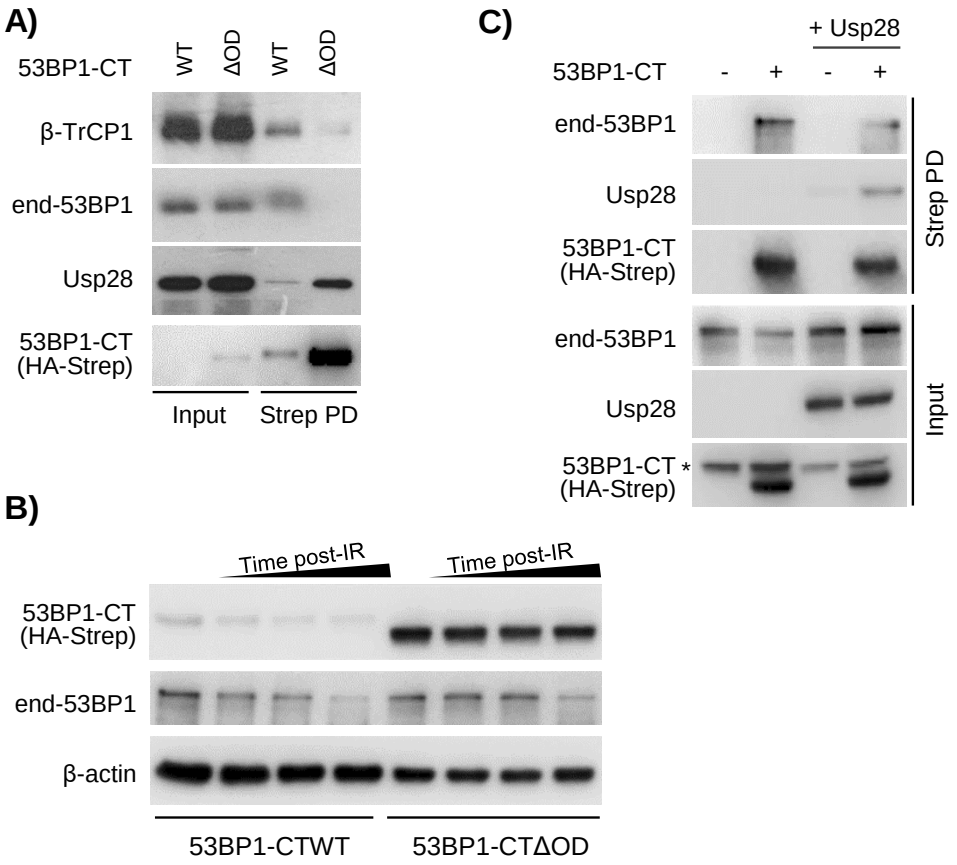

Figure 4.5.4. 53BP1 oligomerization is required for its β-TrCP-dependent destruction[1].

A) Strep-tag pulldowns from MEFs stably expressing 53BP1-CTWT or -CTΔOD showing blocked interaction of 53BP1-CTΔOD with endogenous 53BP1 and β-TrCP.

B) Immunoblots for lysates of MEFs stably expressing 53BP1-CTWT or -CTΔOD demonstrated that the deletion of oligomerization domain attenuated the degradation of 53BP1-CT and endogenous 53BP1 upon IR treatment.

C) Strep-tag pulldowns for 53BP1-CT from transient transfected cells demonstrated that in the presence of ectopic β-TrCP, the levels of 53BP1-CT oligomerization with endogenous 53BP1 was lower upon Usp28 overexpression. Asterisk points a non-specific band that was not detected in the lysates.

4.6 53BP1 destruction promotes activation of β-TrCP upon DNA damage

4.6.1 53BP1 decline precedes Cdc25A degradation mediated by β-TrCP

Figure 4.6.1

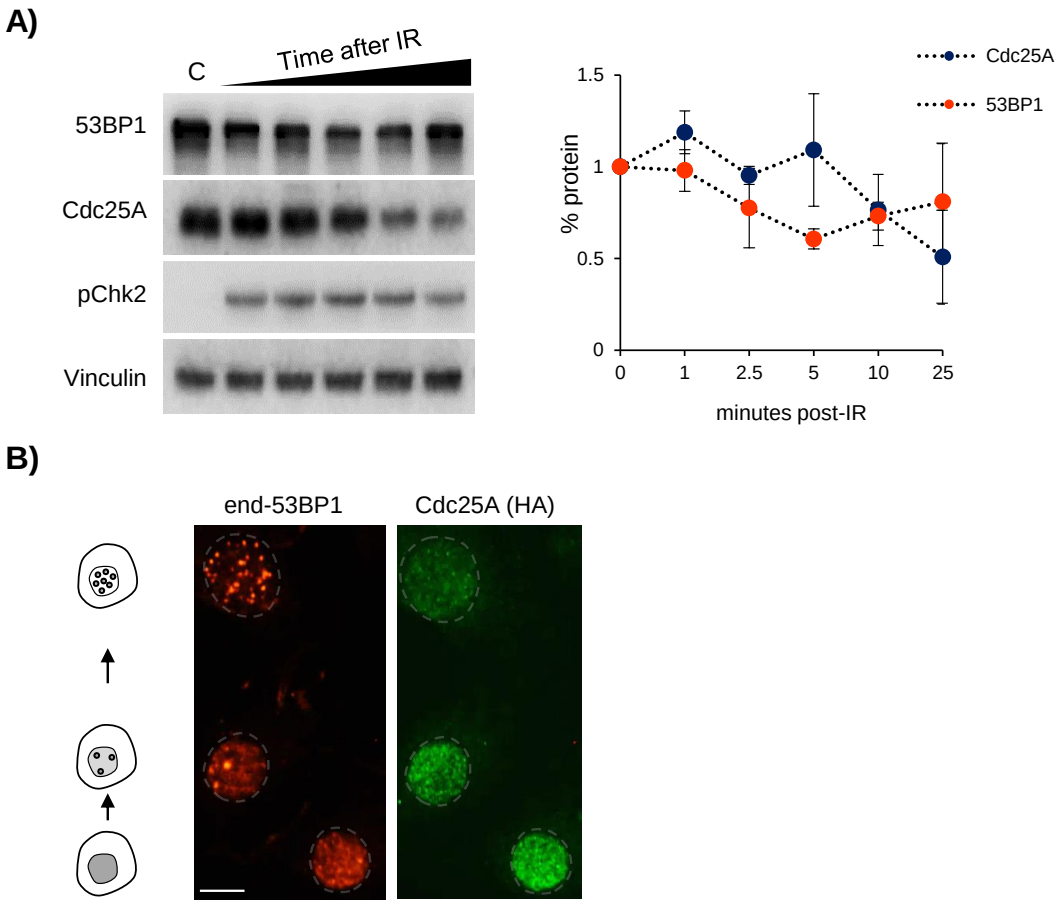

Figure 4.6.1. 53BP1 decline precedes Cdc25A degradation mediated by β-TrCP[1].

A) Protein levels of endogenous 53BP1 and Cdc25A at different timepoints after IR treatment in HeLa cells. The graphic showed quantification of three independent experiments, error bars = SD. 53BP1 and Cdc25A protein abundance was normalized against vinculin levels and then relative to that in non-treated cells.

B) A representative image of IF staining for endogenous 53BP1 and stably expressed HA-tagged Cdc25A in a clonal cell line upon IR, scale bar=20μm. Schematic showed the status of 53BP1 foci formation after IR.

Interestingly, via analyzing the degradation of endogenous 53BP1 and Cdc25A in response to IR at different timepoints, we found that downregulation of 53BP1 constantly occurred ahead of Cdc25A degradation, revealed by immunoblotting (Fig 4.6.1A). IF staining of endogenous 53BP1 and stably expressed HA-tagged Cdc25A in a clonal cell line suggested a strong connection between the localization of 53BP1 to the IRIF and the protein levels of Cdc25A upon IR (Fig 4.6.1B). Cells with homogenous nuclear localization of 53BP1 had higher levels of Cdc25A, whereas cells devoid of nucleoplasmic 53BP1 staining, showing mature 53BP1 foci, had lower levels of Cdc25A (Drane *et al.*, 2017; Hu *et al.*, 2014; Mayca Pozo *et al.*, 2017; Zhang *et al.*, 2017).

4.6.2 53BP1 destruction activates β-TrCP upon DNA damage

To understand the mechanisms behind the priority of 53BP1 degradation upon DNA damage, we generated a non-degradable variant of 53BP1-CT, 53BP1-CTKR. In this variant, all the lysines were substituted by arginines, except K1667 and K1669 that located within a putative nuclear localization signal (NLS). To compare the functions of 53BP1-CTWT and -CTKR, we generated MEFs stably expressing these two plasmids with Strep- and HA-tag. As expected, 53BP1-CTKR exhibited higher stability than 53BP1-CTWT in CHX assays (Fig 4.6.2A). Similar to 53BP1-CTWT, 53BP1-CTKR localized in the nucleus, revealed by immunofluorescence staining for stably expressed 53BP1-CT in MEFs (Fig 4.6.2B). In Strep-tag pulldown assays, both 53BP1-CTWT and -CTKR formed hetero-oligomers with endogenous 53BP1 and bound to chromatin as revealed by interaction with dimethylated histone H4K20 (Fig 4.6.2C).

Upon IR treatment, the degradation of 53BP1-CTKR was attenuated, revealed by immunoblots and IF staining of stably expressed 53BP1-CT in MEFs (Fig 4.6.2D, E). IF staining of HA-53BP1-CT showed that after IR treatment, 53BP1-CTKR retained more notable homogeneous staining in the nucleoplasm compared to 53BP1-CTWT, and the recruitment to IRIF was also partially compromised for the 53BP1-CTKR variant (Fig 4.6.2D). These data were in line with recent studies showing that DNA damage-induced 53BP1 degradation takes place in the soluble nuclear fraction outside of IRIF (Drane *et al.*, 2017; Duheron *et al.*, 2017; Hu *et al.*, 2017; Mayca Pozo *et al.*, 2017).

Figure 4.6.2

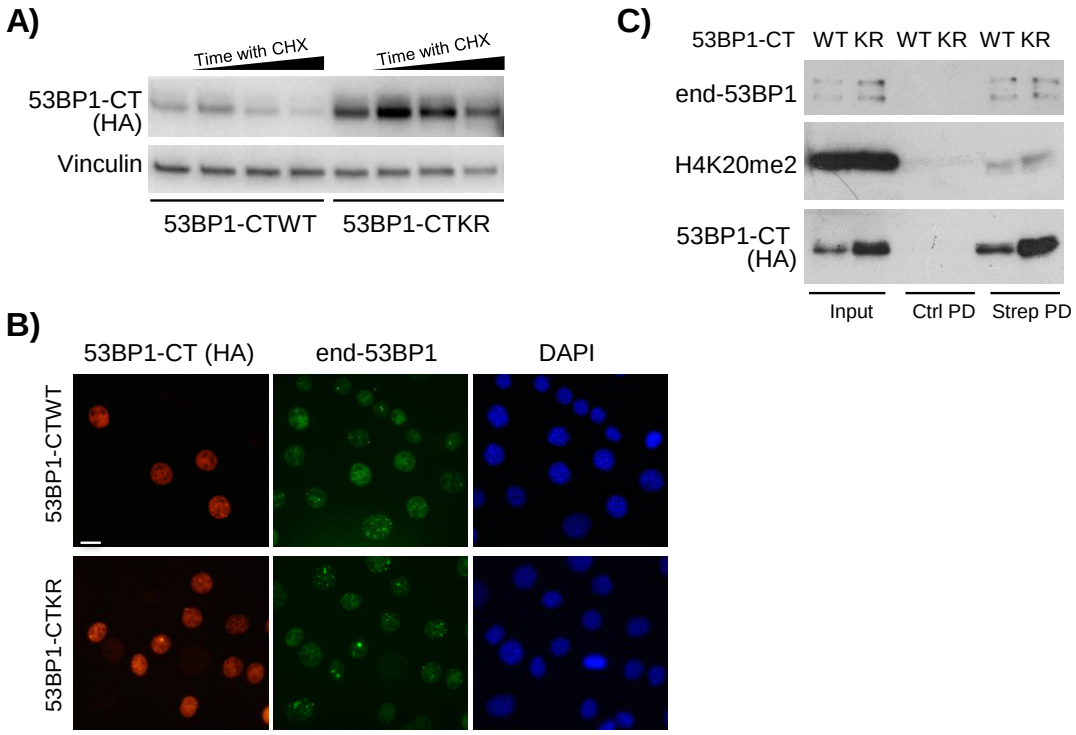

Figure 4.6.2. 53BP1 destruction activates β-TrCP upon DNA damage[1].

A) CHX assay showing impaired turnover of 53BP1-CTKR comparing to 53BP1-CTWT in MEFs stably expressing 53BP1-CT.

B) A representative image for IF staining showing localization and levels of endogenous 53BP1 and stably expressed 53BP1-CTWT or -CTKR with HA-Strep-tag in MEFs. Scale bar = 20 μm.

C) Strep-tag pulldowns for stably expressed HA-Strep-tagged 53BP1-CTWT or -CTKR in MEFs demonstrated the interaction with endogenous 53BP1 and the binding to dimethylated histone H4K20.

Notably, the destruction of endogenous 53BP1 upon IR was delayed in cells stably expressing 53BP1-CTKR, most likely resulting from stabilization by hetero-oligomers with 53BP1-CTKR (Fig 4.6.2D, E). Moreover, IR-induced Cdc25A destruction was diminished by stable expression of 53BP1-CTKR with normal phosphorylation of Chk1 and Chk2 (Fig 4.6.2E and data not shown). These results suggest that 53BP1 destruction upon DNA damage activates β-TrCP, thereby promoting ubiquitination and degradation of Cdc25A.

Figure 4.6.2

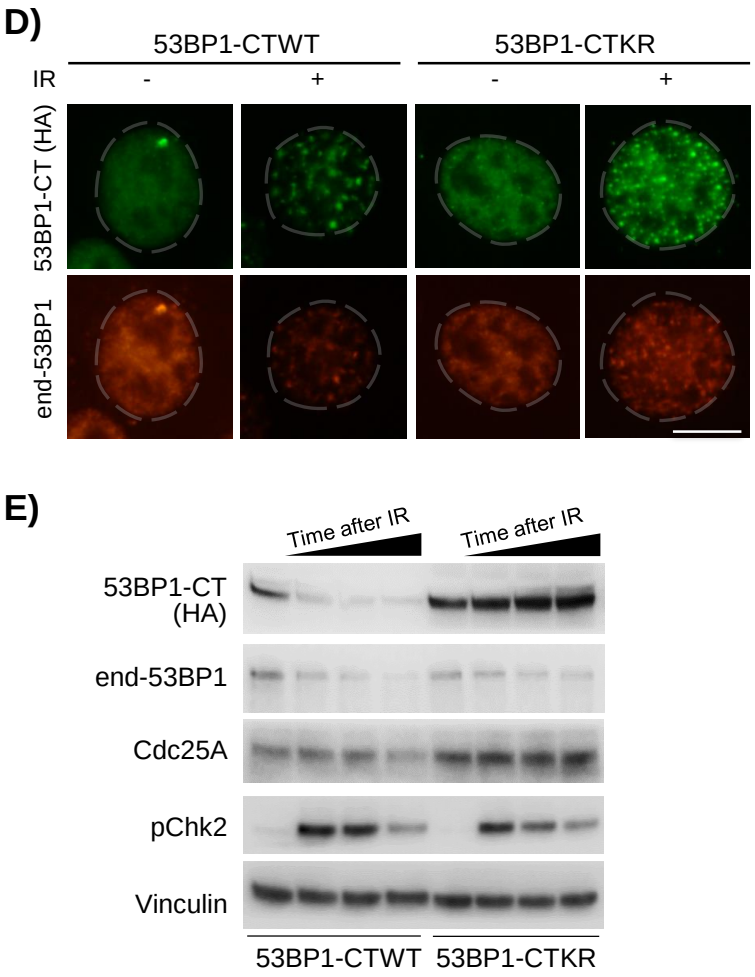

Figure 4.6.2. 53BP1 destruction activates β-TrCP upon DNA damage[1].

D) A representative image showing IF staining of endogenous 53BP1 and stably expressed HA-Strep-tagged 53BP1-CTWT or -CTKR in MEFs upon IR. Scale bar = 20 µm. Cells were stained with HA antibody and 53BP1 antibody which recognize the N-terminal sequences of 53BP1, followed by incubation with corresponding secondary antibodies conjugated to individual fluorescent labels.

E) Immunoblots for lysates of MEFs stably expressing 53BP1-CTWT or -CTKR upon IR.

4.7 53BP1 inhibits β-TrCP dimerization and recruitment to chromatin

4.7.1 Loss of 53BP1 stimulates β-TrCP activity

To understand how 53BP1 degradation activates β-TrCP, we generated 53BP1-null HeLa cells using CRISPR-mediated gene editing. In contrast to cells expressing non-degradable 53BP1-CTKR, 53BP1 knockout cells showed lower protein levels and stability of Cdc25A, as well as some other β-TrCP substrates (*e.g.* BimEL) (Fig 4.7.1A and data not shown). Downregulation of Cdc25A and Bmi1 levels was also observed in siRNA-mediated 53BP1 knockdown HeLa, HCT116 and U2OS cells (Fig 4.7.1B and data not shown). The stable expression of dominant-negative β-TrCP (ΔF-β-TrCP) equalized Cdc25A protein levels in WT and 53BP1 KO HeLa cells (Fig 4.7.1C), demonstrating that β-TrCP activation is responsible for the pronounced Cdc25A degradation in 53BP1-null cells.

Since downregulation of Cdc25A can result in DNA replication blockade, we performed EdU labeling assay to detect DNA replication in WT and 53BP1 KO cells. In line with the low Cdc25A levels, 53BP1 KO cells showed 15% less of EdU-positive cells than WT cells (Fig 4.7.1D). These data point to an impaired DNA replication in 53BP1 null cells.

Figure 4.7.1

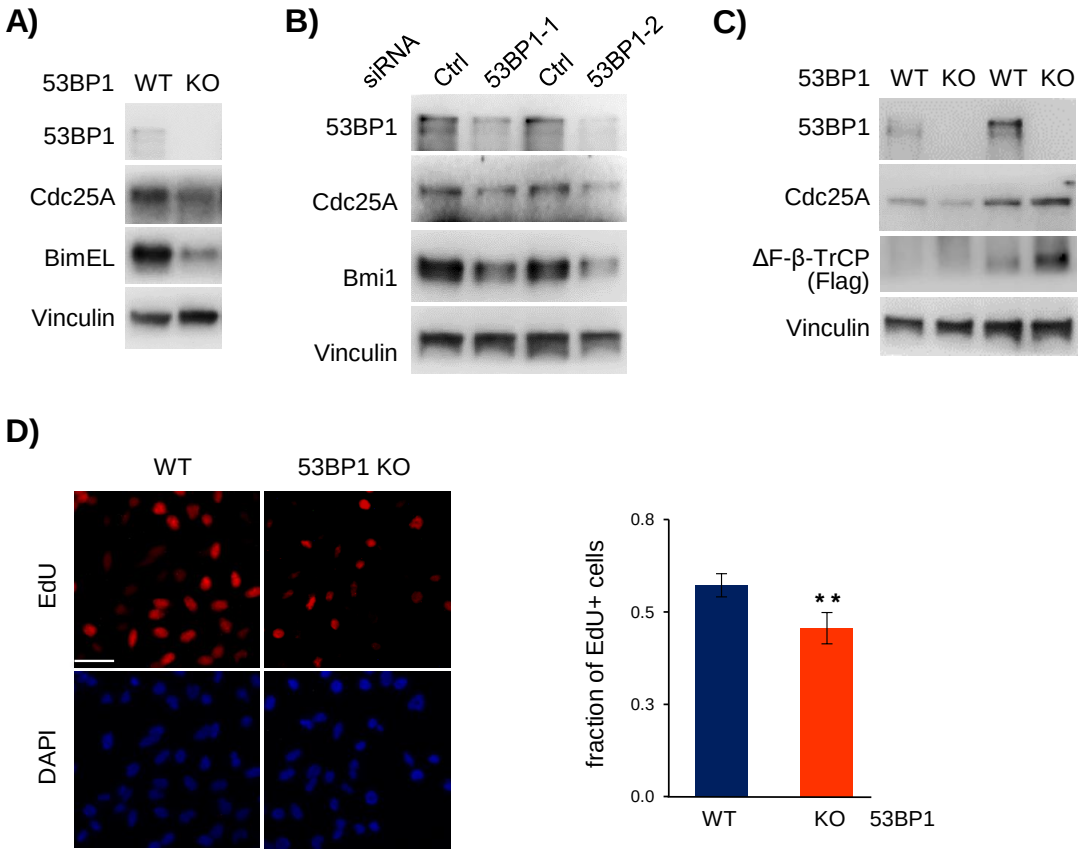

Figure 4.7.1. Loss of 53BP1 stimulates β-TrCP activity[1].

A) Immunoblots showing downregulated protein levels of β-TrCP substrates in 53BP1 KO HeLa cells.

B) Immunoblots for WT and 53BP1 knockdown HeLa cells demonstrating that 53BP1 loss downregulated levels of β-TrCP substrates Cdc25A and Bmi1. Cells were transfected with siRNA of Ctrl, 53BP1-1 or 53BP1-2 (two different siRNAs), collected after 48 h and analyzed with immunoblotting.

C) Cdc25A levels in 53BP1 KO HeLa cells were rescued by expression of dominant-negative β-TrCP. HeLa WT and 53BP1 KO cells were infected for stably expressing HA-ΔF-β-TrCP and collected for immunoblotting.

D) A representative image of EdU labeling assays exhibited impaired DNA replication in 53BP1 KO cells. Scale bar = 200 μm. The schematic documented the quantification for average fractions of EdU-positive cells from three independent experiments. For each experiment and genotype, 200-300 cells were counted. Asterisks indicated p=0.0045 of Student's t-test (two-sided). Error bars = SD.

4.7.2 53BP1 inhibits β-TrCP dimerization and recruitment to chromatin

Since 53BP1 inhibits β-TrCP activity, whereas Usp28 stimulates β-TrCP via promoting dimerization, it is possible that 53BP1 interferes with β-TrCP dimer formation. To test this possibility, we generated HA-tagged β-TrCP stably expressing HeLa WT and 53BP1-null cells via retroviral infection and performed immunoprecipitation of HA-β-TrCP. The results showed that HA-β-TrCP had enhanced ability in dimerization with endogenous β-TrCP1 in 53BP1 KO cells comparing to that in WT cells (Fig 4.7.2A). Moreover, 53BP1-CT preferentially bound to the dimer-deficient β-TrCP, revealed by immunoprecipitation of Flag-tagged β-TrCP-WT or β-TrCP-ΔD in transient transfection experiments (Fig 4.7.2B). These data indicate that 53BP1 suppresses the dimer formation of β-TrCP, thereby inhibiting its activity.

It is well-known that 53BP1 is a chromatin-bound protein (Harrigan *et al.*, 2011; Panier *et al.*, 2014). Therefore, we asked if 53BP1 facilitates β-TrCP recruitment to chromatin to inhibit its activity. Surprisingly, PLA assays with antibodies against HA-β-TrCP and histone H3 showed more pronounced PLA signals in 53BP1 KO cells, suggesting better interaction between HA-β-TrCP and histone H3 (Fig 4.7.2C). β-TrCP binding to histone H2A was also more prominent in 53BP1 KO cells, revealed by immunoprecipitation of stably expressed HA-tagged β-TrCP (Fig 4.7.2A). Consistently, the protein levels of β-TrCP substrates in chromatin fractions was lower in 53BP1 KO cells, whereas they were similar in soluble nuclear fractions of WT and 53BP1 KO cells (Fig 4.7.2D). These results suggest that 53BP1 deletion stimulates β-TrCP recruitment to chromatin and promotes its substrate degradation on chromatin.

Figure 4.7.2

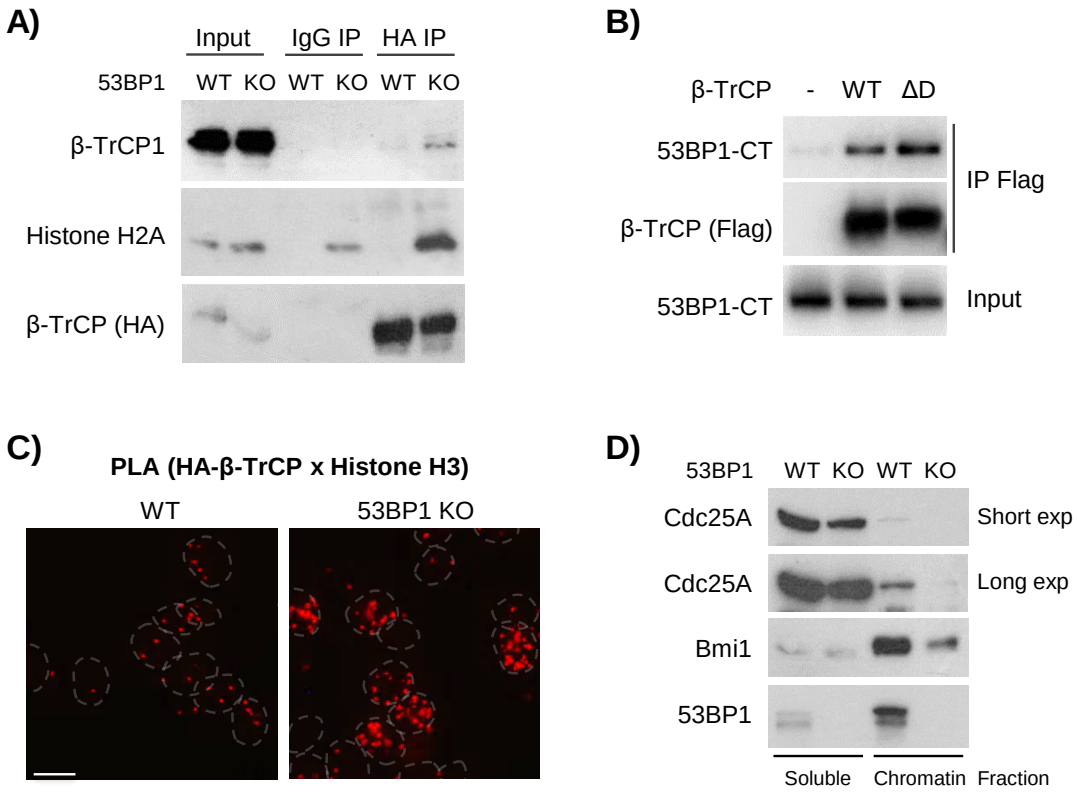

Figure 4.7.2. 53BP1 inhibits β-TrCP dimerization and recruitment to chromatin[1].

A) Immunoprecipitation of stably expressed HA-tagged β-TrCP from HeLa cells showed enhanced dimerization with endogenous β-TrCP and stimulated binding to histone H2A in 53BP1 KO cells.

B) Immunoprecipitation of Flag-tagged β-TrCP exhibited better binding of 53BP1 to the dimer-deficient β-TrCP in transient transfection assays.

C) PLA assays for stably expressed HA-tagged β-TrCP and histone H3 demonstrating enhanced association between them in 53BP1-null HeLa cells. Scale bar = 20 μm.

D) Fractionation assays showing lower protein levels of β-TrCP substrates on the chromatin of 53BP1 KO HeLa cells comparing to that of WT cells, but similar levels in soluble nuclear fractions of WT and 53BP1 KO cells.

4.7.3 β-TrCP relocalization to chromatin overlaps with putative origins of DNA replication

To study the interaction between β-TrCP and chromatin, the genome-wide binding profiles of β-TrCP were determined by ChIP-Sequencing (ChIP-Seq) analysis. For this purpose, ChIP experiments with the antibody against β-TrCP1 were performed from WT and 53BP1 KO HeLa cells, followed by deep sequencing. The bioinformatical analysis of all deep-sequencing data were performed by Dr. Nikita Popov.

Figure 4.7.3

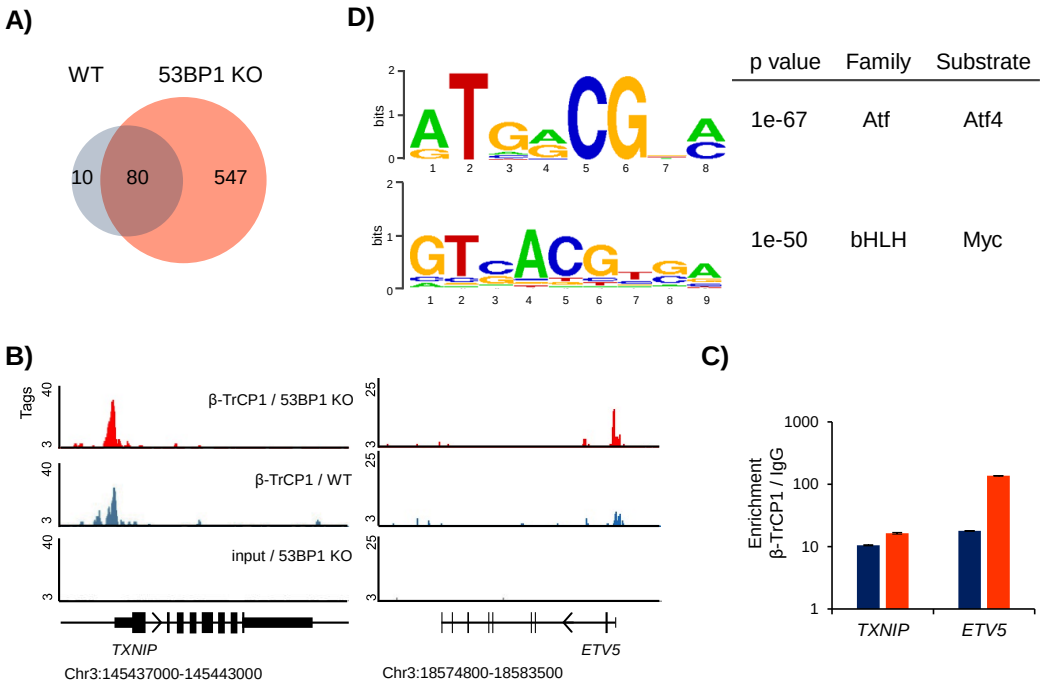

Figure 4.7.3. ChIP-Seq results for endogenous β-TrCP1 in HeLa WT and 53BP1-null cells[1].

A) 90 and 627 peaks were identified by ChIP-Seq with endogenous β-TrCP1 in WT and 53BP1 KO cells.

B) C) Representative tracks of ChIP-Seq signal documenting two β-TrCP binding sites on chromatin 3 in 53BP1-independent (left, *TXNIP*) and -dependent (right, *ETV5*) manner. The graphic (C) displays the validation of these two β-TrCP sites by independent ChIP-qPCR analysis.

D) Representative motifs of β-TrCP-associated transcription factors, Atf and bHLH families that were enriched within β-TrCP binding sites.

The results demonstrated that 53BP1 loss strongly stimulated genomic binding of β-TrCP1 with around 7 times more high-confidence sites comparing to those in WT cells (627 vs 90 sites) (Fig 4.7.3A, B). Consistently, most but not all common sites were bound better by β-TrCP in the absence of 53BP1 (Fig 4.7.3A-C). For example, ChIP-Seq tracks for β-TrCP at the gene *ETV5* on chromatin 3 (Fig 4.7.3B, right) exhibited a much stronger peak for 53BP1 KO cells than that for WT cells, while similar peaks at the gene *TXNIP* (Fig 4.7.3B, left) were identified in WT and 53BP1 KO cells. The sequencing results were validated by qPCR analysis for DNA from independent ChIP assays (Fig 4.7.3C). Moreover, β-TrCP binding sites showed strong association with gene transcription start sites (TSSs), which was supported by enrichment at the motifs for β-TrCP-associated transcription factors, including Atf and bHLH families (Fig 4.7.3D) (Lassot *et al.*, 2001; Loveless *et al.*, 2015; Popov *et al.*, 2010).

The genome ontology analysis showed that the dominant β-TrCP binding sites, especially in 53BP1 KO cells, localized in TSSs containing CpG-rich (CpGi) sequences but no LINE sequences (Fig 4.7.3E, F), which were previously shown to be associated with early replicating domains (Cayrou *et al.*, 2011; Hansen *et al.*, 2010; Sequeira-Mendes *et al.*, 2009).

Figure 4.7.3

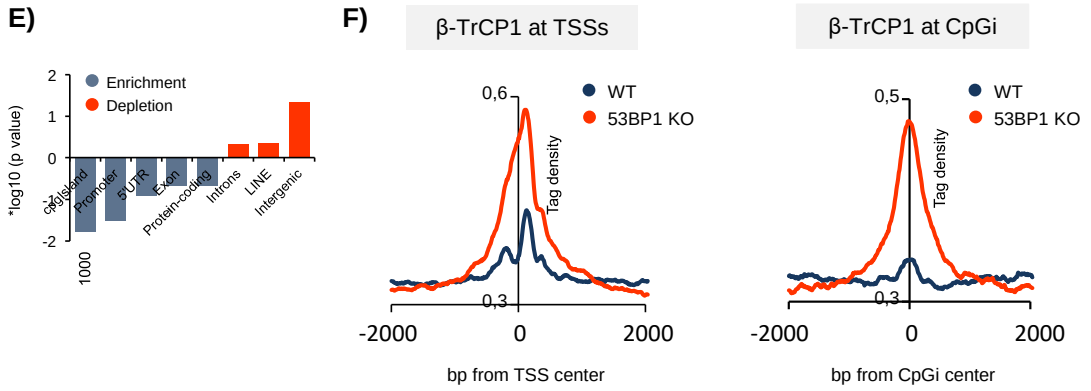

Figure 4.7.3. ChIP-Seq results for endogenous β-TrCP1 in HeLa WT and 53BP1-null cells[1].

E) Genome ontology analysis of β-TrCP binding sites, showing strong enrichment in TSSs containing CpGi sequences and depletion of LINE L1 sequences.

F) Histogram of peak distances showing the coverage of β-TrCP1 ChIP-Seq tags at all TSSs (left) and CpG islands (right).

Figure 4.7.3

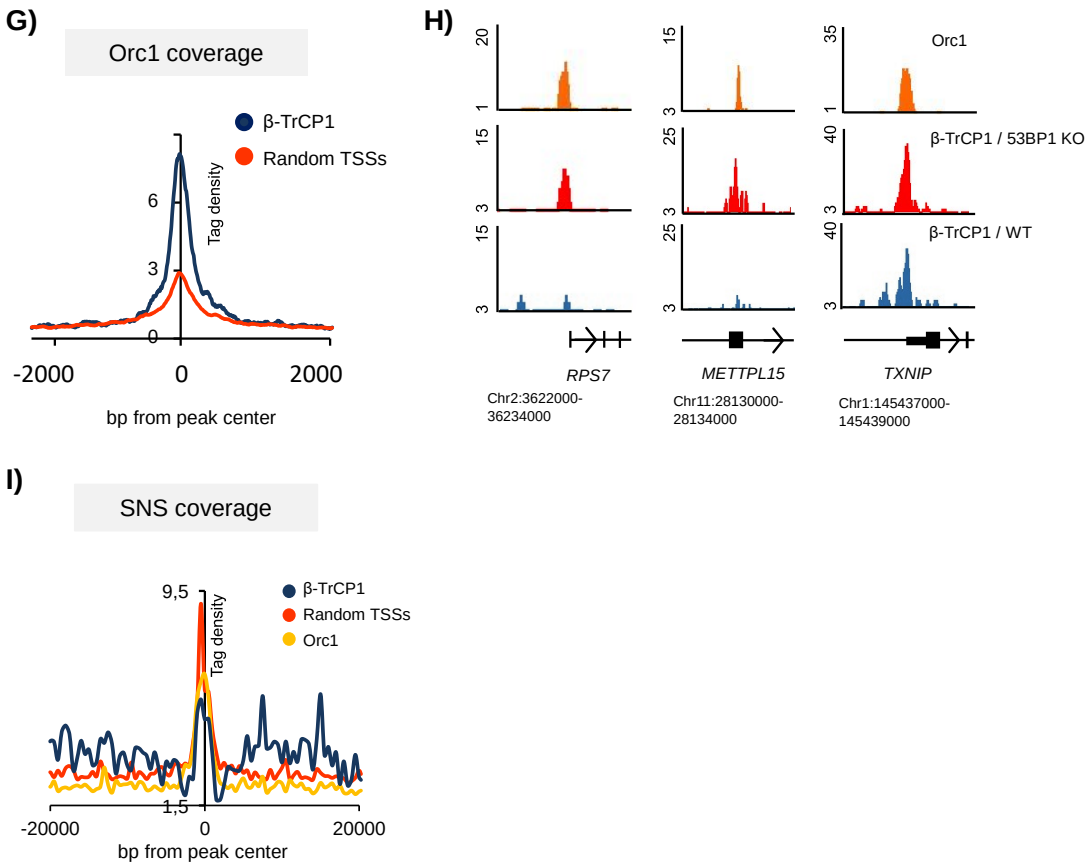

Figure 4.7.3. ChIP-Seq results for endogenous β-TrCP1 in HeLa control and 53BP1-null cells[1].

G) Histogram showing Orc1 ChIP-Seq tag coverage at β-TrCP sites or random TSSs. Average values for 10 different sets were plotted for random TSSs in this and following indicative histograms.

H) Representative tracks of co-localized binding sites of Orc1 and β-TrCP.

I) Tag density plots revealing the coverage of SNS sequencing tags at Orc1 sites, β-TrCP sites and random TSSs.

Intriguingly, β-TrCP binding sites showed strong overlap with the putative origins of replication (Fig 4.7.3G, H), identified by Orc1 ChIP-Seq in HeLa cells (Dellino *et al.*, 2013). Compared to random sets of TSS-associated peaks, the distance of Orc1 binding sites to β-TrCP binding sites was much shorter, indicating prominent co-localization (Fig 4.7.3G). As shown by the representative tracks of ChIP-Seq signal (Fig 4.7.3H), β-TrCP binding at the *RPS7* and *METTPL15* promotors was stimulated

in 53BP1-null cells. Thus, 53BP1 deletion promoted the co-localization of Orc1 and β-TrCP sites.

Short nascent strands (SNS) are the newly synthesized initiation intermediates near replication origins, excluding short Okazaki fragments. Identifying SNS is a sensitive method to map the location of active origins (Besnard *et al.*, 2012; Langley *et al.*, 2016; Staib and Grummt, 1997). β-TrCP binding sites showed overlapping with SNS sequences identified in a previous study (Besnard *et al.*, 2012). Interestingly, the density of SNS sequencing tags was lower at β-TrCP sites comparing to that at Orc1 sites (Fig 4.7.3I). These results support the idea that β-TrCP-mediated localized Cdc25A degradation at replication origins controls DNA replication. Therefore, considering the fact that in 53BP1-null cells and in response to DNA damage, β-TrCP-mediated localized Cdc25A degradation correlates with the regulation of DNA replication, we speculated that β-TrCP recruitment to chromatin sites in the vicinity of replication origins facilitates inhibitory of DNA replication initiation.

4.8 Relocalization of β-TrCP to chromatin upon DNA damage inhibits DNA replication

4.8.1 β-TrCP dissociates from 53BP1 and relocalizes to chromatin in response to DNA damage

Since both 53BP1 deletion and DNA damage stimulate β-TrCP function, we asked whether 53BP1-β-TrCP interaction is affected in response to DNA damage. To study this, we performed immunoprecipitation of endogenous 53BP1 from the soluble nuclear fraction of HeLa cells. The results showed rapid dissociation of 53BP1 from β-TrCP and Usp28 upon IR (Fig 4.8.1A). Since 53BP1 loss stimulates the relocalization of β-TrCP to chromatin, PLA analysis for stably expressed HA-tagged β-TrCP and histone H3 was performed to detect whether DNA damage has similar effect on the chromatin binding of β-TrCP. This assay displayed transient upregulation of PLA signals at 5 min and 30 min after IR, which decreased at 2 h (Fig 4.8.1B), suggesting the transiently enhanced association of β-TrCP to chromatin upon DNA damage.

Figure 4.8.1

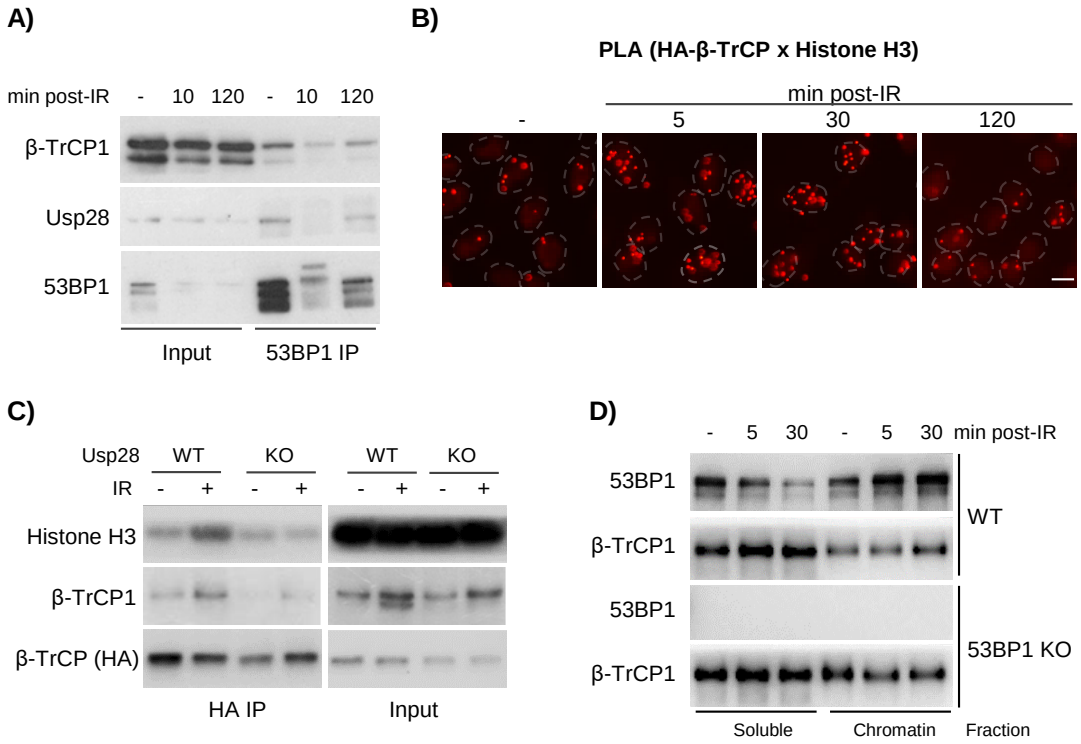

Figure 4.8.1. β-TrCP dissociates from 53BP1 and relocalizes to chromatin in response to DNA damage[1].

A) IP for endogenous 53BP1 from the soluble nuclear fraction of HeLa cells demonstrating transient dissociation of 53BP1 from β-TrCP and Usp28 upon IR.

B) PLA assays for histone H3 and stably expressed HA-β-TrCP in HeLa cells showed transiently increased PLA signals upon IR, suggesting enhanced interaction. Scale bar = 20 µm.

C) IP for stably overexpressed HA-tagged β-TrCP from WT and Usp28 KO HeLa cells revealed enhanced binding to histone H3 and endogenous β-TrCP after IR in WT cells, but not in Usp28 KO cells.

D) Fractionation assay showing protein levels of endogenous 53BP1 and β-TrCP in the soluble and chromatin-associated fractions upon IR in WT and 53BP1 KO HeLa cells.

In accord with this, immunoprecipitation for stably expressed β-TrCP confirmed the increased binding to histone H3 (Fig 4.8.1C). The dimerization of stably expressed β-TrCP with endogenous β-TrCP was also stimulated upon IR. However, these effects were diminished in Usp28-null cells, suggesting that Usp28 is required for β-TrCP dimerization and relocalization to chromatin upon DNA damage (Fig 4.8.1C). Consistently, fractionation assays showed that protein levels of β-TrCP in the

chromatin-associated fraction were upregulated in WT cells after IR (Fig 4.8.1D). In line with the increased binding of β-TrCP to histone H2A and H3 in 53BP1 KO cells (Fig 4.7.2A, C), β-TrCP abundance was higher in the chromatin-associated fraction, but didn't change upon IR (Fig 4.8.1D). These results indicate that β-TrCP dissociates from 53BP1 and relocalizes to chromatin upon DNA damage.

4.8.2 β-TrCP relocalization to chromatin promotes Cdc25A degradation upon DNA damage

As the enhanced association of β-TrCP with chromatin upon DNA damage was accompanied by an increased activity in substrate degradation, we hypothesized that DNA damage-induced substrate degradation by β-TrCP preferentially occurred in the chromatin fraction. In fact, PLA assays for HA-tagged Cdc25A and endogenous histone H3 showed a rapid decrease of PLA signals at 5 min and 15 min after IR treatment (Fig 4.8.2A). Since the total cellular Cdc25A was downregulated later only at 30 min after IR (Fig 4.8.2B), this result suggested rapid degradation of Cdc25A in the chromatin-associated fraction upon IR (Fig 4.8.2A). Consistently, as a target of Cdc25A, phosphorylated Cdk2 quickly accumulated in the chromatin fraction after IR, but remained unaltered in the soluble nuclear fraction at these early timepoints (Fig 4.8.2C). These data suggest that β-TrCP relocalization promotes Cdc25A degradation on chromatin in response to DNA damage.

We then determined recruitment of β-TrCP to genomic sites identified by ChIP-Seq (Fig 4.7.3A) upon DNA damage. HeLa cells were treated with or without IR and collected for ChIP with β-TrCP antibody. The precipitated DNA was analyzed by qPCR with primers as indicated. This experiment showed that IR treatment significantly promoted β-TrCP binding at several tested sites (Fig 4.8.2D, upper panels and data not shown). Importantly, in parallel with the enhanced β-TrCP recruitment, Cdc45 binding was diminished at the co-bound or neighbouring Orc1 sites. At Orc1 sites that didn't recruit β-TrCP, Cdc45 binding increased or remained unaltered upon IR (Fig 4.8.2D, lower panels), in line with partial dissociation of Mcm7-Cdc45 complexes after IR revealed by immunoprecipitation of Cdc45 (Fig 4.2.2F). These data suggest that the stimulation of β-TrCP binding and Cdc45 unloading in response to DNA damage is a specific effect for neighbouring Orc1 and β-TrCP sites.

Figure 4.8.2

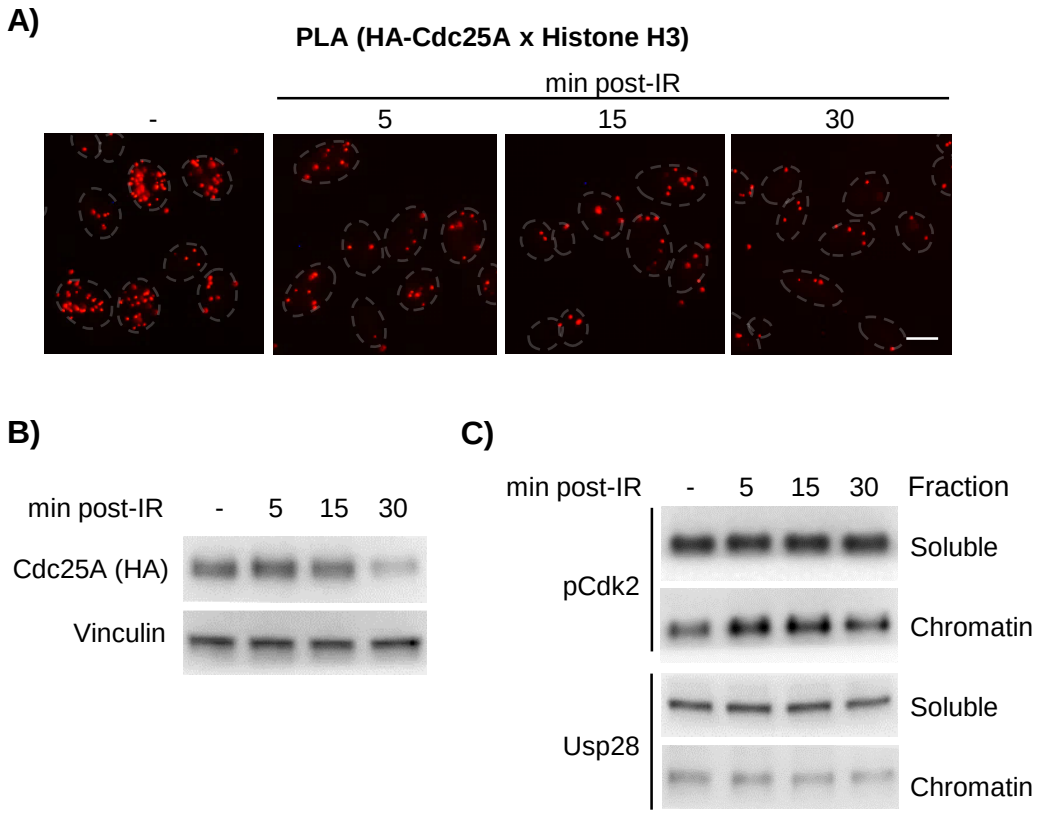

Figure 4.8.2. β-TrCP relocalization to chromatin promotes Cdc25A degradation upon DNA damage[1].

A) PLA assays with histone H3 and stably expressed HA-tagged Cdc25A in HeLa cells showed rapid decrease of PLA signals at 5 min and 15 min after IR, indicating degradation of Cdc25A on chromatin. Scale bar = 20 μm.

B) Immunoblots showing total cellular levels of stably expressed HA-tagged Cdc25A in HeLa cells upon IR.

C) Fractionation assays documented the accumulation of pCdk2 after IR in the chromatin fraction, but not in the soluble nuclear fraction.

Figure 4.8.2

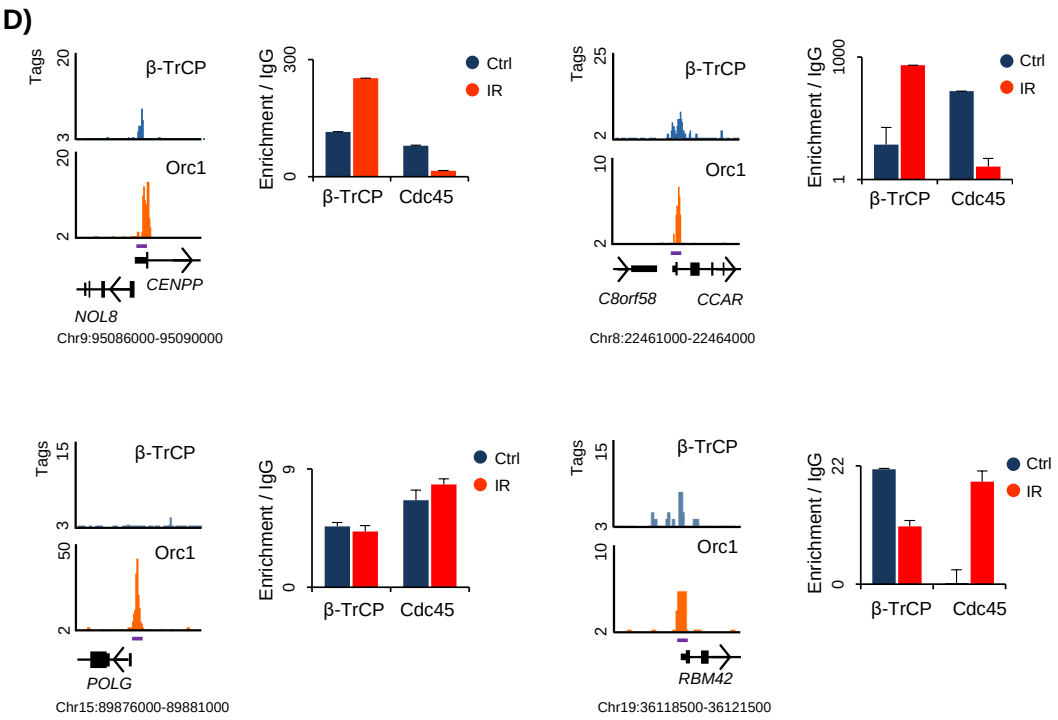

Figure 4.8.2. β-TrCP relocalization to chromatin promotes Cdc25A degradation upon DNA damage[1].

D) ChIP-qPCR assays for β-TrCP demonstrating that upon IR, β-TrCP relocalized to neighbouring Orc1 and β-TrCP sites identified by ChIP-Seq, which was accompanied by dissociation of Cdc45. ChIPs were performed for HeLa cells treated with or without IR and the precipitated DNA was analyzed by qPCR with primers for the amplicons indicated by violet lines.

Collectively, we propose that upon DNA damage, 53BP1 is degraded in the nucleoplasm in a Usp28-dependent manner and releases β-TrCP to relocalize to replication origins, which locally inhibits DNA replication initiation via inducing rapid Cdc25A degradation and phospho-Cdk2 accumulation to suppress Cdc45 loading on the pre-replication complexes (Fig 5.3).

5 Discussion

Previous studies have illustrated that the inhibition of DNA replication upon DNA damage correlates with the SCF(β-TrCP) ligase-mediated degradation of Cdc25A phosphatase. As the substrate recognition subunit of SCF(β-TrCP) ligases, β-TrCP is known to promote substrates destruction and controls cellular responses to DNA damage (Busino *et al.*, 2003; Inuzuka *et al.*, 2010; Peschiaroli *et al.*, 2006), while the modulation of β-TrCP activity upon DNA damage remains unclear. Our results demonstrated that SCF(β-TrCP) ubiquitin ligase is activated upon DNA damage in Usp28- and 53BP1-dependent manner, which specifically inhibit DNA replication.

5.1 Usp28 promotes the activation of β-TrCP

The deubiquitinase Usp28 was previously shown to modulate cell proliferation and tumorigenesis via stabilizing Myc in a Fbw7-dependent manner (Diefenbacher *et al.*, 2014; Popov *et al.*, 2007). Our previous study showed that Usp28 stabilizes Fbw7 and results in dual regulation on Fbw7 substrates, including Myc (Schulein-Volk *et al.*, 2014). Additionally, Usp28 is phosphorylated by ATR/ATM upon DNA damage and controls cellular response via stabilizing 53BP1 and activating Chk2-p53 pathway (Fong *et al.*, 2016; Lambrus *et al.*, 2016; Meitinger *et al.*, 2016; Zhang *et al.*, 2006). However, Knobel *et al.* demonstrated that Usp28 is recruited to DNA damage sites by 53BP1, but is not a critical regulator in 53BP1 stability and DSB response (Knobel *et al.*, 2014).

In our study, Usp28 deletion promoted recovery from DNA damage in several cell lines (Fig 4.1A-C), consistent with the previous study showing that Usp28-deleted H460 cells are more resistant to IR-induced cell death (Zhang *et al.*, 2006). However, in contrast to previous studies showing the involvement of Chk2-p53 pathway (Meitinger *et al.*, 2016; Zhang *et al.*, 2006), the stabilization and activation of p53 in response to DNA damage was not affected by Usp28 deletion (Fig 4.2.1A), indicating additional mechanism for Usp28 to regulate DDR signaling.

In addition to the p53 pathway, Cdc25A is another essential regulator of DNA damage response. DNA damage induces activation of ATR/Chk1 and ATM/Chk2 pathways, which results in phosphorylation of Cdc25A. The phosphorylated Cdc25A

is recognized and degraded by SCF(β-TrCP) ubiquitin ligase (Busino *et al.*, 2003; Jin *et al.*, 2003). Cdc25A degradation promotes accumulation of inactive pCdk2, which inhibits Cdc45 loading onto pre-RCs to block the initiation of DNA replication (Falck *et al.*, 2002). In fact, our study showed that Usp28 loss attenuated the blockade of DNA replication (Fig 4.2.1B, C) and the proteasomal destruction of Cdc25A (Fig 4.2.2A-E), as well as dissociation of Cdc45 from the pre-RCs component Mcm7 (Fig 4.2.2F) upon DNA damage. Taken together, these results indicate the crucial role of Cdc25A in Usp28-dependent modulation of DDR signaling.

As a well-established substrate of SCF(β-TrCP) ubiquitin ligase (Busino *et al.*, 2003; Falck *et al.*, 2001; Jin *et al.*, 2003), Cdc25A, as well as other β-TrCP substrates were stabilized by Usp28 loss (Fig 4.3.1A-C). Conversely, the overexpression of Usp28 promotes β-TrCP-mediated degradation of substrates (*e.g.*, Cdc25A, Bmi1, BimEL) (Fig 4.3.1E, F). β-TrCP substrates are phosphorylated by various kinases. For example, phosphorylation of Cdc25A is dependent on Chk2 and Chk1 activation (Busino *et al.*, 2003; Falck *et al.*, 2001; Jin *et al.*, 2003). The turnover of Bmi1 is dependent on its phosphorylation by CK1α (Banerjee Mustafi *et al*., 2017). Thus, the regulation of β-TrCP substrate degradation by Usp28 is not dependent on specific kinases. Additionally, the DNA damage-induced degradation of Cdc25A, BimEL and Bmi1 was attenuated in Usp28-deficient cells (Fig 4.3.1D). The kinases for the phosphorylation of some substrates are not checkpoint kinases, such as BimEL that relies on Rsk1/2 and Erk1/2 kinases (Dehan *et al.*, 2009), suggesting that Usp28 promotes the activation of β-TrCP directly, instead of regulating checkpoint kinases.

5.2 Usp28 stimulates β-TrCP dimerization via deubiquitination

Usp28 has been reported to deubiquitinate and stabilize F-box protein Fbw7, which requires its catalytic activity (Diefenbacher *et al.*, 2014; Popov *et al.*, 2007; Schulein-Volk *et al.*, 2014). Our data showed the association between Usp28 and β-TrCP in immunoprecipitation and PLA assays (Fig 4.3.2A, B). The analysis mapping interaction sites showed that Usp28 bound to the WD40 repeats of β-TrCP, but not via the substrates binding surface (Fig 4.3.2C, D). Furthermore, the reconstitution of WT but not catalytic-inactive Usp28 in Usp28 KO cells downregulated the protein levels of Cdc25A, suggesting the importance of Usp28 catalytic activity (Fig 4.3.3A). β-TrCP was deubiquitinated by Usp28 *in vivo* and *in vitro*, which as well required the

catalytic activity of Usp28 and was stimulated upon DNA damage (4.3.3B-D). Usp28 is phosphorylated by ATM or ATR upon DNA damage and the phosphorylation has been suggested to be necessary for regulation of multiple proteins in DDR pathways (*e.g.*, 53BP1, Chk2, Claspin) (Bassermann *et al.*, 2008; Zhang *et al.*, 2006). Thus, the stimulation of Usp28 activity in β-TrCP deubiquitination upon DNA damage might also result from Usp28 phosphorylation.

Distinct from stabilizing Fbw7, Usp28 didn't affect the stability of β-TrCP protein, thereby regulated β-TrCP activity in a non-proteolytic manner (Fig 4.3.3E). It is known that K48-linked polyubiquitin chains typically target proteins for proteasomal degradation, while K63-linked chains are shown to be essential in DDR and kinase signaling pathways as non-proteolytic modifications (Doil *et al.*, 2009; Stewart *et al.*, 2009). Therefore, it is possible that Usp28 deubiquitinates K63-linked chains from β-TrCP that affect its activity. To study this, *in vitro* deubiquitination assays could be performed with K63-linked chains, β-TrCP and Usp28 proteins under proper conditions, followed by immunoblotting.

The self-ubiquitination of E3 ligases has been shown to regulate their activities. For instance, the self-ubiquitination of RING1B ligase and BRCA1 promotes their activity in substrate ubiquitination, and RING1B ubiquitination is non-proteolytic (Ben-Saadon *et al.*, 2006; Mallery *et al.*, 2002). In fact, β-TrCP ubiquitination directly regulated its activity since non-ubiquitinated β-TrCP (β-TrCP-KR) was more active in substrate ubiquitination and degradation (Fig 4.4.2A-C). Unlike β-TrCP-WT that was deubiquitinated by Usp28, β-TrCP-KR was ubiquitination-deficient, thereby its activity was not stimulated by Usp28 (Fig 4.4.2A, C).

Additionally, the self-ubiquitination of certain E3 ligases inversely correlates with their dimerization- for example, the dimer-deficient Fbw7 and Cdc4 are highly auto-ubiquitinated and show impaired activity in substrate ubiquitination comparing to the dimers (Min *et al.*, 2012; Tang *et al.*, 2007). The self-association of Trim ligases and Cullin3 has been reported to be necessary for their activities (Choo and Hagen, 2012; Koliopoulos *et al.*, 2016; Streich *et al.*, 2013). In line with these studies, the dimer-deficient β-TrCP was highly ubiquitinated and inactive in Cdc25A ubiquitination and degradation (Fig 4.4.1A-C), supporting previous data that showed dimeric β-TrCP is more active in IκB ubiquitination (Suzuki *et al.*, 2000). The dimerization ability of β-TrCP was impaired in Usp28-null cells (Fig 4.4.1E), indicating that deubiquitination of β-TrCP by Usp28 promoted its dimerization and consequently activated β-TrCP.

Indeed, additional expression of Usp28 stimulated Cdc25A degradation mediated by WT but not dimer-deficient β-TrCP (Fig 4.4.1D).

The activity of ubiquitination-deficient β-TrCP was dependent on its dimerization (Fig 4.4.2C), indicating that dimerization is crucial for β-TrCP function. We also provided the evidence that ubiquitinated β-TrCP was strongly impaired in dimerization via sequential pulldown assays (Fig 4.4.2D). It has been suggested that Fbw7 dimerization is required for stable binding to SREBP1/2 (Welcker *et al.*, 2013). In agreement with this idea, ectopic dimer-deficient β-TrCP bound weaker to endogenous Wee1 in transient transfection assays (data not shown). Thus, the enhanced activity of β-TrCP dimer is likely to be a consequence of more efficient interaction with its substrates. It is also possible that β-TrCP dimer stimulates ubiquitin conjugation via utilizing different oriented ubiquitin acceptor sites on substrates, as suggested in the previous study demonstrating that Cdc4 dimerization strongly stimulates ubiquitination of its substrate Sic1 (Tang *et al.*, 2007). The dimerization has also been reported to be required for the binding of XIAP to E2 and E2-ubiquitin conjugate (Nakatani *et al.*, 2013). Another likely mechanism is that the dimer brings the substrates close to the E2-bound ubiquitin and promotes ubiquitin transfer via preferentially binding and activating the E2-ubiquitin thioester bond across the dimer, which has been demonstrated for RNF4 (Liew *et al.*, 2010; Plechanovova *et al.*, 2011).

Since the ubiquitin acceptor sites in β-TrCP were unknown, we performed mass spectrometry analysis for overexpressed β-TrCP2. A single lysine at K430 in β-TrCP2 (corresponding to K491 in β-TrCP1) was identified as a ubiquitin acceptor in the WD40 repeats of β-TrCP (Fig 4.4.3A, B). However, although the mutation of K430R inhibited this site-specific ubiquitination, this β-TrCP mutant was still ubiquitinated in transient transfection assays (data not shown). Since we didn't treat cells with the proteasomal inhibitors that can result in accumulation of ubiquitination, it is possible that we only identified the lysine which is ubiquitinated to a certain level. Another possibility is that when Lys430 is mutated, the nearby lysines become targeted for ubiquitination as alternate sites, as shown for some proteins in previous studies (Bhat *et al.*, 2010; Pickart, 2001; Treier *et al.*, 1994).

The K430R mutant showed enhanced activity in Cdc25A ubiquitination and degradation, especially in Usp28-deleted cells (Fig 4.4.3C-E). Interestingly, K430 is located in a ubiquitin binding region, which was identified previously in a functionally

diverse set of proteins including F-box proteins (Pashkova *et al.*, 2010). Pashkova *et al.* demonstrated that ubiquitin binding at this particular region promotes auto-ubiquitination and degradation of yeast F-box proteins Doa1 and Cdc4. Our model of dimeric β-TrCP1-Skp1 complex suggested that ubiquitination at K491 in β-TrCP1 might disrupt the formation of β-TrCP dimer via interfering with the orientation of the propeller domains (Fig 4.4.4A, B). Experimental data confirmed that the site-specific ubiquitination inhibited β-TrCP activity by preventing its dimerization (Fig 4.4.3F). Thus, our study suggests that site-specific ubiquitination can non-proteolytically regulate the activity of F-box proteins via inhibiting dimer formation. Additionally, the deubiquitination of F-box proteins might be a common mechanism for the activation of SCF E3 ligases, which complements substrate phosphorylation stimulated by DNA damage.

Figure 5.1

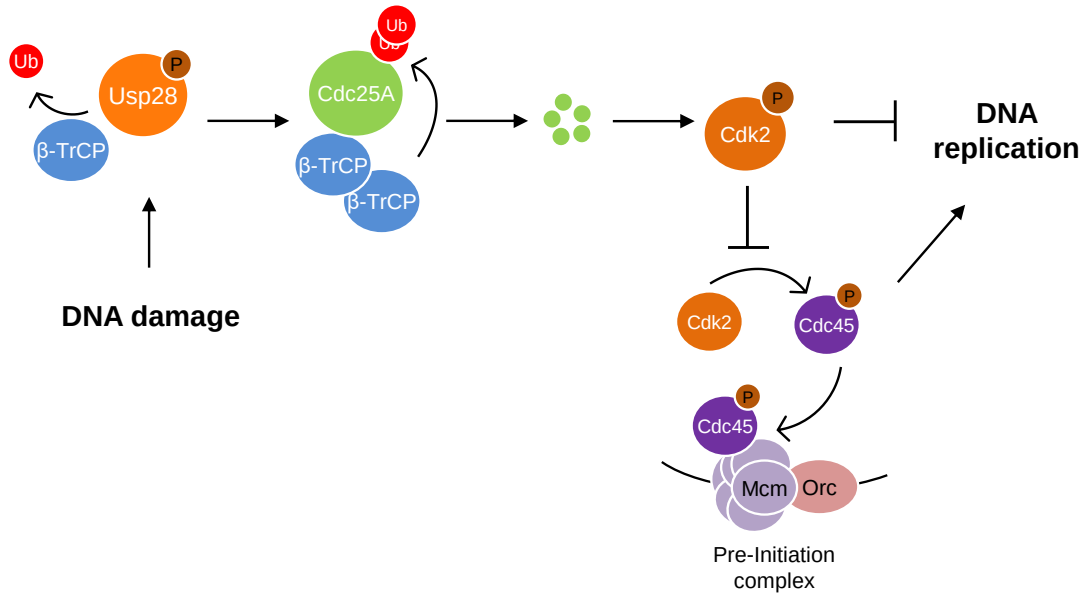

Figure 5.1. A model for β-TrCP-dependent DNA replication blockade upon DNA damage promoted by Usp28.

Upon DNA damage, Usp28 is activated to deubiquitinate β-TrCP. The deubiquitinated β-TrCP forms dimer and becomes active in Cdc25A degradation, which results in accumulation of inactive phospho-Cdk2. As a critical mediator for the loading of Cdc45 onto pre-RCs to form pre-ICs, Cdk2 is inactivated by phosphorylation, which thereby suppresses initiation of DNA replication.

Taken together, we propose that deubiquitination of β-TrCP by Usp28 upon DNA damage promotes β-TrCP dimerization, which stimulates Cdc25A ubiquitination and degradation. Cdc25A degradation leads to the accumulation of its target phospho-Cdk2. As an inactive form of Cdk2, pCdk2 suppresses the loading of Cdc45 onto pre-RCs and thereby inhibits DNA replication initiation (Fig 5.1).

5.3 Usp28 promotes β-TrCP-dependent degradation of 53BP1 oligomers

Previous studies suggested that Usp28 stabilizes 53BP1 upon DNA damage, which subsequently regulates cellular response via Chk2-p53 pathway (Zhang *et al.*, 2006). However, another study indicated that Usp28 has minor effects on 53BP1 stability and plays non-essential role in DNA damage response (Knobel *et al.*, 2014). On the other hand, several studies suggested that 53BP1-Usp28 cooperation is crucial for cellular response to DNA damage and centrosome loss (Cuella-Martin *et al.*, 2016; Fong *et al.*, 2016; Lambrus *et al.*, 2016; Meitinger *et al.*, 2016). Cuella-Martin *et al.* demonstrated that the interaction between 53BP1 and Usp28 is crtical for DNA damage-induced activation of p53 pathway, but is dispensable for 53BP1-mediated DNA repair (Cuella-Martin *et al.*, 2016).

Our results demonstrated a role of SCF(β-TrCP) ligase in 53BP1- and Usp28-dependent regulation in DDR. 53BP1 degradation induced by IR treatment was attenuated by Usp28 deletion (Fig 4.5.1A), similar to known β-TrCP substrates. Moreover, the protein levels of 53BP1 accumulated in β-TrCP KO HCT116 cells and HeLa cells stably expressing dominant-negative β-TrCP (Fig 4.5.1B-F). IR-induced destruction of 53BP1 was also attenuated by dominant-negative β-TrCP (Fig 4.5.1F). These results suggest that 53BP1 is degraded in a β-TrCP-dependent manner.

The interaction between 53BP1 and β-TrCP was revealed by immunoprecipitation and PLA assays (Fig 4.5.3A, B). 53BP1 BRCT domain interacted with the substrate binding surface of β-TrCP WD40 repeats (Fig 4.5.3C-F), consistent with the study showing that the WD40 domain of E3 ligase APC/C binds to 53BP1 BRCT domain (Kucharski *et al.*, 2017).

It was previously shown that 53BP1 oligomerization partially facilitates its recruitment to chromatin and promotes NHEJ (Bothmer *et al.*, 2011; Zgheib *et al.*,

2009), while another study demonstrated that OD-deleted 53BP1 is sufficient to mediate NHEJ (Lottersberger *et al.*, 2013). Moreover, 53BP1 oligomerization stabilizes the interaction of BRCT domain with p53 and is necessary for p53 pathway activation upon DNA damage (Cuella-Martin *et al.*, 2016). We showed that 53BP1 oligomerization is required for its β-TrCP-dependent degradation upon DNA damage (Fig 4.5.4B). Since the OD does not have any ubiquitin acceptor lysines that could mediate proteasomal degradation, or sequences similar to β-TrCP degrons, 53BP1 oligomers are likely to be the targets of β-TrCP for degradation, in line with the studies demonstrating that oligomerization of Nrdp1 and p53 is necessary for their efficient ubiquitination and degradation (Maki, 1999; Printsev *et al.*, 2014). Analogous to Fbw7, which requires dimerization for productive interaction with SREBP1/2 (Welcker *et al.*, 2013), 53BP1 oligomerization stimulated its binding to β-TrCP (Fig 4.5.4A), which likely stimulates β-TrCP interaction with the low-affinity binding sites in 53BP1, in concert with Cdc4 binding to multiple weak Cdc4 phospho-degrons in its substrate Sic1 (Nash *et al.*, 2001). Moreover, 53BP1 oligomer formation might stimulate binding of various E3 ligases which cooperate to sequentially ubiquitinate 53BP1, analogous to the data showing that ARIH mediates monoubiquitination of several SCF substrates to allow further ubiquitination by SCF ligases (Scott *et al.*, 2016). As dimeric F-box proteins have better access to substrates (Tang *et al.*, 2007), the oligomerization of 53BP1 might allow additional accessibility to its ubiquitin acceptors for the ligases. Collectively, our data indicate that 53BP1 oligomerization plays an essential role in β-TrCP-dependent degradation in response to DNA damage.

Like the substrates of β-TrCP (*e.g.*, Cdc25A), ectopic and endogenous 53BP1 were downregulated by overexpression of WT but not dimer-deficient β-TrCP (Fig 4.5.2A). Since Usp28 stimulates the activity of β-TrCP, β-TrCP-mediated 53BP1 destruction was promoted by overexpression of Usp28 (Fig 4.5.2B). The non-ubiquitinated β-TrCP-KR showed higher activity in degrading 53BP1, but was not stimulated by Usp28 (Fig 4.5.2B). The reconstitution of WT but not catalytic-inactive Usp28 downregulated the protein levels of 53BP1 and promoted its degradation upon DNA damage (Fig 4.5.2C). Furthermore, in the presence of β-TrCP, the levels of 53BP1 oligomerization were lower in cells overexpressing Usp28 (Fig 4.5.4C), suggesting that Usp28 promotes β-TrCP-mediated degradation of 53BP1 oligomers.

The conflicting observations of Usp28 on 53BP1 from previous studies and our data indicate that Usp28 might have dual regulation on 53BP1 via β-TrCP, which is similar to the effects on Fbw7 substrates (Schulein-Volk *et al.*, 2014). Low levels of Usp28 was previously shown to stabilize Fbw7 and thereby promotes its substrate degradation, while high level of Usp28 stabilizes Fbw7 and its substrates directly. Analogously, we speculate that at low expression levels, Usp28 stimulates β-TrCP-dependent 53BP1 degradation, but at high protein levels of Usp28 or when β-TrCP activity is not able to be promoted by Usp28 (*e.g.,* expression of non-ubiquitinated β-TrCP-KR), Usp28 might directly deubiquitinate and stabilize 53BP1. We showed that DNA damage-induced activation of Usp28, which has been suggested to be stimulated by ATM- or ATR-dependent phosphorylation (Zhang *et al.*, 2006), promotes the deubiquitination and dimerization of β-TrCP, which results in β-TrCP-dependent destruction of 53BP1 and Cdc25A.

5.4 53BP1 inhibits β-TrCP activity and excludes β-TrCP from chromatin

53BP1 was shown to be an inhibitor of the E3 ligase APC/C via interacting with its co-activators Cdc20 and Cdh1 (Kucharski *et al.*, 2017). Our study demonstrated that 53BP1 degradation invariably preceded Cdc25A destruction upon DNA damage (Fig 4.6.1A, B). To investigate whether 53BP1 degradation upon DNA damage plays a role in regulating β-TrCP activity, we generated 53BP1-CTKR with all lysines replaced by arginines, except K1667 and K1669 that located within a putative nuclear localization signal (NLS). As expected, this 53BP1-CT variant was more stable, but was still degraded at later timepoints of CHX assays (Fig 4.6.2A), which likely resulted from K1667 and K1669 remained in 53BP1-CTKR. 53BP1-CTKR had similar subcellular localization, oligomerization and association with chromatin compared to 53BP1-CTWT (Fig 4.6.2B, C). Interestingly, stably expression of 53BP1-CTKR inhibited IR-induced destruction of Cdc25A by β-TrCP (Fig 4.6.2E), suggesting that 53BP1 degradation activates SCF(β-TrCP) ligase in response to DNA damage. The destruction of endogenous 53BP1 upon DNA damage was also attenuated in cells expressing 53BP1-CTKR (Fig 4.6.2D, E), likely as a consequence of oligomerization between endogenous 53BP1 and 53BP1-CTKR. Moreover, comparing to 53BP1-CTWT, the rather homogenous IF staining of 53BP1-CTKR confirmed that 53BP1 was degraded in nucleoplasm (Fig 4.6.2D). This supports the recent studies showing

that 53BP1 destruction occurs in the nucleoplasm, not at the DNA damage sites (Drane *et al.*, 2017; Duheron *et al.*, 2017; Hu *et al.*, 2017; Mayca Pozo *et al.*, 2017). Our study revealed that this effect is required not only for 53BP1 recruitment to DNA damage sites that was suggested previously (Drane *et al.*, 2017; Zhang *et al.*, 2017), but also for the activation of SCF(β-TrCP) ligase. Previous study showed that the DNA damage-induced degradation of unbound bulk 53BP1 is dependent on RNF8 and RNF168 (Drane *et al.*, 2017; Hu *et al.*, 2014). Our data suggest a novel mechanism and function of 53BP1 destruction in a β-TrCP-dependent manner in the nucleoplasm upon DNA damage. To study whether β-TrCP, RNF8 and RNF168 all play essential roles in regulating 53BP1 stability in response to DNA damage, single knockout and double or triple knockout cell lines could be generated and compared.

In line with the idea that β-TrCP is activated by destruction of 53BP1 upon DNA damage, the protein levels of β-TrCP substrates were downregulated by 53BP1 deletion and rescued by expression of dominant-negative β-TrCP (Fig 4.7.1A-C). Consistent with the low Cdc25A levels, the DNA replication was impaired in 53BP1 KO cells (Fig 4.7.1D). Thus, 53BP1 loss stimulated β-TrCP activity in substrate turnover, thereby resulted in regulation of cellular processes.

Additionally, 53BP1 deletion promoted the dimerization of β-TrCP (Fig 4.7.2A) and 53BP1 preferentially bound to monomeric β-TrCP (Fig 4.7.2B). Surprisingly, 53BP1 excluded β-TrCP from chromatin, revealed by enhanced association of β-TrCP with histones in 53BP1 KO cells (Fig 4.7.2A, C). The protein levels of β-TrCP substrates were lower in the chromatin fraction of 53BP1-null cells comparing to those in WT cells (Fig 4.7.2D), suggesting that in the absence of 53BP1, β-TrCP relocalizes to chromatin to promote chromatin-associated substrate degradation. ChIP-Seq data for β-TrCP confirmed that 53BP1 deletion strongly stimulated β-TrCP relocalization to chromatin with much more binding sites and stronger affinity (Fig 4.7.3A-C).

Since DNA damage induces 53BP1 degradation in the nucleoplasm, it is possible that 53BP1-β-TrCP interaction is disrupted upon DNA damage. Indeed, β-TrCP transiently dissociated from 53BP1 after IR treatment, formed dimer and relocalized to chromatin (Fig 4.8.1A-D). Importantly, these effects were attenuated in Usp28-null cells (Fig 4.8.1C). The relocalization of β-TrCP upon DNA damage promoted the degradation of chromatin-associated Cdc25A, which resulted in accumulation of pCdk2 (Fig 4.8.2A-C).

Figure 5.2

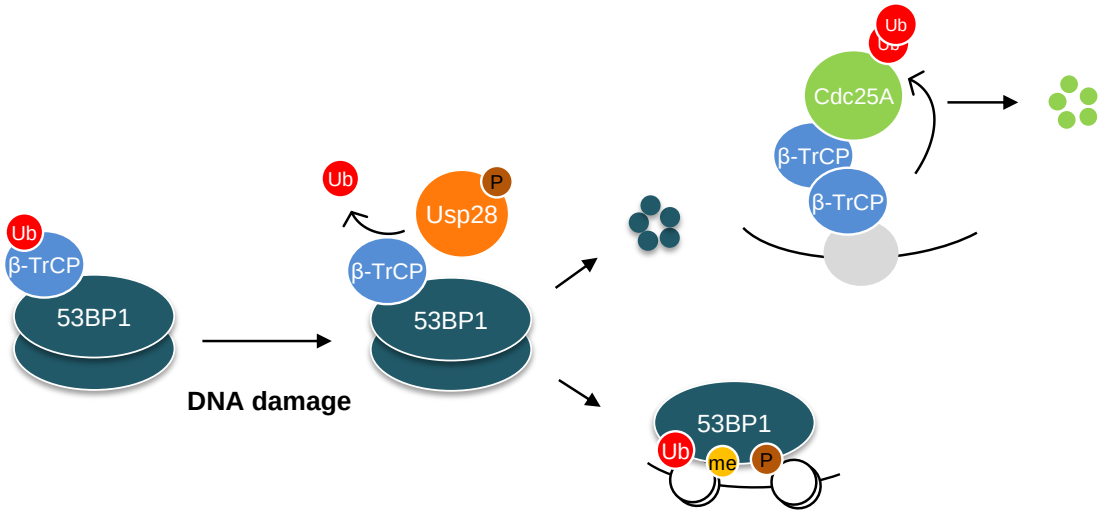

Figure 5.2. A model for 53BP1- and Usp28- dependent activation of β-TrCP upon DNA damage.

Under normal conditions, 53BP1 oligomers inhibits β-TrCP activity by binding and retaining β-TrCP in the nucleoplasm. Upon DNA damage, Usp28 is activated and promotes 53BP1 oligomer degradation in a β-TrCP-dependent manner, and stimulates β-TrCP dimerization. Subsequently, the dimeric β-TrCP is released and relocalizes to chromatin to degrade localized Cdc25A.

Taken together, we propose that DNA damage-induced activation of Usp28 promotes the proteolytic dissociation of 53BP1-β-TrCP complexes in the nucleoplasm, which stimulates 53BP1 accumulation at the DNA damage sites and releases β-TrCP to form dimer. The dimeric β-TrCP relocalizes to chromatin and mediates the degradation of chromatin-associated Cdc25A (Fig 5.2). It has been shown that the subcellular localization is essential for the function of proteins such as p53, RNF144, and SCCRO5 (Bommelje *et al.*, 2014; Ho *et al.*, 2015; Laine and Ronai, 2007). Importantly, self-association affects the subcellular localization and function of proteins. For example, induction of Parkin self-association results in stimulation of its ubiquitination activity and attachment to its substrates on mitochondria (Lazarou *et al.*, 2013). The self-association-deficient SPOP (speckle-type POZ protein) cannot localize to liquid nuclear speckles as wildtype SPOP (Marzahn *et al.*, 2016). Inhibition of E1B-55 kDa oligomerization impairs its localization to the cytoplasmic clusters (Morawska-Onyszczuk *et al.*, 2010). Thus, the Usp28-stimulated β-TrCP dimerization might play a critical role in the interactions

with the effectors that mediate β-TrCP recruitment to chromatin. In fact, ChIP-Seq data revealed that β-TrCP binding sites on chromatin mostly localized at transcription start sites and were enriched at the motifs for β-TrCP-associated transcription factors, including Atf and bHLH families (Fig 4.7.3D). Thus, the dimeric β-TrCP accumulation to chromatin is potentially via interaction with its associated transcription factors, such as Atf4, Myc, NFκB, β-Catenin/Tcf, and CREB-H (Cheng *et al.*, 2016; Fuchs *et al.*, 2004; Lassot *et al.*, 2001; Loveless *et al.*, 2015; Popov *et al.*, 2010).

To experimentally study whether dimerization of β-TrCP is important for its recruitment to chromatin, the fractionation assays for cells expressing WT or dimer-deficient β-TrCP upon DNA damage could be performed. Immunoprecipitation and PLA assays for detecting the interaction between WT or dimer-deficient β-TrCP with histones could also be used.

5.5 DNA damage-induced β-TrCP relocalization to chromatin regulates DNA replication

ChIP-Seq data demonstrated that most of the β-TrCP binding sites on chromatin localized within TSS and CpG-rich sequences (Fig 4.7.3E, F), which are the features associated with replication origins (Cayrou *et al.*, 2011; Hansen *et al.*, 2010; Sequeira-Mendes *et al.*, 2009). β-TrCP sites also showed strong overlap with Orc1 binding sites identified by Repli-seq (Fig 4.7.3G) (Dellino *et al.*, 2013). Mapping of SNS sequence to β-TrCP binding sites showed that β-TrCP bound to the region with multiple origins for replication initiation (Fig 4.7.3I) (Petryk *et al.*, 2016). Additionally, β-TrCP sites preferentially located to the early replicating domains (data not shown) (Hansen *et al.*, 2010). These results suggest that chromatin-associated β-TrCP potentially suppresses firing of replication origins.

53BP1 deletion and DNA damage significantly stimulated β-TrCP recruitment to the co-bound or neighbouring Orc1 sites on chromatin identified by ChIP-Seq (Fig 4.7.3H, Fig 4.8.2D), corresponding to the promoted Cdc25A degradation and impaired DNA replication in our data and previous studies (Busino *et al.*, 2003; Falck *et al.*, 2001; Falck *et al.*, 2002). The chromatin-associated Cdc25A destruction by β-TrCP neighboring putative replication origins led to the inactivation of Cdc25A target, Cdk2 (Fig 4.8.2A-C), which can consequently suppress the assembly of pre-initiation complexes (pre-ICs). Cdk2-dependent loading of Cdc45 onto the pre-RCs is a critical

step for pre-ICs formation and DNA replication initiation (Falck *et al.*, 2002). In fact, Cdc45 dissociated from the pre-RCs component Mcm7 upon DNA damage in a Usp28-dependent manner (Fig 4.2.2F). Supportively, Cdc45 loading to the co-bound or neighbouring Orc1 and β-TrCP sites was downregulated upon IR treatment, accompanied by upregulation of β-TrCP binding (Fig 4.8.2D). These data are consistent with the studies demonstrating that DNA damage slows DNA replication via suppressing origin firing with Cdk2 inhibitory phosphorylation, but not via limiting fork progression rates (Hughes *et al.*, 2013; Iyer *et al.*, 2017; Merrick *et al.*, 2004).

To further confirm the overlap of β-TrCP sites with active replication origin sites upon DNA damage, Repli-Seq analysis could be performed (Hansen *et al.*, 2010). To this end, cells would be treated with or without IR and incubated with BrdU. BrdU-labeled DNA and β-TrCP-associated chromatin would be precipitated with antibodies against BrdU and β-TrCP, followed by ChIP library preparation and deep sequencing. The BrdU sites that indicates active replication origin sites would be mapped to β-TrCP sites and the results from non-treated and IR-treated cells would be compared. β-TrCP ChIP-Seq analysis could also be performed for WT and Usp28-null cells to determine if Usp28 is essential for the relocalization of β-TrCP to the replication initiation sites.

On the other hand, Cdk2 inhibitory phosphorylation is necessary for the normal fork progression and cell recovery from replication stress (Hughes *et al.*, 2013). Accordingly, it is likely that the localized degradation of Cdc25A upon DNA damage plays stronger role in suppressing replication origin firing, rather than in fork progression. Although the induction of Cdk2 phosphorylation is attenuated in Usp28 KO cells, the basal levels of phospho-Cdk2 is elevated (Fig 4.2.2B), which might result from the suppression of Wee1 degradation by β-TrCP since Wee1 phosphorylates Cdk2 and regulates replication fork speed (Chen *et al.*, 2004; Dominguez-Kelly *et al.*, 2011; Watanabe *et al.*, 2004; Watanabe *et al.*, 1995; Wu *et al.*, 2001). The elevated basal levels of pCdk2 might be responsible for the robust fork progression and better recovery from DNA damage overserved in Usp28-null cells. Despite the inhibition of β-TrCP on origin firing upon DNA damage, the silenced origins by β-TrCP might act as a reserve to facilitate the restart of stalled replication forks (Blow *et al.*, 2011; Hills and Diffley, 2014; Iyer *et al.*, 2017). This hypothesis is in line with the studies showing that β-TrCP promotes cell recovery from DNA damage

or replication stress (Mailand *et al.*, 2006; Mamely *et al.*, 2006; Peschiaroli *et al.*, 2006).

During S-phase of normal cell cycle, the low level of checkpoint signaling activity might moderately stimulate the activity of β-TrCP via the motifs enriched on β-TrCP binding sites (*e.g.* Myc, bHLH or Atf4), thereby exhibits restricted effects on DNA replication (Busino *et al.*, 2003). We speculate that, in addition to regulation of DNA replication, activation of β-TrCP on chromatin results in the degradation of multiple chromatin substrates, including transcription factors and histone modifiers, which regulates many cellular processes.

Collectively, we propose a novel mechanism of 53BP1- and Usp28- dependent activation of SCF(β-TrCP) ligase that results in the arrest of DNA replication (Fig 5.3). During normal cell cycle processes, oligomeric 53BP1 binds to β-TrCP and retains it in the nucleoplasm to keep it inactive. Upon DNA damage, Usp28 is activated to deubiquitinate β-TrCP and promote β-TrCP dimerization. Nucleoplasmic 53BP1 oligomers are degraded in a β-TrCP-dependent manner and release β-TrCP. The dimeric β-TrCP binds to the genomic sites which are neighboring putative origins of replication and degrades chromatin-associated Cdc25A. Cdc25A destruction by β-TrCP at origins inactivates Cdk2, inhibits Cdc45 loading to pre-RCs, thereby suppressing the initiation of DNA replication. This model might provide a novel mechanism for the rapid activation of SCF ubiquitin ligases upon DNA damage via deubiquitination and dimerization of F-box proteins and give a new insight into the function of 53BP1 oligomerization and nucleoplasmic destruction induced by DNA damage.

Figure 5.3

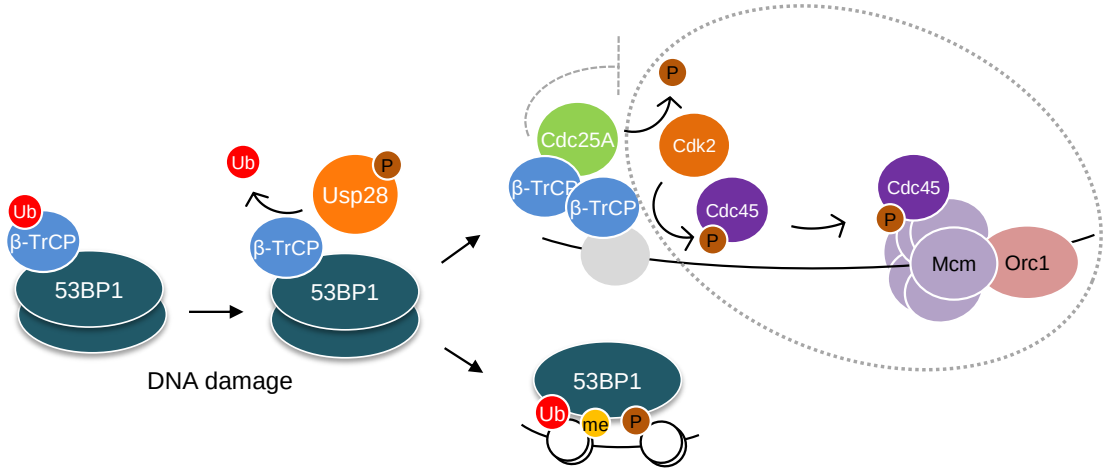

Figure 5.3. Proposed model for 53BP1- and Usp28- dependent activation of SCF (β-TrCP) ligase that leads to arrest of DNA replication upon DNA damage via Cdc25A pathway.

In unstressed cells, 53BP1 oligomers form complexes with β-TrCP in the nucleoplasm to inhibit its activity. Upon DNA damage, Usp28 promotes 53BP1 oligomer degradation in a β-TrCP-dependent manner, resulting in release of β-TrCP. β-TrCP deubiquitination by Usp28 promotes its dimerization. The dimeric β-TrCP relocalizes to DNA replication origins and locally suppresses the initiation of DNA replication via promoting Cdc25A destruction, and subsequent accumulation of inactive pCdk2 to inhibits Cdc45 loading on the pre-RCs.

6 Bibliography

Adams, M. M. and Carpenter, P. B. (2006). Tying the loose ends together in DNA double strand break repair with 53BP1. Cell Div *1*: 19.

Andreassen, P. R., Ho, G. P. and D'Andrea, A. D. (2006). DNA damage responses and their many interactions with the replication fork. Carcinogenesis *27* (5): 883-892.

Aravind, L. and Koonin, E. V. (2000). The U box is a modified RING finger - a common domain in ubiquitination. Curr Biol *10* (4): R132-134.

Banath, J. P., Klokov, D., MacPhail, S. H., Banuelos, C. A. and Olive, P. L. (2010). Residual gammaH2AX foci as an indication of lethal DNA lesions. BMC Cancer *10*: 4.

Banerjee Mustafi, S., Chakraborty, P. K., Dwivedi, S. K., Ding, K., Moxley, K. M., Mukherjee, P. and Bhattacharya, R. (2017). BMI1, a new target of CK2alpha. Mol Cancer *16* (1): 56.

Barenz, F., Inoue, D., Yokoyama, H., Tegha-Dunghu, J., Freiss, S., Draeger, S., Mayilo, D., Cado, I., Merker, S., Klinger, M., Hoeckendorf, B., Pilz, S., Hupfeld, K., Steinbeisser, H., Lorenz, H., Ruppert, T., Wittbrodt, J. and Gruss, O. J. (2013). The centriolar satellite protein SSX2IP promotes centrosome maturation. J Cell Biol *202* (1): 81-95.

Bartek, J. and Lukas, J. (2001). Mammalian G1- and S-phase checkpoints in response to DNA damage. Curr Opin Cell Biol *13* (6): 738-747.

Bassermann, F., Frescas, D., Guardavaccaro, D., Busino, L., Peschiaroli, A. and Pagano, M. (2008). The Cdc14B-Cdh1-Plk1 axis controls the G2 DNA-damage-response checkpoint. Cell *134* (2): 256-267.

Batonnet, S., Leibovitch, M. P., Tintignac, L. and Leibovitch, S. A. (2004). Critical role for lysine 133 in the nuclear ubiquitin-mediated degradation of MyoD. J Biol Chem *279* (7): 5413-5420.

Baud, V., Liu, Z. G., Bennett, B., Suzuki, N., Xia, Y. and Karin, M. (1999). Signaling by proinflammatory cytokines: oligomerization of TRAF2 and TRAF6 is sufficient for JNK and IKK activation and target gene induction via an amino-terminal effector domain. Genes Dev *13* (10): 1297-1308.

Ben-Saadon, R., Zaaroor, D., Ziv, T. and Ciechanover, A. (2006). The polycomb protein Ring1B generates self atypical mixed ubiquitin chains required for its in vitro histone H2A ligase activity. Mol Cell *24* (5): 701-711.

Besnard, E., Babled, A., Lapasset, L., Milhavet, O., Parrinello, H., Dantec, C., Marin, J. M. and Lemaitre, J. M. (2012). Unraveling cell type-specific and reprogrammable

human replication origin signatures associated with G-quadruplex consensus motifs. Nat Struct Mol Biol *19* (8): 837-844.

Bhat, K. P., Truax, A. D. and Greer, S. F. (2010). Phosphorylation and ubiquitination of degron proximal residues are essential for class II transactivator (CIITA) transactivation and major histocompatibility class II expression. J Biol Chem *285* (34): 25893-25903.

Blow, J. J., Ge, X. Q. and Jackson, D. A. (2011). How dormant origins promote complete genome replication. Trends Biochem Sci *36* (8): 405-414.

Bohgaki, M., Bohgaki, T., El Ghamrasni, S., Srikumar, T., Maire, G., Panier, S., Fradet-Turcotte, A., Stewart, G. S., Raught, B., Hakem, A. and Hakem, R. (2013). RNF168 ubiquitylates 53BP1 and controls its response to DNA double-strand breaks. Proc Natl Acad Sci U S A *110* (52): 20982-20987.

Bommelje, C. C., Weeda, V. B., Huang, G., Shah, K., Bains, S., Buss, E., Shaha, M., Gonen, M., Ghossein, R., Ramanathan, S. Y. and Singh, B. (2014). Oncogenic function of SCCRO5/DCUN1D5 requires its Neddylation E3 activity and nuclear localization. Clin Cancer Res *20* (2): 372-381.

Bothmer, A., Robbiani, D. F., Di Virgilio, M., Bunting, S. F., Klein, I. A., Feldhahn, N., Barlow, J., Chen, H. T., Bosque, D., Callen, E., Nussenzweig, A. and Nussenzweig, M. C. (2011). Regulation of DNA end joining, resection, and immunoglobulin class switch recombination by 53BP1. Mol Cell *42* (3): 319-329.

Bouwman, P., Aly, A., Escandell, J. M., Pieterse, M., Bartkova, J., van der Gulden, H., Hiddingh, S., Thanasoula, M., Kulkarni, A., Yang, Q., Haffty, B. G., Tommiska, J., Blomqvist, C., Drapkin, R., Adams, D. J., Nevanlinna, H., Bartek, J., Tarsounas, M., Ganesan, S. and Jonkers, J. (2010). 53BP1 loss rescues BRCA1 deficiency and is associated with triple-negative and BRCA-mutated breast cancers. Nat Struct Mol Biol *17* (6): 688-695.

Brinkmann, K., Schell, M., Hoppe, T. and Kashkar, H. (2015). Regulation of the DNA damage response by ubiquitin conjugation. Front Genet *6*: 98.

Budenholzer, L., Cheng, C. L., Li, Y. and Hochstrasser, M. (2017). Proteasome Structure and Assembly. J Mol Biol.

Bunting, S. F., Callen, E., Wong, N., Chen, H. T., Polato, F., Gunn, A., Bothmer, A., Feldhahn, N., Fernandez-Capetillo, O., Cao, L., Xu, X., Deng, C. X., Finkel, T., Nussenzweig, M., Stark, J. M. and Nussenzweig, A. (2010). 53BP1 inhibits homologous recombination in Brca1-deficient cells by blocking resection of DNA breaks. Cell *141* (2): 243-254.

Busino, L., Donzelli, M., Chiesa, M., Guardavaccaro, D., Ganoth, D., Dorrello, N. V., Hershko, A., Pagano, M. and Draetta, G. F. (2003). Degradation of Cdc25A by beta-TrCP during S phase and in response to DNA damage. Nature *426* (6962): 87-91.

Cano, F., Rapiteanu, R., Sebastiaan Winkler, G. and Lehner, P. J. (2015). A non-proteolytic role for ubiquitin in deadenylation of MHC-I mRNA by the RNA-binding E3-ligase MEX-3C. Nat Commun *6*: 8670.

Cardozo, T. and Pagano, M. (2004). The SCF ubiquitin ligase: insights into a molecular machine. Nat Rev Mol Cell Biol *5* (9): 739-751.

Cayrou, C., Coulombe, P., Vigneron, A., Stanojcic, S., Ganier, O., Peiffer, I., Rivals, E., Puy, A., Laurent-Chabalier, S., Desprat, R. and Mechali, M. (2011). Genome-scale analysis of metazoan replication origins reveals their organization in specific but flexible sites defined by conserved features. Genome Res *21* (9): 1438-1449.

Chapman, J. R., Taylor, M. R. and Boulton, S. J. (2012). Playing the end game: DNA double-strand break repair pathway choice. Mol Cell *47* (4): 497-510.

Chen, S. and Gardner, D. G. (2004). Suppression of WEE1 and stimulation of CDC25A correlates with endothelin-dependent proliferation of rat aortic smooth muscle cells. J Biol Chem *279* (14): 13755-13763.

Chen, Z. J. and Sun, L. J. (2009). Nonproteolytic functions of ubiquitin in cell signaling. Mol Cell *33* (3): 275-286.

Cheng, Y., Gao, W. W., Tang, H. M., Deng, J. J., Wong, C. M., Chan, C. P. and Jin, D. Y. (2016). beta-TrCP-mediated ubiquitination and degradation of liver-enriched transcription factor CREB-H. Sci Rep *6*: 23938.

Choo, Y. Y. and Hagen, T. (2012). Mechanism of cullin3 E3 ubiquitin ligase dimerization. PLoS One *7* (7): e41350.

Ciccia, A. and Elledge, S. J. (2010). The DNA damage response: making it safe to play with knives. Mol Cell *40* (2): 179-204.

Citterio, E. (2015). Fine-tuning the ubiquitin code at DNA double-strand breaks: deubiquitinating enzymes at work. Front Genet *6*: 282.

Cuella-Martin, R., Oliveira, C., Lockstone, H. E., Snellenberg, S., Grolmusova, N. and Chapman, J. R. (2016). 53BP1 Integrates DNA Repair and p53-Dependent Cell Fate Decisions via Distinct Mechanisms. Mol Cell *64* (1): 51-64.

Davis, M., Hatzubai, A., Andersen, J. S., Ben-Shushan, E., Fisher, G. Z., Yaron, A., Bauskin, A., Mercurio, F., Mann, M. and Ben-Neriah, Y. (2002). Pseudosubstrate regulation of the SCF(beta-TrCP) ubiquitin ligase by hnRNP-U. Genes Dev *16* (4): 439-451.

de Bie, P. and Ciechanover, A. (2011). Ubiquitination of E3 ligases: self-regulation of the ubiquitin system via proteolytic and non-proteolytic mechanisms. Cell Death Differ *18* (9): 1393-1402.

Dehan, E., Bassermann, F., Guardavaccaro, D., Vasiliver-Shamis, G., Cohen, M., Lowes, K. N., Dustin, M., Huang, D. C., Taunton, J. and Pagano, M. (2009). betaTrCP- and Rsk1/2-mediated degradation of BimEL inhibits apoptosis. Mol Cell *33* (1): 109-116.

Dellino, G. I., Cittaro, D., Piccioni, R., Luzi, L., Banfi, S., Segalla, S., Cesaroni, M., Mendoza-Maldonado, R., Giacca, M. and Pelicci, P. G. (2013). Genome-wide mapping of human DNA-replication origins: levels of transcription at ORC1 sites regulate origin selection and replication timing. Genome Res *23* (1): 1-11.

Deshaies, R. J. (1999). SCF and Cullin/Ring H2-based ubiquitin ligases. Annu Rev Cell Dev Biol *15*: 435-467.

Diefenbacher, M. E., Popov, N., Blake, S. M., Schulein-Volk, C., Nye, E., Spencer-Dene, B., Jaenicke, L. A., Eilers, M. and Behrens, A. (2014). The deubiquitinase USP28 controls intestinal homeostasis and promotes colorectal cancer. J Clin Invest *124* (8): 3407-3418.

Ding, Q., He, X., Hsu, J. M., Xia, W., Chen, C. T., Li, L. Y., Lee, D. F., Liu, J. C., Zhong, Q., Wang, X. and Hung, M. C. (2007). Degradation of Mcl-1 by beta-TrCP mediates glycogen synthase kinase 3-induced tumor suppression and chemosensitization. Mol Cell Biol *27* (11): 4006-4017.

Dobin, A., Davis, C. A., Schlesinger, F., Drenkow, J., Zaleski, C., Jha, S., Batut, P., Chaisson, M. and Gingeras, T. R. (2013). STAR: ultrafast universal RNA-seq aligner. Bioinformatics *29* (1): 15-21.

Doil, C., Mailand, N., Bekker-Jensen, S., Menard, P., Larsen, D. H., Pepperkok, R., Ellenberg, J., Panier, S., Durocher, D., Bartek, J., Lukas, J. and Lukas, C. (2009). RNF168 binds and amplifies ubiquitin conjugates on damaged chromosomes to allow accumulation of repair proteins. Cell *136* (3): 435-446.

Dominguez-Kelly, R., Martin, Y., Koundrioukoff, S., Tanenbaum, M. E., Smits, V. A., Medema, R. H., Debatisse, M. and Freire, R. (2011). Wee1 controls genomic stability during replication by regulating the Mus81-Eme1 endonuclease. J Cell Biol *194* (4): 567-579.

Drane, P., Brault, M. E., Cui, G., Meghani, K., Chaubey, S., Detappe, A., Parnandi, N., He, Y., Zheng, X. F., Botuyan, M. V., Kalousi, A., Yewdell, W. T., Munch, C., Harper, J. W., Chaudhuri, J., Soutoglou, E., Mer, G. and Chowdhury, D. (2017). TIRR regulates 53BP1 by masking its histone methyl-lysine binding function. Nature *543* (7644): 211-216.

Duheron, V., Nilles, N., Pecenko, S., Martinelli, V. and Fahrenkrog, B. (2017). Localisation of Nup153 and SENP1 to nuclear pore complexes is required for 53BP1 mediated DNA double-strand break repair. J Cell Sci.

Falck, J., Mailand, N., Syljuasen, R. G., Bartek, J. and Lukas, J. (2001). The ATM-Chk2-Cdc25A checkpoint pathway guards against radioresistant DNA synthesis. Nature *410* (6830): 842-847.

Falck, J., Petrini, J. H., Williams, B. R., Lukas, J. and Bartek, J. (2002). The DNA damage-dependent intra-S phase checkpoint is regulated by parallel pathways. Nat Genet *30* (3): 290-294.

Fang, S., Jensen, J. P., Ludwig, R. L., Vousden, K. H. and Weissman, A. M. (2000). Mdm2 is a RING finger-dependent ubiquitin protein ligase for itself and p53. J Biol Chem *275* (12): 8945-8951.

Flick, K., Raasi, S., Zhang, H., Yen, J. L. and Kaiser, P. (2006). A ubiquitin-interacting motif protects polyubiquitinated Met4 from degradation by the 26S proteasome. Nat Cell Biol *8* (5): 509-515.

Fong, C. S., Mazo, G., Das, T., Goodman, J., Kim, M., O'Rourke, B. P., Izquierdo, D. and Tsou, M. F. (2016). 53BP1 and USP28 mediate p53-dependent cell cycle arrest in response to centrosome loss and prolonged mitosis. Elife *5*.

Fragkos, M., Ganier, O., Coulombe, P. and Mechali, M. (2015). DNA replication origin activation in space and time. Nat Rev Mol Cell Biol *16* (6): 360-374.

Freire, R., van Vugt, M. A., Mamely, I. and Medema, R. H. (2006). Claspin: timing the cell cycle arrest when the genome is damaged. Cell Cycle *5* (24): 2831-2834.

Frescas, D. and Pagano, M. (2008). Deregulated proteolysis by the F-box proteins SKP2 and beta-TrCP: tipping the scales of cancer. Nat Rev Cancer *8* (6): 438-449.

Fuchs, S. Y., Chen, A., Xiong, Y., Pan, Z. Q. and Ronai, Z. (1999). HOS, a human homolog of Slimb, forms an SCF complex with Skp1 and Cullin1 and targets the phosphorylation-dependent degradation of IkappaB and beta-catenin. Oncogene *18* (12): 2039-2046.

Fuchs, S. Y., Spiegelman, V. S. and Kumar, K. G. (2004). The many faces of beta-TrCP E3 ubiquitin ligases: reflections in the magic mirror of cancer. Oncogene *23* (11): 2028-2036.

Galan, J. M. and Peter, M. (1999). Ubiquitin-dependent degradation of multiple F-box proteins by an autocatalytic mechanism. Proc Natl Acad Sci U S A *96* (16): 9124-9129.

Ginjala, V., Nacerddine, K., Kulkarni, A., Oza, J., Hill, S. J., Yao, M., Citterio, E., van Lohuizen, M. and Ganesan, S. (2011). BMI1 is recruited to DNA breaks and contributes to DNA damage-induced H2A ubiquitination and repair. Mol Cell Biol *31* (10): 1972-1982.

Guardavaccaro, D., Kudo, Y., Boulaire, J., Barchi, M., Busino, L., Donzelli, M., Margottin-Goguet, F., Jackson, P. K., Yamasaki, L. and Pagano, M. (2003). Control of meiotic and mitotic progression by the F box protein beta-Trcp1 in vivo. Dev Cell *4* (6): 799-812.

Gudjonsson, T., Altmeyer, M., Savic, V., Toledo, L., Dinant, C., Grofte, M., Bartkova, J., Poulsen, M., Oka, Y., Bekker-Jensen, S., Mailand, N., Neumann, B., Heriche, J. K., Shearer, R., Saunders, D., Bartek, J., Lukas, J. and Lukas, C. (2012). TRIP12 and UBR5 suppress spreading of chromatin ubiquitylation at damaged chromosomes. Cell *150* (4): 697-709.

Hakem, R. (2008). DNA-damage repair; the good, the bad, and the ugly. EMBO J *27* (4): 589-605.

Han, X., Zhang, L., Chung, J., Mayca Pozo, F., Tran, A., Seachrist, D. D., Jacobberger, J. W., Keri, R. A., Gilmore, H. and Zhang, Y. (2014). UbcH7 regulates 53BP1 stability and DSB repair. Proc Natl Acad Sci U S A *111* (49): 17456-17461.

Hansen, R. S., Thomas, S., Sandstrom, R., Canfield, T. K., Thurman, R. E., Weaver, M., Dorschner, M. O., Gartler, S. M. and Stamatoyannopoulos, J. A. (2010). Sequencing newly replicated DNA reveals widespread plasticity in human replication timing. Proc Natl Acad Sci U S A *107* (1): 139-144.

Harper, J. W. and Elledge, S. J. (2007). The DNA damage response: ten years after. Mol Cell *28* (5): 739-745.

Harrigan, J. A., Belotserkovskaya, R., Coates, J., Dimitrova, D. S., Polo, S. E., Bradshaw, C. R., Fraser, P. and Jackson, S. P. (2011). Replication stress induces 53BP1-containing OPT domains in G1 cells. J Cell Biol *193* (1): 97-108.

Hart, M., Concordet, J. P., Lassot, I., Albert, I., del los Santos, R., Durand, H., Perret, C., Rubinfeld, B., Margottin, F., Benarous, R. and Polakis, P. (1999). The F-box protein beta-TrCP associates with phosphorylated beta-catenin and regulates its activity in the cell. Curr Biol *9* (4): 207-210.

Hattori, K., Hatakeyama, S., Shirane, M., Matsumoto, M. and Nakayama, K. (1999). Molecular dissection of the interactions among IkappaBalpha, FWD1, and Skp1 required for ubiquitin-mediated proteolysis of IkappaBalpha. J Biol Chem *274* (42): 29641-29647.

Herman-Bachinsky, Y., Ryoo, H. D., Ciechanover, A. and Gonen, H. (2007). Regulation of the Drosophila ubiquitin ligase DIAP1 is mediated via several distinct ubiquitin system pathways. Cell Death Differ *14* (4): 861-871.

Hershko, A. and Ciechanover, A. (1998). The ubiquitin system. Annu Rev Biochem *67*: 425-479.

Hicke, L. (2001). Protein regulation by monoubiquitin. Nat Rev Mol Cell Biol *2* (3): 195-201.

Hills, S. A. and Diffley, J. F. (2014). DNA replication and oncogene-induced replicative stress. Curr Biol *24* (10): R435-444.

Ho, S. R., Lee, Y. J. and Lin, W. C. (2015). Regulation of RNF144A E3 Ubiquitin Ligase Activity by Self-association through Its Transmembrane Domain. J Biol Chem *290* (38): 23026-23038.

Hoeijmakers, J. H. (2001). DNA repair mechanisms. Maturitas *38* (1): 17-22; discussion 22-13.

Honaker, Y. and Piwnica-Worms, H. (2010). Casein kinase 1 functions as both penultimate and ultimate kinase in regulating Cdc25A destruction. Oncogene *29* (23): 3324-3334.

Honda, R. and Yasuda, H. (1999). Association of p19(ARF) with Mdm2 inhibits ubiquitin ligase activity of Mdm2 for tumor suppressor p53. EMBO J *18* (1): 22-27.

Hu, G. and Fearon, E. R. (1999). Siah-1 N-terminal RING domain is required for proteolysis function, and C-terminal sequences regulate oligomerization and binding to target proteins. Mol Cell Biol *19* (1): 724-732.

Hu, Q., Botuyan, M. V., Cui, G., Zhao, D. and Mer, G. (2017). Mechanisms of Ubiquitin-Nucleosome Recognition and Regulation of 53BP1 Chromatin Recruitment by RNF168/169 and RAD18. Mol Cell *66* (4): 473-487 e479.

Hu, Y., Wang, C., Huang, K., Xia, F., Parvin, J. D. and Mondal, N. (2014). Regulation of 53BP1 protein stability by RNF8 and RNF168 is important for efficient DNA double-strand break repair. PLoS One *9* (10): e110522.

Hughes, B. T., Sidorova, J., Swanger, J., Monnat, R. J., Jr. and Clurman, B. E. (2013). Essential role for Cdk2 inhibitory phosphorylation during replication stress revealed by a human Cdk2 knockin mutation. Proc Natl Acad Sci U S A *110* (22): 8954-8959.

Inuzuka, H., Tseng, A., Gao, D., Zhai, B., Zhang, Q., Shaik, S., Wan, L., Ang, X. L., Mock, C., Yin, H., Stommel, J. M., Gygi, S., Lahav, G., Asara, J., Xiao, Z. X., Kaelin, W. G., Jr., Harper, J. W. and Wei, W. (2010). Phosphorylation by casein kinase I promotes the turnover of the Mdm2 oncoprotein via the SCF(beta-TRCP) ubiquitin ligase. Cancer Cell *18* (2): 147-159.

Isaacs, J. S., Chiao, C., Merrick, B. A., Selkirk, J. K., Barrett, J. C. and Weissman, B. E. (1997). p53-dependent p21 induction following gamma-irradiation without concomitant p53 induction in a human peripheral neuroepithelioma cell line. Cancer Res *57* (14): 2986-2992.

Iwabuchi, K., Basu, B. P., Kysela, B., Kurihara, T., Shibata, M., Guan, D., Cao, Y., Hamada, T., Imamura, K., Jeggo, P. A., Date, T. and Doherty, A. J. (2003). Potential role for 53BP1 in DNA end-joining repair through direct interaction with DNA. J Biol Chem *278* (38): 36487-36495.

Iyer, D. R. and Rhind, N. (2017). The Intra-S Checkpoint Responses to DNA Damage. Genes (Basel) *8* (2).

Iyer, D. R. and Rhind, N. (2017). Replication fork slowing and stalling are distinct, checkpoint-independent consequences of replicating damaged DNA. PLoS Genet *13* (8): e1006958.

Jaenicke, L. A., von Eyss, B., Carstensen, A., Wolf, E., Xu, W., Greifenberg, A. K., Geyer, M., Eilers, M. and Popov, N. (2016). Ubiquitin-Dependent Turnover of MYC Antagonizes MYC/PAF1C Complex Accumulation to Drive Transcriptional Elongation. Mol Cell *61* (1): 54-67.

Jin, J., Shirogane, T., Xu, L., Nalepa, G., Qin, J., Elledge, S. J. and Harper, J. W. (2003). SCFbeta-TRCP links Chk1 signaling to degradation of the Cdc25A protein phosphatase. Genes Dev *17* (24): 3062-3074.

Jones, R. M. and Petermann, E. (2012). Replication fork dynamics and the DNA damage response. Biochem J *443* (1): 13-26.

Kim, W., Bennett, E. J., Huttlin, E. L., Guo, A., Li, J., Possemato, A., Sowa, M. E., Rad, R., Rush, J., Comb, M. J., Harper, J. W. and Gygi, S. P. (2011). Systematic and quantitative assessment of the ubiquitin-modified proteome. Mol Cell *44* (2): 325-340.

Kipreos, E. T. and Pagano, M. (2000). The F-box protein family. Genome Biol *1* (5): REVIEWS3002.

Kirkpatrick, D. S., Hathaway, N. A., Hanna, J., Elsasser, S., Rush, J., Finley, D., King, R. W. and Gygi, S. P. (2006). Quantitative analysis of in vitro ubiquitinated cyclin B1 reveals complex chain topology. Nat Cell Biol *8* (7): 700-710.

Knobel, P. A., Belotserkovskaya, R., Galanty, Y., Schmidt, C. K., Jackson, S. P. and Stracker, T. H. (2014). USP28 is recruited to sites of DNA damage by the tandem BRCT domains of 53BP1 but plays a minor role in double-strand break metabolism. Mol Cell Biol *34* (11): 2062-2074.

Kobe, B. and Kajava, A. V. (2001). The leucine-rich repeat as a protein recognition motif. Curr Opin Struct Biol *11* (6): 725-732.

Koliopoulos, M. G., Esposito, D., Christodoulou, E., Taylor, I. A. and Rittinger, K. (2016). Functional role of TRIM E3 ligase oligomerization and regulation of catalytic activity. EMBO J *35* (11): 1204-1218.

Komander, D., Clague, M. J. and Urbe, S. (2009). Breaking the chains: structure and function of the deubiquitinases. Nat Rev Mol Cell Biol *10* (8): 550-563.

Komander, D. and Rape, M. (2012). The ubiquitin code. Annu Rev Biochem *81*: 203-229.

Kucharski, T. J., Minshall, P. E., Moustafa-Kamal, M., Turnell, A. S. and Teodoro, J. G. (2017). Reciprocal Regulation between 53BP1 and the Anaphase-Promoting Complex/Cyclosome Is Required for Genomic Stability during Mitotic Stress. Cell Rep *18* (8): 1982-1995.

Laine, A. and Ronai, Z. (2007). Regulation of p53 localization and transcription by the HECT domain E3 ligase WWP1. Oncogene *26* (10): 1477-1483.

Lambrus, B. G., Daggubati, V., Uetake, Y., Scott, P. M., Clutario, K. M., Sluder, G. and Holland, A. J. (2016). A USP28-53BP1-p53-p21 signaling axis arrests growth after centrosome loss or prolonged mitosis. J Cell Biol *214* (2): 143-153.

Langley, A. R., Graf, S., Smith, J. C. and Krude, T. (2016). Genome-wide identification and characterisation of human DNA replication origins by initiation site sequencing (ini-seq). Nucleic Acids Res *44* (21): 10230-10247.

Lassot, I., Segeral, E., Berlioz-Torrent, C., Durand, H., Groussin, L., Hai, T., Benarous, R. and Margottin-Goguet, F. (2001). ATF4 degradation relies on a phosphorylation-dependent interaction with the SCF(betaTrCP) ubiquitin ligase. Mol Cell Biol *21* (6): 2192-2202.

Latres, E., Chiaur, D. S. and Pagano, M. (1999). The human F box protein beta-Trcp associates with the Cul1/Skp1 complex and regulates the stability of beta-catenin. Oncogene *18* (4): 849-854.

Lazarou, M., Narendra, D. P., Jin, S. M., Tekle, E., Banerjee, S. and Youle, R. J. (2013). PINK1 drives Parkin self-association and HECT-like E3 activity upstream of mitochondrial binding. J Cell Biol *200* (2): 163-172.

Lee, D. H. and Goldberg, A. L. (1996). Selective inhibitors of the proteasome-dependent and vacuolar pathways of protein degradation in Saccharomyces cerevisiae. J Biol Chem *271* (44): 27280-27284.

Lee, J. H., Goodarzi, A. A., Jeggo, P. A. and Paull, T. T. (2010). 53BP1 promotes ATM activity through direct interactions with the MRN complex. EMBO J *29* (3): 574-585.

Li, D. and Roberts, R. (2001). WD-repeat proteins: structure characteristics, biological function, and their involvement in human diseases. Cell Mol Life Sci *58* (14): 2085-2097.

Li, H., Okamoto, K., Peart, M. J. and Prives, C. (2009). Lysine-independent turnover of cyclin G1 can be stabilized by B'alpha subunits of protein phosphatase 2A. Mol Cell Biol *29* (3): 919-928.

Li, M. Z. and Elledge, S. J. (2007). Harnessing homologous recombination in vitro to generate recombinant DNA via SLIC. Nat Methods *4* (3): 251-256.

Li, Y., Gazdoiu, S., Pan, Z. Q. and Fuchs, S. Y. (2004). Stability of homologue of Slimb F-box protein is regulated by availability of its substrate. J Biol Chem *279* (12): 11074-11080.

Liew, C. W., Sun, H., Hunter, T. and Day, C. L. (2010). RING domain dimerization is essential for RNF4 function. Biochem J *431* (1): 23-29.

Liu, P., Barkley, L. R., Day, T., Bi, X., Slater, D. M., Alexandrow, M. G., Nasheuer, H. P. and Vaziri, C. (2006). The Chk1-mediated S-phase checkpoint targets initiation factor Cdc45 via a Cdc25A/Cdk2-independent mechanism. J Biol Chem *281* (41): 30631-30644.

Lorick, K. L., Jensen, J. P., Fang, S., Ong, A. M., Hatakeyama, S. and Weissman, A. M. (1999). RING fingers mediate ubiquitin-conjugating enzyme (E2)-dependent ubiquitination. Proc Natl Acad Sci U S A *96* (20): 11364-11369.

Lottersberger, F., Bothmer, A., Robbiani, D. F., Nussenzweig, M. C. and de Lange, T. (2013). Role of 53BP1 oligomerization in regulating double-strand break repair. Proc Natl Acad Sci U S A *110* (6): 2146-2151.

Loveless, T. B., Topacio, B. R., Vashisht, A. A., Galaang, S., Ulrich, K. M., Young, B. D., Wohlschlegel, J. A. and Toczyski, D. P. (2015). DNA Damage Regulates Translation through beta-TRCP Targeting of CReP. PLoS Genet *11* (6): e1005292.

Mah, L. J., El-Osta, A. and Karagiannis, T. C. (2010). gammaH2AX: a sensitive molecular marker of DNA damage and repair. Leukemia *24* (4): 679-686.

Mailand, N., Bekker-Jensen, S., Bartek, J. and Lukas, J. (2006). Destruction of claspin by SCF beta TrCP restrains Chk1 activation and facilitates recovery from genotoxic stress. Molecular Cell *23* (3): 307-318.

Maki, C. G. (1999). Oligomerization is required for p53 to be efficiently ubiquitinated by MDM2. J Biol Chem *274* (23): 16531-16535.

Mallery, D. L., Vandenberg, C. J. and Hiom, K. (2002). Activation of the E3 ligase function of the BRCA1/BARD1 complex by polyubiquitin chains. EMBO J *21* (24): 6755-6762.

Mamely, I., van Vugt, M. A., Smits, V. A., Semple, J. I., Lemmens, B., Perrakis, A., Medema, R. H. and Freire, R. (2006). Polo-like kinase-1 controls proteasome-dependent degradation of Claspin during checkpoint recovery. Curr Biol *16* (19): 1950-1955.

Marechal, A. and Zou, L. (2013). DNA damage sensing by the ATM and ATR kinases. Cold Spring Harb Perspect Biol *5* (9).

Margottin-Goguet, F., Hsu, J. Y., Loktev, A., Hsieh, H. M., Reimann, J. D. and Jackson, P. K. (2003). Prophase destruction of Emi1 by the SCF(betaTrCP/Slimb)

ubiquitin ligase activates the anaphase promoting complex to allow progression beyond prometaphase. Dev Cell *4* (6): 813-826.

Marzahn, M. R., Marada, S., Lee, J., Nourse, A., Kenrick, S., Zhao, H., Ben-Nissan, G., Kolaitis, R. M., Peters, J. L., Pounds, S., Errington, W. J., Prive, G. G., Taylor, J. P., Sharon, M., Schuck, P., Ogden, S. K. and Mittag, T. (2016). Higher-order oligomerization promotes localization of SPOP to liquid nuclear speckles. EMBO J *35* (12): 1254-1275.

Mayca Pozo, F., Tang, J., Bonk, K. W., Keri, R. A., Yao, X. and Zhang, Y. (2017). Regulatory cross-talk determines the cellular levels of 53BP1 protein, a critical factor in DNA repair. J Biol Chem *292* (14): 5992-6003.

McDowell, G. S. and Philpott, A. (2013). Non-canonical ubiquitylation: mechanisms and consequences. Int J Biochem Cell Biol *45* (8): 1833-1842.

Meitinger, F., Anzola, J. V., Kaulich, M., Richardson, A., Stender, J. D., Benner, C., Glass, C. K., Dowdy, S. F., Desai, A., Shiau, A. K. and Oegema, K. (2016). 53BP1 and USP28 mediate p53 activation and G1 arrest after centrosome loss or extended mitotic duration. J Cell Biol *214* (2): 155-166.

Merrick, C. J., Jackson, D. and Diffley, J. F. (2004). Visualization of altered replication dynamics after DNA damage in human cells. J Biol Chem *279* (19): 20067-20075.

Min, S. H., Lau, A. W., Lee, T. H., Inuzuka, H., Wei, S., Huang, P., Shaik, S., Lee, D. Y., Finn, G., Balastik, M., Chen, C. H., Luo, M., Tron, A. E., Decaprio, J. A., Zhou, X. Z., Wei, W. and Lu, K. P. (2012). Negative regulation of the stability and tumor suppressor function of Fbw7 by the Pin1 prolyl isomerase. Mol Cell *46* (6): 771-783.

Morawska-Onyszczuk, M., Bienkowska-Szewczyk, K. and Dobbelstein, M. (2010). Self-association of adenovirus type 5 E1B-55 kDa as well as p53 is essential for their mutual interaction. Oncogene *29* (12): 1773-1786.

Nacerddine, K., Beaudry, J. B., Ginjala, V., Westerman, B., Mattiroli, F., Song, J. Y., van der Poel, H., Ponz, O. B., Pritchard, C., Cornelissen-Steijger, P., Zevenhoven, J., Tanger, E., Sixma, T. K., Ganesan, S. and van Lohuizen, M. (2012). Akt-mediated phosphorylation of Bmi1 modulates its oncogenic potential, E3 ligase activity, and DNA damage repair activity in mouse prostate cancer. J Clin Invest *122* (5): 1920-1932.

Nakatani, Y., Kleffmann, T., Linke, K., Condon, S. M., Hinds, M. G. and Day, C. L. (2013). Regulation of ubiquitin transfer by XIAP, a dimeric RING E3 ligase. Biochem J *450* (3): 629-638.

Nakayama, K., Hatakeyama, S., Maruyama, S., Kikuchi, A., Onoe, K., Good, R. A. and Nakayama, K. I. (2003). Impaired degradation of inhibitory subunit of NF-kappa B (I kappa B) and beta-catenin as a result of targeted disruption of the beta-TrCP1 gene. Proc Natl Acad Sci U S A *100* (15): 8752-8757.

Nash, P., Tang, X., Orlicky, S., Chen, Q., Gertler, F. B., Mendenhall, M. D., Sicheri, F., Pawson, T. and Tyers, M. (2001). Multisite phosphorylation of a CDK inhibitor sets a threshold for the onset of DNA replication. Nature *414* (6863): 514-521.

Natarajan, C. and Takeda, K. (2017). Regulation of various DNA repair pathways by E3 ubiquitin ligases. J Cancer Res Ther *13* (2): 157-169.

Noon, A. T. and Goodarzi, A. A. (2011). 53BP1-mediated DNA double strand break repair: insert bad pun here. DNA Repair (Amst) *10* (10): 1071-1076.

Panier, S. and Boulton, S. J. (2014). Double-strand break repair: 53BP1 comes into focus. Nat Rev Mol Cell Biol *15* (1): 7-18.

Pashkova, N., Gakhar, L., Winistorfer, S. C., Yu, L., Ramaswamy, S. and Piper, R. C. (2010). WD40 repeat propellers define a ubiquitin-binding domain that regulates turnover of F box proteins. Mol Cell *40* (3): 433-443.

Peschiaroli, A., Dorrello, N. V., Guardavaccaro, D., Venere, M., Halazonetis, T., Sherman, N. E. and Pagano, M. (2006). SCFbetaTrCP-mediated degradation of Claspin regulates recovery from the DNA replication checkpoint response. Mol Cell *23* (3): 319-329.

Petroski, M. D. and Deshaies, R. J. (2005). Function and regulation of cullin-RING ubiquitin ligases. Nat Rev Mol Cell Biol *6* (1): 9-20.

Petryk, N., Kahli, M., d'Aubenton-Carafa, Y., Jaszczyszyn, Y., Shen, Y., Silvain, M., Thermes, C., Chen, C. L. and Hyrien, O. (2016). Replication landscape of the human genome. Nat Commun *7*: 10208.

Pickart, C. M. (2001). Mechanisms underlying ubiquitination. Annu Rev Biochem *70*: 503-533.

Pickart, C. M. and Eddins, M. J. (2004). Ubiquitin: structures, functions, mechanisms. Biochim Biophys Acta *1695* (1-3): 55-72.

Plechanovova, A., Jaffray, E. G., McMahon, S. A., Johnson, K. A., Navratilova, I., Naismith, J. H. and Hay, R. T. (2011). Mechanism of ubiquitylation by dimeric RING ligase RNF4. Nat Struct Mol Biol *18* (9): 1052-1059.

Popov, N., Herold, S., Llamazares, M., Schulein, C. and Eilers, M. (2007). Fbw7 and Usp28 regulate myc protein stability in response to DNA damage. Cell Cycle *6* (19): 2327-2331.

Popov, N., Schulein, C., Jaenicke, L. A. and Eilers, M. (2010). Ubiquitylation of the amino terminus of Myc by SCF(beta-TrCP) antagonizes SCF(Fbw7)-mediated turnover. Nat Cell Biol *12* (10): 973-981.

Popov, N., Wanzel, M., Madiredjo, M., Zhang, D., Beijersbergen, R., Bernards, R., Moll, R., Elledge, S. J. and Eilers, M. (2007). The ubiquitin-specific protease USP28 is required for MYC stability. Nat Cell Biol *9* (7): 765-774.

Printsev, I., Yen, L., Sweeney, C. and Carraway, K. L., 3rd (2014). Oligomerization of the Nrdp1 E3 ubiquitin ligase is necessary for efficient autoubiquitination but not ErbB3 ubiquitination. J Biol Chem *289* (12): 8570-8578.

Raynard, S., Niu, H. and Sung, P. (2008). DNA double-strand break processing: the beginning of the end. Genes Dev *22* (21): 2903-2907.

Reyes-Turcu, F. E., Ventii, K. H. and Wilkinson, K. D. (2009). Regulation and cellular roles of ubiquitin-specific deubiquitinating enzymes. Annu Rev Biochem *78*: 363-397.

Rother, K., Kirschner, R., Sanger, K., Bohlig, L., Mossner, J. and Engeland, K. (2007). p53 downregulates expression of the G1/S cell cycle phosphatase Cdc25A. Oncogene *26* (13): 1949-1953.

Ryan, P. E., Davies, G. C., Nau, M. M. and Lipkowitz, S. (2006). Regulating the regulator: negative regulation of Cbl ubiquitin ligases. Trends Biochem Sci *31* (2): 79-88.

Sadowski, M. and Sarcevic, B. (2010). Mechanisms of mono- and poly-ubiquitination: Ubiquitination specificity depends on compatibility between the E2 catalytic core and amino acid residues proximal to the lysine. Cell Div *5*: 19.

Sadowski, M., Suryadinata, R., Tan, A. R., Roesley, S. N. and Sarcevic, B. (2012). Protein monoubiquitination and polyubiquitination generate structural diversity to control distinct biological processes. IUBMB Life *64* (2): 136-142.

Schulein-Volk, C., Wolf, E., Zhu, J., Xu, W., Taranets, L., Hellmann, A., Janicke, L. A., Diefenbacher, M. E., Behrens, A., Eilers, M. and Popov, N. (2014). Dual regulation of Fbw7 function and oncogenic transformation by Usp28. Cell Rep *9* (3): 1099-1109.

Scott, D. C., Rhee, D. Y., Duda, D. M., Kelsall, I. R., Olszewski, J. L., Paulo, J. A., de Jong, A., Ovaa, H., Alpi, A. F., Harper, J. W. and Schulman, B. A. (2016). Two Distinct Types of E3 Ligases Work in Unison to Regulate Substrate Ubiquitylation. Cell *166* (5): 1198-1214 e1124.

Sequeira-Mendes, J., Diaz-Uriarte, R., Apedaile, A., Huntley, D., Brockdorff, N. and Gomez, M. (2009). Transcription initiation activity sets replication origin efficiency in mammalian cells. PLoS Genet *5* (4): e1000446.

Shanbhag, N. M., Rafalska-Metcalf, I. U., Balane-Bolivar, C., Janicki, S. M. and Greenberg, R. A. (2010). ATM-dependent chromatin changes silence transcription in cis to DNA double-strand breaks. Cell *141* (6): 970-981.

Sharma, N., Zhu, Q., Wani, G., He, J., Wang, Q. E. and Wani, A. A. (2014). USP3 counteracts RNF168 via deubiquitinating H2A and gammaH2AX at lysine 13 and 15. Cell Cycle *13* (1): 106-114.

Sharma, R., Williams, P. J., Gupta, A., McCluskey, B., Bhaskaran, S., Munoz, S. and Oyajobi, B. O. (2015). A dominant-negative F-box deleted mutant of E3 ubiquitin ligase, beta-TrCP1/FWD1, markedly reduces myeloma cell growth and survival in mice. Oncotarget *6* (25): 21589-21602.

Skaar, J. R., Pagan, J. K. and Pagano, M. (2013). Mechanisms and function of substrate recruitment by F-box proteins. Nat Rev Mol Cell Biol *14* (6): 369-381.

Staib, C. and Grummt, F. (1997). Mapping replication origins by nascent DNA strand length. Methods *13* (3): 293-300.

Stewart, G. S., Panier, S., Townsend, K., Al-Hakim, A. K., Kolas, N. K., Miller, E. S., Nakada, S., Ylanko, J., Olivarius, S., Mendez, M., Oldreive, C., Wildenhain, J., Tagliaferro, A., Pelletier, L., Taubenheim, N., Durandy, A., Byrd, P. J., Stankovic, T., Taylor, A. M. and Durocher, D. (2009). The RIDDLE syndrome protein mediates a ubiquitin-dependent signaling cascade at sites of DNA damage. Cell *136* (3): 420-434.

Streich, F. C., Jr., Ronchi, V. P., Connick, J. P. and Haas, A. L. (2013). Tripartite motif ligases catalyze polyubiquitin chain formation through a cooperative allosteric mechanism. J Biol Chem *288* (12): 8209-8221.

Suzuki, H., Chiba, T., Suzuki, T., Fujita, T., Ikenoue, T., Omata, M., Furuichi, K., Shikama, H. and Tanaka, K. (2000). Homodimer of two F-box proteins betaTrCP1 or betaTrCP2 binds to IkappaBalpha for signal-dependent ubiquitination. J Biol Chem *275* (4): 2877-2884.

Tang, W., Pavlish, O. A., Spiegelman, V. S., Parkhitko, A. A. and Fuchs, S. Y. (2003). Interaction of Epstein-Barr virus latent membrane protein 1 with SCFHOS/beta-TrCP E3 ubiquitin ligase regulates extent of NF-kappaB activation. J Biol Chem *278* (49): 48942-48949.

Tang, X., Orlicky, S., Lin, Z., Willems, A., Neculai, D., Ceccarelli, D., Mercurio, F., Shilton, B. H., Sicheri, F. and Tyers, M. (2007). Suprafacial orientation of the SCFCdc4 dimer accommodates multiple geometries for substrate ubiquitination. Cell *129* (6): 1165-1176.

Treier, M., Staszewski, L. M. and Bohmann, D. (1994). Ubiquitin-dependent c-Jun degradation in vivo is mediated by the delta domain. Cell *78* (5): 787-798.

Villamil, M. A., Liang, Q. and Zhuang, Z. (2013). The WD40-repeat protein-containing deubiquitinase complex: catalysis, regulation, and potential for therapeutic intervention. Cell Biochem Biophys *67* (1): 111-126.

Visintin, R., Prinz, S. and Amon, A. (1997). CDC20 and CDH1: a family of substrate-specific activators of APC-dependent proteolysis. Science *278* (5337): 460-463.

Vodermaier, H. C. (2004). APC/C and SCF: controlling each other and the cell cycle. Curr Biol *14* (18): R787-796.

Walter, J. and Newport, J. (2000). Initiation of eukaryotic DNA replication: origin unwinding and sequential chromatin association of Cdc45, RPA, and DNA polymerase alpha. Mol Cell *5* (4): 617-627.

Wang, Z., Inuzuka, H., Zhong, J., Fukushima, H., Wan, L., Liu, P. and Wei, W. (2012). DNA damage-induced activation of ATM promotes beta-TRCP-mediated Mdm2 ubiquitination and destruction. Oncotarget *3* (9): 1026-1035.

Ward, I., Kim, J. E., Minn, K., Chini, C. C., Mer, G. and Chen, J. (2006). The tandem BRCT domain of 53BP1 is not required for its repair function. J Biol Chem *281* (50): 38472-38477.

Watanabe, N., Arai, H., Nishihara, Y., Taniguchi, M., Watanabe, N., Hunter, T. and Osada, H. (2004). M-phase kinases induce phospho-dependent ubiquitination of somatic Wee1 by SCFbeta-TrCP. Proc Natl Acad Sci U S A *101* (13): 4419-4424.

Watanabe, N., Broome, M. and Hunter, T. (1995). Regulation of the human WEE1Hu CDK tyrosine 15-kinase during the cell cycle. EMBO J *14* (9): 1878-1891.

Welchman, R. L., Gordon, C. and Mayer, R. J. (2005). Ubiquitin and ubiquitin-like proteins as multifunctional signals. Nat Rev Mol Cell Biol *6* (8): 599-609.

Welcker, M., Larimore, E. A., Swanger, J., Bengoechea-Alonso, M. T., Grim, J. E., Ericsson, J., Zheng, N. and Clurman, B. E. (2013). Fbw7 dimerization determines the specificity and robustness of substrate degradation. Genes Dev *27* (23): 2531-2536.

Willis, N. and Rhind, N. (2009). Regulation of DNA replication by the S-phase DNA damage checkpoint. Cell Div *4*: 13.

Winston, J. T., Strack, P., Beer-Romero, P., Chu, C. Y., Elledge, S. J. and Harper, J. W. (1999). The SCFbeta-TRCP-ubiquitin ligase complex associates specifically with phosphorylated destruction motifs in IkappaBalpha and beta-catenin and stimulates IkappaBalpha ubiquitination in vitro. Genes Dev *13* (3): 270-283.

Woelk, T., Oldrini, B., Maspero, E., Confalonieri, S., Cavallaro, E., Di Fiore, P. P. and Polo, S. (2006). Molecular mechanisms of coupled monoubiquitination. Nat Cell Biol *8* (11): 1246-1254.

Wu, C. L., Kirley, S. D., Xiao, H., Chuang, Y., Chung, D. C. and Zukerberg, L. R. (2001). Cables enhances cdk2 tyrosine 15 phosphorylation by Wee1, inhibits cell growth, and is lost in many human colon and squamous cancers. Cancer Res *61* (19): 7325-7332.

Wu, G., Xu, G., Schulman, B. A., Jeffrey, P. D., Harper, J. W. and Pavletich, N. P. (2003). Structure of a beta-TrCP1-Skp1-beta-catenin complex: destruction motif binding and lysine specificity of the SCF(beta-TrCP1) ubiquitin ligase. Mol Cell *11* (6): 1445-1456.

Wu, X., Yen, L., Irwin, L., Sweeney, C. and Carraway, K. L., 3rd (2004). Stabilization of the E3 ubiquitin ligase Nrdp1 by the deubiquitinating enzyme USP8. Mol Cell Biol *24* (17): 7748-7757.

Yin, Q., Lin, S. C., Lamothe, B., Lu, M., Lo, Y. C., Hura, G., Zheng, L., Rich, R. L., Campos, A. D., Myszka, D. G., Lenardo, M. J., Darnay, B. G. and Wu, H. (2009). E2 interaction and dimerization in the crystal structure of TRAF6. Nat Struct Mol Biol *16* (6): 658-666.

Zaaroor-Regev, D., de Bie, P., Scheffner, M., Noy, T., Shemer, R., Heled, M., Stein, I., Pikarsky, E. and Ciechanover, A. (2010). Regulation of the polycomb protein Ring1B by self-ubiquitination or by E6-AP may have implications to the pathogenesis of Angelman syndrome. Proc Natl Acad Sci U S A *107* (15): 6788-6793.

Zgheib, O., Pataky, K., Brugger, J. and Halazonetis, T. D. (2009). An oligomerized 53BP1 tudor domain suffices for recognition of DNA double-strand breaks. Mol Cell Biol *29* (4): 1050-1058.

Zhang, A., Peng, B., Huang, P., Chen, J. and Gong, Z. (2017). The p53-binding protein 1-Tudor-interacting repair regulator complex participates in the DNA damage response. J Biol Chem *292* (16): 6461-6467.

Zhang, D., Zaugg, K., Mak, T. W. and Elledge, S. J. (2006). A role for the deubiquitinating enzyme USP28 in control of the DNA-damage response. Cell *126* (3): 529-542.

Zimmermann, M. and de Lange, T. (2014). 53BP1: pro choice in DNA repair. Trends Cell Biol *24* (2): 108-117.

Zong, D., Callen, E., Pegoraro, G., Lukas, C., Lukas, J. and Nussenzweig, A. (2015). Ectopic expression of RNF168 and 53BP1 increases mutagenic but not physiological non-homologous end joining. Nucleic Acids Res *43* (10): 4950-4961.

7 Appendix

7.1 Abbreviations

Prefixes

c	centi
k	kilo
m	milli
n	nano
µ	micro

Units

A	
°C	degree celsius
Da	dalton
g	gram
h	hour
l	liter
m	meter
M	mol/l
min	minute
s	second
U	unit
v/v	volume / volume percent
w/v	weight / volume percent

Other Abbreviations

A, Ala	alanine
AA	amino acid
APC/C	anaphase-promoting complex / cyclosome
APS	ammoniumpersulfate
ATCC	American type culture collection
ATP	adenosin-5'-triphosphate
ATM	ataxia telangiectasia mutated
ATR	ATM and Rad3-related
BCA	Bicinchoninic acid assay
bp	basepairs
BrdU	bromodeoxyuridine
BSA	bovine serum albumine
C	cytosine
Cdc	cell division cycle
Cdk	cyclin-dependent kinase
cDNA	complementary DNA
ChIP	chromatin immunoprecipitation
ChIP-Seq	chromatin immunoprecipitation sequencing
Chk	checkpoint kinase
CHX	cycloheximide
Cul	cullin
Ctrl	control
CT	C-terminal fragment
Δ	deletion
ΔD	dimer deficient

ΔOD	oligomerization domain deleted
ddH2O	double-distilled water
DDR	DNA damage response
DMEM	Dulbecco's Modified Eagle-Medium
DMSO	dimethylsulfoxide
DNA	deoxyribonucleic acid
dNTPs	deoxyribonucleoside-5'-triphosphate (dATP, dCTP, dGTP, dTTP)
DSBs	double-strand breaks
dsDNA	double-strand DNA
DTT	dithiothreitol
DUB	deubiquitinating enzyme
E, Glu	glutamic acid
E1	ubiquitin-activating enzyme
E2	ubiquitin-conjugating enzyme
E3	ubiquitin ligase
E.coli	Escherichia coli
EDTA	ethylendiamintetraacetate
e.g.	exempli gratia (for example)
FACS	fluorescence-activated cell sorting
FBP	F-box protein
FBS	fetal bovine serum
Fbw	F-box/WD40 repeat containing
Fig	figure
FL	full length

g	relative centrifugal force
GFP	green fluorescent protein
HECT	homologous to E6AP carboxy terminus
histone H2AK15ub	ubiquitinated histone H2A at K15
histone H4K20me2	dimethylated histone H4K20
HRP	horseradish peroxidase
IB	immunoblot
IgG	immunoglobulin
IF	immunofluorescence
IP	immunoprecipitation
IR	irradiation
IRIF	ionizing radiation induced foci
K, Lys	lysine
Knockdown	KD
Knockout	KO
KR	lysines replaced by arginines
LB	lysogeny broth
M-MLV RT	Moloney murine leukemia virus reverse transcriptase
mRNA	messenger RNA
NHEJ	non-homologous endjoining
NLS	nuclear localization signal
NP-40	nonyl phenoxypolyethoxylethanol-40
NTA	nitrilotriacetic acid
p	phospho
PAGE	Polyacrylamide gel electrophoresis
PBS	phosphate-buffered saline

PBS-T	phosphate-buffered saline with tween20
PCR	polymerase chain reaction
PD	pulldown
PEI	polyethyleneimine
Phleo	phleomycin
PI	Propidium iodide
PVDF	polyvinylidene difluoride
Pol	DNA polymerases
pre-ICs	pre-initiation complexes
pre-RCs	pre-replication complexes
qPCR	quantitative PCR
R, Arg	arginine
RING	really interesting new gene
RNA	ribonucleic acid
RNase	ribonuclease
RT	room temperature
T, Thr	threonine
TAE	Tris-acetate-EDTA
TBS	Tris-buffered saline
TBS-T	Tris-buffered saline with tween-20
TE	Tris-EDTA buffer
TEMED	N,N,N’,N’-Tetramethylethylenediamine
TNT	Tris-NaCl-Triton X100
Tris	Tris-(hydroxymethyl)-aminomethane
Y, Tyr	tyrosine
S, Ser	serine

SCF complex	Skp1-Cul1-F-box complex
SD	standard deviation
SDS	sodium dodecyl sulfate
SDS-PAGE	SDS polyacrylamide gelelectrophoresis
SEM	standard error of the mean
siRNA	small interfering RNA
S-phase	synthesis phase
ssDNA	single-strand DNA
Ub	ubiquitin
U-box	UFD2 homology
UV	ultraviolet radiation
UPS	ubiquitin-proteasome system
WT	wildtype

7.2 Acknowledgements

I would like to express my sincerest gratitude to all those who helped me during my doctoral study.

First and foremost, I would like to thank my primary supervisor **Dr. Nikita Popov** for providing me the opportunity to work on this project, for giving constant guidance and encouragement on my work, for supervising this thesis, and for the bioinformatic analysis of ChIP-Seq data.

I am grateful to **Dr. Sonja Lorenz** and **Prof. Dr. Alexander Buchberger** for being my committee members and providing valuable suggestions, especially for the structural analysis done by **Dr. Sonja Lorenz**. I also thank **Dr. Thomas Ruppert** for performing the mass spectrometry analysis.

My great gratitude also goes to **Theresa Klemm** and **Prof. Dr. Caroline Kisker** for providing the purified proteins for the *in vitro* assays. I would like to thank **Prof. Dr. Martin Eilers**, **Dr. Markus Diefenbacher, Dr. Elmar Wolf**, **Apoorva Baluapuri**, **Prof. Dr. Michael Flentje**, **Dr. Konrad Förster** for advice and discussions toward this project, and **Dr. Matthias Rosenfeldt** for providing the murine PDAC KPC cells. I also thank **Lena Ries** for helping me write the summary of this thesis in German.

I am thankful to all my former and current labmates for all the discussions and technical supports. I especially thank **Lyudmyla Taranets, Ravi Babu Kollampally, Ksenia Popova, Jing Zhu** for all their help inside and outside the lab, and for the great time we spent together.

I would like to thank the financial support for this project from the **German Research Foundation (DFG)** grant PO-1458/4-1 and the core support from the **Department of Radiation Oncology**. I also thank the **Graduate School of Life Sciences** in University of Würzburg for providing the opportunities to participate in excellent workshops and courses and the financial support to conferences.

Lastly, my great appreciation goes to my parents for their endless love, encouragement and support throughout my life.

7.3 Publications

During PhD study,

1. **Xu W**, Taranets L, Babu R, Ruppert T, Djuzenova C, Klemm T, Sauer F, Fink S, Stühmer T, Kisker C, Flentje M, Lorenz S, Popov N. The Usp28 deubiquitinase promotes destruction of Cdc25A to inhibit DNA replication in response to genotoxic stress. *(Manuscript in preparation)*.

2. Sander B, **Xu W**, Eilers M, Popov N, Lorenz S. A conformational switch regulates the ubiquitin ligase HUWE1. Elife*,* 2017, 6.

3. Jaenicke LA, von Eyss B, Carstensen A, Wolf E, **Xu W**, Greifenberg AK, Geyer M, Eilers M, Popov N. Ubiquitin-Dependent Turnover of MYC Antagonizes MYC/PAF1C Complex Accumulation to Drive Transcriptional Elongation. Mol Cell*,* 2016, 61(1): 54-67.

4. Schulein-Volk C, Wolf E, Zhu J, **Xu W**, Taranets L, Hellmann A, Janicke LA, Diefenbacher ME, Behrens A, Eilers M, Popov N. Dual regulation of Fbw7 function and oncogenic transformation by Usp28. Cell Rep*,* 2014, 9(3): 1099-1109.

5. **Xu W**, Taranets L, Popov N. Regulating Fbw7 on the road to cancer. Semin Cancer Biol*,* 2016, 36:62-70. *(Review)*.

6. Taranets L, Zhu J, **Xu W,** Popov N. Fbw7 and Usp28 - enemies and allies. Mol Cell Oncol, 2015, 23: 2(3). *(Review)*.

During Master study,

1. **Xu WS**, Dang YY, Guo JJ, Wu GS, Lu JJ, Chen XP, Wang YT. Furanodiene induces endoplasmic reticulum stress and presents antiproliferative activities in lung cancer cells. Evidence-Based Complementary and Alternative Medicine*,* 2012, 2012: 426521.

2. **Xu WS**, Dang YY, Chen XP, Lu JJ, Wang YT. Furanodiene presents synergistic anti-proliferative activity with paclitaxel via altering cell cycle and integrin signaling in 95-D lung cancer cells. Phytotherapy Research*,* 2013. [Epub ahead of print]

3. **Xu WS**, Li T, Wu GS, Dang YY, Hao WH, Chen XP, Lu JJ, Wang YT. Effects of furanodiene on 95-D lung cancer cells: apoptosis, autophagy and G1 phase cell cycle arrest. Am J Chin Med, 2014, 42(1):243-55*.*

4. Li T*, **Xu WS***, Wu GS, Chen XP, Wang YT, Lu JJ. Platycodin D induces apoptosis, and inhibits adhesion, migration and invasion in HepG2 hepatocellular carcinoma cells. Asian Pac J Cancer Prev, 2014, 15(4):1745-9. (* *authors contributed equally*).

5. Li T, Tang ZH, **Xu WS**, Wu GS, Wang YF, Chang LL, Zhu H, Chen XP, Wang YT, Chen Y, Lu JJ. Platycodin D triggers autophagy through activation of extracellular signal-regulated kinase in hepatocellular carcinoma HepG2 cells. Eur J Pharmacol, 2015, 15(749):81-8.

6. Lu JJ, Bao JL, Wu GS, **Xu WS**, Huang MQ, Chen XP, Wang YT: Quinones derived from plant secondary metabolites as anti-cancer agents. Anti-Cancer Agents in Medicinal Chemistry, 2012. [Epub ahead of print]

7. Chen XP, Guo JJ, Bao JL, **Xu WS**, Huang Yanjuan, Wang YT: Screening Neuroprotective Agents Through 4-hydroxynonenal, Ethanol, High Glucose, Homocysteine, Okadaic Acid, Rotenone, and Oxygen-Glucose Deprivation Induced PC12 Injury Models: A Review. Current Psychopharmacology, 2012, 1: 103-10.

8. Lu JJ, Dang YY, Huang M, **Xu WS**, Wang YT: Anti-cancer properties of terpenoids isolated from Rhizoma Curcumae - A review. Journal of Ethnopharmacology, 2012, 143: 406-11.

9. Wu GS, Qian ZM, Guo JJ, Hu DJ, Bao JL, Xie J, **Xu WS**, Lu JJ, Chen XP, Wang YT: *Ganoderma lucidum* extract induces G1 cell cycle arrest, and apoptosis in human breast cancer cells. The American Journal of Chinese Medicine, 2012, 40(3): 631-42.

10. **Xu WS**, Huang MQ, Chen XP, Wang YT: Natural products with aromatase inhibitory activity. Lishizhen Medicine and Materia Medicine Research, 2012, 23(4): 1008-11. *(In Chinese)*

11. **Xu WS**, Lu JJ, Chen XP, Wang YT: Anti-cancer drug research and development based on endoplasmic reticulum stress. Chinese Pharmacological Bulletin, 2012, 28(12): 1659-65. *(In Chinese).*

12. Chen XP, Lu JJ, Guo JJ, Bao JL, **Xu WS**, Ding Q, Wang YT. Inspirations from natural products based drug research and development for Chinese medicine research - Analysis of natural products recorded in TTD. Acta Pharmaceutica Sinica B, 2012, 47(11): 1423-7. *(In Chinese).*

13. Wang YT. Progress of the modern research techniques for investigating anti-cancer Traditional Chinese Medicine. Beijing: People's Medical Publishing House, 2012. ISBN 978-7-117-16227-2/R·16228. (*In Chinese*) (I wrote Chapter 7 in Volume 2, which is about the techniques to investigate anti-multidrug resistance in tumor cells.)

7.4 Curriculum vitae

7.5 Affidavit

I hereby confirm that my thesis entitled "**Regulation of the DNA Damage Response by the Ubiquitin System**" is the result of my own work. I did not receive any help or support from commercial consultants. All sources and / or materials applied are listed and specified in the thesis.

Furthermore, I confirm that this thesis has not yet been submitted as part of another examination process neither in identical nor in similar form.

_____ _____

Place, Date Signature

Eidesstattliche Erklärung

Hiermit erkläre ich an Eides statt, die Dissertation "**Regulierung der DNA-Schadensreaktion durch das Ubiquitin System**" eigenständig, d.h. insbesondere selbständig und ohne Hilfe eines kommerziellen Promotionsberaters, angefertigt und keine anderen als die von mir angegebenen Quellen und Hilfsmittel verwendet zu haben.

Ich erkläre außerdem, dass die Dissertation weder in gleicher noch in ähnlicher Form bereits in einem anderen Prüfungsverfahren vorgelegen hat.

_____ _____

Ort, Datum Unterschrift